**PREPARATION AND CHARACTERIZATION OF
MODIFIED POLYETHER ETHER KETONE (PEEK-WC) MEMBRANES FOR
POLYMER ASSISTED ULTRAFILTRATION OF Cu^{2+} IONS FROM WATER**

by

FİRUZE OKYAY ÖNER

**Submitted to the Graduate School of Engineering and Natural Sciences
in partial fulfillment of
the requirements for the degree of
Doctor of Philosophy**

**Sabancı University
January 2014**

PREPARATION AND CHARACTERIZATION OF
MODIFIED POLYETHER ETHER KETONE (PEEK-WC) MEMBRANES
FOR POLYMER ASSISTED ULTRAFILTRATION OF Cu^{2+} IONS FROM
WATER

APPROVED BY:

Prof. Dr. Yuda Yürüm

(Thesis Supervisor)

Prof. Dr. Ferhat Yardım

Assoc. Prof. Dr. Melih Papila

Assoc. Prof. Dr. Selmiye Alkan Gürsel

Asst. Prof. Dr. Fevzi Çakmak Cebeci

DATE OF APPROVAL: 13/01/2014

To my beloved family

PREPARATION AND CHARACTERIZATION OF
MODIFIED POLYETHER ETHER KETONE (PEEK-WC) MEMBRANES FOR
POLYMER ASSISTED ULTRAFILTRATION OF Cu^{2+} IONS FROM WATER

Firuze OKYAY ÖNER

MAT, Doctor of Philosophy Thesis, 2014

Thesis Advisor: Prof Dr. Yuda Yürüm

Abstract

Membrane technology is one of the most important topics in today's research for achieving metal removal and/or recovery from water. In this study, modified polyether ether ketone (PEEK-WC) membranes ranging from microfiltration to nanofiltration membranes depending on the coagulation bath, evaporation time and temperature were produced by phase inversion method. Produced asymmetric porous ultrafiltration membranes were preferred for PAUF processes. In the meantime, bonding conditions (pH and polymer/metal concentration) of various heavy metals (Cu^{2+}, Ni^{2+}, Co^{2+}) with PEI were optimized. Optimum pH of 6 and 1:1 Cu^{2+}:B-PEI (weight ratio) conditions were used to prepare feed solution for PAUF tests. In conclusion, a denser structure of PEEK-WC membranes, DW-120, corresponded to a higher rejection of Cu^{2+} (98%), although there was a sharp reduction in permeance. All membranes showed a constant permeance profile with respect to time. This strongly indicated that there was no effect of concentration polarization on the membranes. Also, both long-term and short-term stability (in means of flux and selectivity) of these membranes validated the reduction of fouling effect due to the chemical stabilility of PEEK-WC. In spite of the decrease in permeances, reusability and almost complete recovery (94.5%) of the used membranes make these membranes an attractive alternative for industrial applications. Specifically, almost full recovery of performance of PEEK-WC membranes, just by washing with water, makes them significant among commercially used membranes.

POLİETER ETER KETON (PEEK-WC) MEMBRANLARIN ÜRETİMİ, KARAKTERİZASYONU VE SUDAN BAKIR(II) İYONLARININ POLİMER DESTEKLİ ULTRAFİLTRASYON PROSESİ İLE GİDERİMİ

Firuze OKYAY ÖNER

MAT, Doktora Tezi, 2014

Tez Danışmanı: Prof. Dr. Yuda Yürüm

Anahtar Kelimeler: Membran, Modifiye edilmiş polyeter eter keton (PEEK-WC), Ultrafiltrasyon, Nanofiltrasyon, Polimer destekli ultrafiltrasyon

Özet

Membranlar, günümüzde ağır metallerin sudan giderimi ve/veya geri kazanımı araştırmalarında en dikkat çeken teknolojilerden birisidir. Bu çalışmada, modifiye edilmiş polieter eter ketone (PEEK-WC) kullanılarak mikrofiltrasyondan nanofiltrasyona kadar uzanan özelliklere sahip membranlar faz ayrıştırma metodunun koagülasyon banyosu, evaporasyon süresi ve sıcaklığı gibi parametreleri kontrol edilerek üretilmişlerdir. Üretilen asimetrik gözenekli membranlardan ultrafiltrasyon özelliklerine sahip olanları, polimer destekli ultrafiltrasyon proseslerinde kullanılmak üzere seçilmişlerdir. Aynı zamanda, polimer destekli ultrafiltrasyon işlemi öncesi PEI ve bazı ağır metallerin bağlanma kapasitelerini etkileyen pH ve metal konsantrasyon değerleri optimize edilmiştir. Bu sonuçlardan, bakır(II)'ye ait olan optimum koşulları, pH=6 ve ağırlık oranınca 1:1-Cu^{2+}:B-PEI, göz önüne alınarak model bakır(II) atık suyu hazırlanmıştır. Polimer destekli ultrafiltrasyon sonucunda, daha az gözenekli olan DW-2 membranının %98'lik Cu^{2+} giderimi yapabildiği görülmüştür. Bu yüksek seçiciliğe karşın, membranın geçirgenliğinde keskin bir azalma gözlemlenmiştir. Öte yandan, bütün membranlar zamana karşı sabit bir geçirgenlik profili göstermişlerdir. Bu da membran kirliliğinin PEEK-WC'nin kimyasal ve mekanik kararlılığının sayesinde, ticari olarak kullanılan polimer membranlara kıyasla, az olduğunun bir kanıtıdır. DW-120 membranlarının geçirgenliği 33,9 l/h·m^2·bar değerine düşmesine rağmen, sadece su ile yıkanarak performanslarını %94,5 gibi yüksek bir oranda geri kazanabildikleri görülmüştür. Böylece, membranların yeniden kullanılabilmesinin sağlanmasıyla maliyeti düşecek ve ticari olarak kullanılabilecek potansiyel bir ürün olduğu görülmüştür.

ACKNOWLEDGEMENTS

TABLE OF CONTENTS

LIST OF FIGURES

LIST OF TABLES

LIST OF ABBREVIATIONS

CGIAR   Consultative Group on International Agricultural Research

DMA   *N,N* Dimethyl acetemide

DMF   *N,N* Dimethyl formamide

FAO   Food and Agriculture Organization

IPA   Isopropyl Alcohol

MF   Microfiltration

MWCO   Molecular Weight Cut-off

NF   Nanofiltration

NMP   N-Methyl-2-Pyrrolidone

PAA   Polyacrylic Acid

PAUF   Polymer Assisted Ultrafiltration

PDEHED   Poly(dimethylamine–co–epichlorohydrin–co– ethylenediamine)

PEEK   Polyether ether ketone

PEEK-WC   Modified Polyether ether ketone

PEI   Polyethylenemine

RO   Reverse Osmosis

SEM   Scanning Electron Microscopy

TIPS   Temperature Induced Phase Separation

TMP   Transmembrane Pressure

UF   Ultrafiltration

WHO   World Health Organization

CHAPTER 1

INTRODUCTION

Today, there is a high demand and competition for limited water sources since water pollution has become one of the most serious environmental problems. Consultative Group on International Agricultural Research (CGIAR) predicts that 2.7 billion people will be living in "water scarce" regions by 2025 whereas the World Water Council predicts this number will be 3.9 billion people by 2030 [1,2]. As the human population grows, the demand for water will increase exponentially. Demand of water will not increase only due to the population, but it will increase also due to agriculture, industry, and energy consumption. Unfortunately, water scarce is not the only problem due to rising water pollution in many regions of the world. Most of the researches show today water pollutants are not only present in wastewater, but they are also found in surface and ground water, which are the main sources for sustainable drinking water [1,3-6]. The World Health Organization (WHO) states that 2.6 billion people suffer from water hygiene whereas 1.1 billion people suffer from poor quality in drinking water [7]. Unfortunately, the lack of water supply and hygiene lead to countless diseases in many regions, especially in Africa and Asia [8]. Food and Agriculture Organization (FAO) reported that 4 billion people face with diarrhea every year and 2.2 billion of them lose their lives. Moreover, malaria causes death of 1 million children under age of five every year [8]. Considering this problem, better water

treatment technologies are needed to supply the growing demand in clean water. In order to be able to overcome these problems, the contaminants and the source of these contaminants should be investigated deeply.

Rapid and intensive industrialization presents large volumes of aqueous wastes containing hazardous materials, such as heavy metals, into the environment [9] Some of these industries can be listed as metal finishing, mining, battery, paper, chemical and electronic industries and pesticides [9,13]. Heavy metal contamination is one of the most serious problems in water pollution. Heavy metal ions, such as copper, nickel, cobalt, cadmium, lead, zinc and/or their compounds are non-biodegradable and can be toxic and carcinogenic even at very low concentrations, creating a serious threat to the environmental and public health [9-13]. In *this thesis*, we mainly focused on copper, nickel and cobalt due to their treat against human health. Even though copper is essential to human life and health, its excess in the human body leads to stomach and intestinal distress, such as nausea, diarrhea and stomach cramps [14,15]. Moreover, the toxicity of copper has been implicated in various neurodegenerative disorders, such as Wilson's disease and Alzheimer's disease. In fact, free copper in the brain has been associated with neuronal and cellular damage, promoting free radical production [16]. On the other hand, nickel is known as a human carcinogen and it can cause gastrointestinal distress, pulmonary fibrosis, skin dermatitis, lung and kidney problems [15,17]. Cobalt is also determined as a possible human carcinogen by the International Agency for Research on Cancer [18]. Some experiments on animals show that exposure to high cobalt concentrations can cause problems in fetus growth during pregnancy. Animal studies have found problems with the development of the fetus in animals exposed to high concentrations of cobalt during pregnancy. As a consequence, these heavy metals should be removed from water.

Even tough it is very necessary to remove heavy metals from water, it is more important to recover them with respect to decline of their availability. As a result, there is a growing demand for most of the heavy metals due to a decrease in grade of available ores and strict environmental regulations [19]. For this reason, there is a high potential to develop efficient and low-cost treatment methods to separate and regenerate these toxic heavy metals from water, especially wastewater. The main treatments to remove heavy metals from wastewater can be listed as [3-20],

- chemical precipitation,

- ion exchange,
- adsorption,
- coagulation and flocculation,
- flotation,
- electrochemical treatment, and
- membrane filtration.

Chemical precipitation is a widely used method due its simple processing and inexpensive capital cost. However, chemical precipitation method produces high amounts of sludge, which will be difficult to treat as well it, will also prevent the regeneration of heavy metals. Also, it is not an effective method to deal with low concentration of metal ions in wastewater [15]. To sum up, chemical precipitation will not be an economical and efficient treatment to retain and recover metal ions. On the other hand, adsorption is an emerging wastewater treatment due to its ability to treat both high and low concentrated wastewaters. However, the cost and efficiency of adsorption technique is highly depending on the choice of the adsorbent [15]. Ion exchange is another technique applied in for separating heavy metals from wastewater. Due to its high cost and pollution problems during regeneration step, it is not preferred for large-scale application [15,21]. In coagulation and flocculation method is a two-step process in which large amount of sludge is produced and a lot of chemicals are used [15]. When it comes to flotation, it presents high metal removal efficiency, high overflow and low operation cost. However, its high capital, maintenance and operation costs are serious drawbacks [15,22]. On the other hand, membrane separation technology is a promising approach due to its high efficiency, simple operation, ease of scale-up, and efficient energy usage. Depending on the membrane filtration technique, cost, process complexity, flux rate and membrane fouling can be the possible problems of this treatment.

The membrane processes used for heavy metal removal are reverse osmosis (RO), nanofiltration (NF), electrodialysis and ultrafiltration (UF). During the reverse osmosis, which comprises at least 20 % of the world's desalination capacity, high efficiencies in removal of heavy metal ions were obtained. However, it is necessary to apply high transmembrane pressures, which will increase the operating cost due to the high-energy consumption. Nanofiltration is also providing high removal efficiency of

heavy metals from wastewater. NF membranes are operating under lower transmembrane pressures (2-30 bar) with respect to RO membranes (1-100 bar), but still higher pressures are applied than UF membranes (0.5-5 bar). Although the reduction of applied transmembrane pressure reduces the cost of NF treatment, it is still consuming much more energy than UF applications [15]. Also, RO and NF operations are yielding low permeate flow rates. In fact, ultrafiltration process takes place at low transmembrane pressures. Even though this would reduce the operation cost of the filtration processes, low molecular weight complexes and metal ions may still pass easily through ultrafiltration membranes as a result of their large pore sizes. In order to overcome these problems a solution for the removal of heavy metals from water, called polymer-assisted ultrafiltration (PAUF), has been proposed [15,23-25]. The PAUF method uses water-soluble polymers that form macromolecular complexes with metallic ions. The UF membranes, having a smaller molecular weight cut-off than the molecular weight of the metal-polymer complex, will block the macromolecular complexes, while still allowing the non-complexed metal ions to pass through the membrane. The main advantages of PAUF are high flux rates, low transmembrane pressure, low operation cost, high selectivity, and regeneration of retained heavy metals [23-25]. Although PAUF processes has not widespread in industry, Koch Membrane Systems Inc. (KMS) introduced industrial tubular ultrafiltration systems, incorporating ULTRA-COR™, INDUCOR™, and FEG PLUS™ membrane modules, which are capable of separating heavy metals from wastewater by increasing pH of wastewater to precipitate insoluble metal hydroxides [15,26].

Considering the high demand and competition for limited water sources, due to heavy metal pollution in water, among water treatment methods PAUF process is found to be a challenging treatment to be used *in this work*, which satisfies the following requirements

- ✓ high water flux,
- ✓ low transmembrane pressures,
- ✓ high metal ion retention (depends on binding conditions between metal ions and polymer),
- ✓ low cost,
- ✓ possibility to regenerate metal ions after separation.

Even tough PAUF has many advantages, it needs certain improvements for becoming a widespread industrial application. Some of these requirements can be listed as,

- high water flux (low capital cost),
- high metal retention (high water quality and high metal recovery),
- long-term stability of water flux and rejection (membrane fouling),
- recovery and reusability of membranes (low capital cost),
- mechanical, chemical and thermal stability of membranes,
- minimum pre-treatment (back-flushing and chemical treatment),
- simple and large-scale processability,
- inexpensive

Considering these requirements, the objectives of this dissertation are set as: 1) to produce and modify the morphology of polymer membranes for desired application by simple and inexpensive method; 2) to ensure high selectivity and high water flux of membranes; 3) to produce anti-fouling membranes that can be recovered to its initial performance by simple washing procedures. Thus, achieving these aims will be result with a high performance, recyclable polymer membrane that will be a good candidate for industrial applications.

In this manner, modified polyether ether ketone (PEEK-WC) is chosen as polymer of interest due to its outstanding mechanical, chemical, and thermal properties. To complement the advantageous material characteristics of PEEK-WC, it also enables the production of both asymmetrically dense and porous membranes, depending on the proper choice of solvent/non-solvent system [27]. Additionally, the low-cost and simple, single-step preparation of PEEK-WC membranes is a compelling advantage over commercial composite hydrophilic membranes [28]. Also, it should be noted that flat PEEK-WC membranes are used for water purification applications for the first time, in literature, in *this work*. Preparation, characterization and application of PEEK-WC membranes were carried out at laboratories of ITM-CNR under supervision of Prof. Dr. Enrico Drioli, Dr. Catia Algieri, Dr. Laura Donato and Dr. Teresa Poerio.

In *Chapter 2,* asymmetric PEEK-WC membranes were produced by phase inversion method. Phase inversion method enabled the alteration of morphologies of PEEK-WC membranes by tuning parameters of evaporation time, non-solvent selection, and evaporation temperature. PEEK-WC membranes ranging from UF to NF were

produced by a simple and single-step preparation. Based on the results, three UF membranes were chosen as good candidates, which can be used in PAUF applications for separation of heavy metal ions, due to their high water flux values.

Chapter 3 is a complementary section that includes the optimization step of the complexation of selected heavy metals (Cu^{2+}, Ni^{2+}, and Co^{2+}) with water-soluble polyethylenimine (PEI) prior to PAUF tests. The optimum conditions for maximum binding capacities of metal-PEI were investigated by varying the pH and metal concentrations of the prepared model wastewater solutions. Branched-PEI (B-PEI) provided a high metal uptake of 1:1 (B-PEI:M^{2+} weight ratio), when the optimum conditions were satisfied. In literature, most of the studies showed a lower metal uptake PEI, so this result was very important to show that PEI (especially B-PEI) can be preferred for further studies since its higher bonding capacity allows reduction of the polymer amount, thereby reducing the cost and the probability of membrane fouling and/or concentration polarization that can be faced during PAUF processes.

In *Chapter 4,* produced UF membranes DW-0, DW-1, and DW-2 (*Chapter 2*) and optimized conditions for the PEI-Cu complex (*Chapter 3*) were combined to investigate the performance of PEEK-WC membranes during PAUF tests. The removal of the B-PEI-Cu^{2+} complex from aqueous solutions was carried out by using flat PEEK-WC membranes prepared at lab-scale. The aim of *this part of our study* was to show the development of an alternative typology of membranes with respect to those normally employed for the Cu^{2+} extraction, able to reduce the fouling of membrane, while ensuring good rejection of Cu^{2+} transport from the feed to the extractant. DW-120 membranes performed 98% retention of B-PEI-Cu^{2+} with a long-term stability of permeate flux. In particular, these membranes showed almost full recovery after washing with water for 2-3 minutes. High selectivity, reduced fouling, long-term stability, almost full recovery, and reusability of these membranes make them potential candidates for industrial applications.

Chapter 5 covers the preliminary studies on production and characterization of zeolite membranes for water purification. In this manner, tubular FAU and ZSM-5 type supported membranes were prepared by a secondary growth method. The novel seeding procedure designed by Algieri et.al [3] was applied in this study to form a uniform and selective zeolite membrane on the inner surface of α-Al_2O_3 supports. The pH of the

6

seeding suspension and its stabilization was important to form better seal of the inter-crystalline spaces improving the performance of the membrane whereas applying a two-step hydrothermal treatment with shorter times improved the selectivity of the membrane. These results were due to a better uniform and compact zeolite layer formation on the inner surface of the α-Al_2O_3 support.

Chapter 6 summarizes major conclusions of this thesis, ongoing and future works on characterization and application of both polymeric and zeolite membranes.

REFERENCES

[1] Radjenovic J., Petrovic M., Ventura F., Barcelo D. Rejection of pharmaceuticals in nanofiltration and reverse osmosis membrane drinking water treatment. *Water Research*, 2008;42: 3601-3610.

[2]Urban Urgency, Water Caucus Summary, World Water Council (WWC), Marseille, France, 2007.

[3] Halling-Sørensen B., Nors Nielsen S., Lanzky P.F., Ingerslev F., Holten Lützhøft H.C., Jørgensen S.E. Occurrence, fate and effects of pharmaceutical substances in the environment – A review. *Chemosphere*, 1998;36(2): 357–393.

[4] Kolpin D.W., Furlong E.T., Meyer M.T., Thurman E.M., Zaugg S. D., Barber L.D., Buxton H.T. Pharmaceuticals, hormones, and other organic wastewater contaminants in U.S. streams, 1999–2000: Anational reconnaissance. *Environmental Science and Technology*, 2002;36(6):1202–121.

[5] Snyder S.A., Westerhoff P., Yoon Y., Sedlak D.L. Pharmaceuticals, personal care products, and endocrine disruptors in water: implications for the water industry. *Environmental Engineering Science*, 2003;20(5):449–469.

[6] Ternes, T.A. Occurrence of drugs in German sewage treatment plants and rivers. *Water Research*, 1998;32(11):3245–3260.7.

[7] WHO and UNICEF. *Progress on Sanitation and Drinking-Water.* World Health Organization (WHO)/ United Nations International Children's Fund (UNICEF) Joint Monitoring Programme for Water Supply and Sanitation, 2010.

[8] United Nations (UN) Water. *Coping with water scarcity-Challenge of the twenty-first century.* Food and Agricultural Association (FAO), 2007.

[9] Khan M.N., Wahab M.F. Characterization of chemically modified corncobs and its application in the removal of metal ions from aqueous solution. *Journal of Hazardous Materials*, 2007;141: 237–244.

[10] Liu C., Bai R., Ly Q.S. Selective removal of copper and lead ions by diethylenetriamine- functionalized adsorbent behaviours and mechanisms. *Water Research*, 2008;42:1511–1522.

[11] Vilar V.J.P., Botelho C.M.S., Boaventura R.A.R. Copper desorption from Gelidium algal biomass. *Water Research*, 2007;41:1569–1579.

[12] Dobson R.S., Burgess J.E. Biological treatment of precious metal refinery wastewater: A review. *Minerals Engineering*, 2007;20:519–532.

[13] Aziz H.A., Adlan M.N., Ariffin K.S. Heavy metals (Cd, Pb, Zn, Ni;Cu and Cr(III)) removal from water in Malysia: Post treatment by high quality limestone. *Bioresource Technology*, 2008;99:1578–1583.

[14] Bertinato J., L'Abbé M.R. Maintaining copper homeostasis: Regulation of copper-trafficking proteins in response to copper deficiency or overload. *Journal of Nutritional Biochemistry*, 2004;15:316–322.

[15] Fu F., Wang Q. Removal of heavy metal ions from wastewaters: A review. *Journal of Environmental Management*, 2011;92:407-418.

[16] Parmar P., Daya S. The effect of copper on (3H)-tryptophan metabolism in organ cultures of rat pineal glands. *Metabolic Brain Disease*, 2001;16(3-4):199–205.

[17] Borba, C.E., Guirardello, R., Silva, E.A., Veit, M.T., Tavares, C.R.G. Removal of nickel(II) ions from aqueous solution by biosorption in a fixed bed column: experimental and theoretical breakthrough curves. *Biochemical Engineering Journal*, 2006;30:184-191.

[18] IARC. Cobalt in hard metals and cobalt sulfate, gallium arsenide, indium phosphide and vanadium pentoxide. *IARC Monographs on the Evaluation of Carcinogenic Risks to Humans*, 2006;86.

[19] Rivas B.L., Pereira D. Moreno-Villoslada I. Water-soluble polymer-metal ion interations. *Progress in Polymer Science*, 2003;28:173-208.

[20] Ku Y., Jung I.L. Photocatalytic reduction of Cr(VI) in aqueous solutions by UV irradiation with the presence of titanium dioxide. *Water Research*, 2001;35(1):135-142.

[21] Barakat M.A. New trends in removing heavy metals from industrial wastewater. *Arabian Journal of Chemistry*, 2011;4(4):361–377.

[22] Rubio I., Souza M.L., Smith R.W. Overview of flotation as a wastewater treatment technique. *Minerals Engineering*, 2002;15(3):139-155.

[23] Molinari R., Argurio P., Poerio T. Ultrafiltration of polymer-metal complexes for metal ion removal from wastewaters. *Macromolar Symposia*, 2006;235(1):206–214.

[24] Molinari R., Argurio P., Poerio T. Comparison of polyethylenimine, polyacrylic acid and poly(dimethylamine-co-epichlorohydrin-co-ethylenediamme) in Cu^{2+} removal from wastewaters by polymer-assisted ultrafiltration. *Desalination*, 2004;162:217–228.

[25] Molinari R., Poerio T., Argurio P. Selective separation of copper(II) and nickel(II) from aqueous media using the complexation–ultrafiltration process. *Chemosphere*, 2008;70:341-348.

[26] Koch Membranes, Ultrafiltration in Heavy Metal Treatment, 2014. [online] http://www.kochmembrane.com/Resources/Application-Bulletins/Ultrafiltration-in-Heavy-Metals-Treatment.aspx.

[27] Yampolskii Y., Pinnau I., Freeman B.D. *Materials Science of Membranes for Gas and Vapor Separation*. Wiley, Chichester, 2006.

[28] Buonomenna M.G., Golemme G., Jansen J.C., Choi S.-H. Asymmetric PEEKWC membranes for treatment of organic solvent solutions. *Journal of Membrane Science*, 2011;368(1-2):144-149.

CHAPTER 2

PRODUCTION AND CHARACTERIZATION OF MODIFIED POLYETHER ETHER KETONE (PEEK-WC) MEMBRANES

2.1 Literature Review

2.1.1 Membranes

Membrane, illustrated in Figure 2.1, can be defined as a "selective barrier between two phases" [1]. In fact, it should be noted that this definition does not reveal anything about the structure or the function of the membrane. Membranes can be homogeneous or heterogeneous with different thicknesses and pore sizes. They can be neutral or they may carry positive or negative charges, or functional groups with specific binding/complexing abilities. Membrane transport driven by pressure, concentration, chemical or electrical gradients can be active or passive. Their electrical resistance may vary from more than 1,000,000 ohm•cm^2 to less than one ohm•cm^2 [2]. So, these structures need to be classified in order to be more precise. The main classification of membranes is by their nature; biological or synthetic membranes. The biological membranes have a subdivision, which are the living and non-living biological membranes. The details of biological membranes will not be described here since it will

extend the scope of this work. The detailed classification will be limited to synthetic membranes since they are main focus of this thesis.
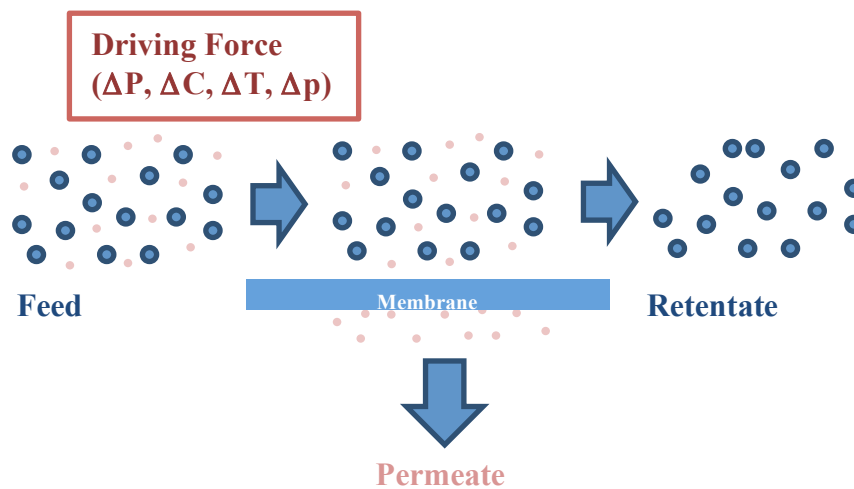
Figure 2.1 Schematic presentation of membrane

Although it is very difficult to make a comprehensive and exact definition, synthetic membranes can be described as an interphase, which separates two phases and restricts the transport of various components in a specific manner [3]. Figure 2.2 illustrates the large diversity in the materials, the structures and the configuration of the synthetic membranes. The most general classification of solid synthetic membranes emerges due to their structure. They can be asymmetric or symmetric. Symmetric membranes show indistinguishable transport properties due to their steady structure across cross-section. They usually have a thickness varying from 10 to 200 μm [1], which determines the flux of the membrane. The permeation rate increases as the membrane becomes thinner. It is important to have thin symmetric membranes to achieve high flux rates, so that they might be a feasible choice in industrial applications. However as the thickness of symmetric membranes decrease, they begin to suffer from their mechanical resistance. Symmetric membranes are used today mainly in dialysis, electrodialysis and microfiltration [2]. On the other hand, a new era for industrial applications has begun with the development of asymmetric membranes. Asymmetric membranes show anisotropic structure and transport properties across the membrane cross-section. In asymmetric membranes, a thick porous sublayer (50-150

Membrane Materials

- Polymers
- Ceramics
- Metals
- Glass
- Liquids

Membrane Structures

Symmetric
- cylindrical porous
- porous
- homogeneous

Asymmetric
- composite structures
  - homogeneous skin layer
- integral asymmetric
  - porous skin layer
  - homogeneous skin layer

Membrane Configurations

- Flat sheet
- Spiral wound
- Tubular
- Capillary
- Hollow fiber
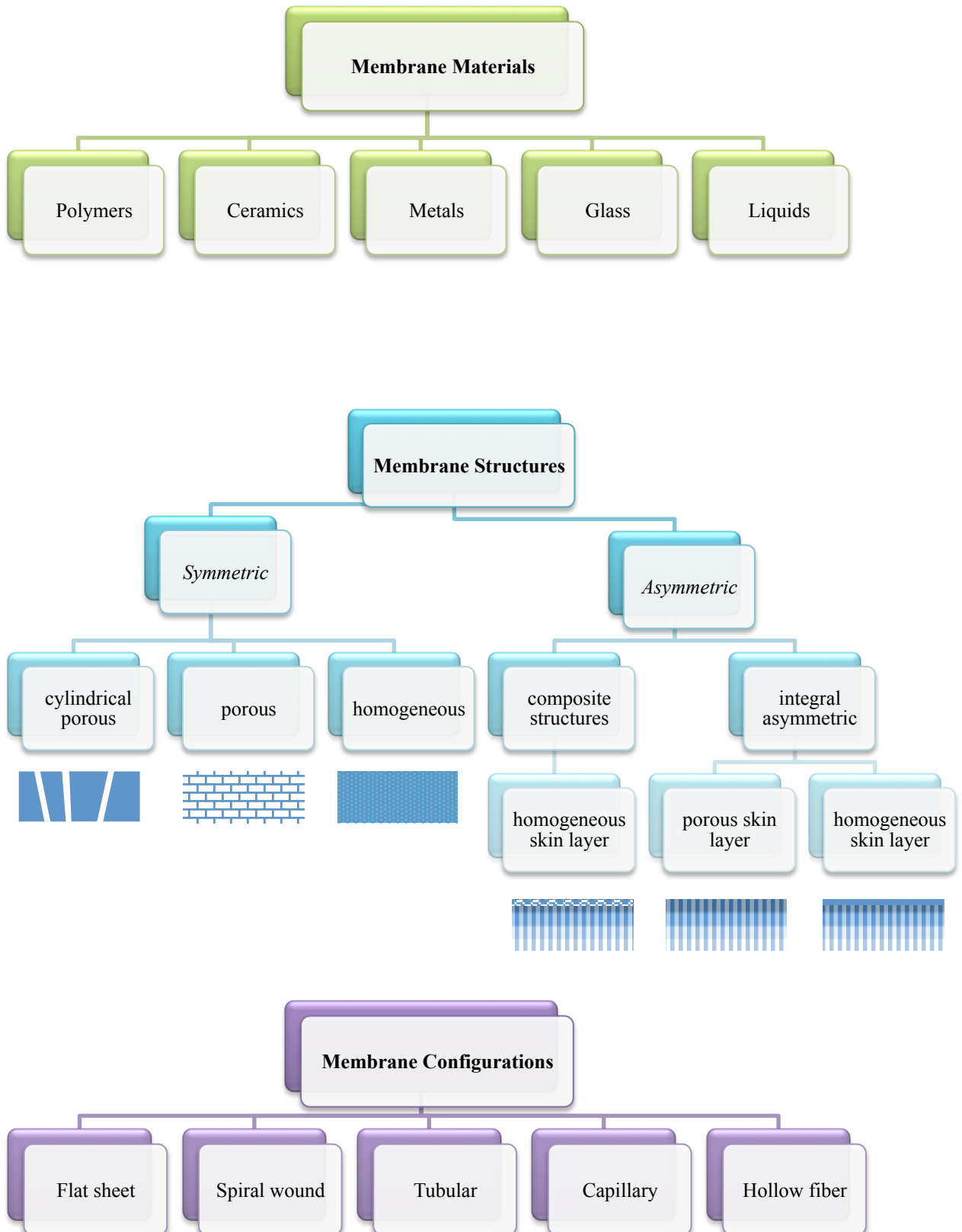
Figure 2.2 Schematic representation of various materials, structures and configurations of synthetic membranes

13

μm) supports a thin, dense skin layer having a thickness between 0.1 to 1μm [1,2]. This thin and dense skin layer acts as main selective membrane. In this manner, membrane material and the pore structure of the skin layer controls the separation characteristics of the membrane. Although the selectivity of membrane strongly depends on the material nature and pore structure of the skin layer, the thickness of this skin layer changes the mass transport rate remarkably. Also, the porous support layer may have a slight effect on the flux and selectivity of membrane; its key role is to enhance mechanical strength by supporting the fragile skin layer. Due to their morphology, asymmetric membranes provide superior properties within high flux (thin membrane), high permeability (dense membrane) and good mechanical strength (thick support layer). Asymmetric membranes are used today mainly in ultrafiltration, nanofiltration, reverse osmosis, gas and vapor separation [1,2].

Taking into consideration that the term "membrane" covers a diverse group of materials, configurations and structures, it may be more precise to define a membrane with respect to its functional properties. All materials functioning as membranes have one characteristic property in common: They restrict the passage of predefined components in a very specific manner [2].

2.1.2 Membrane Processes

Separation mechanism in membranes mainly regulated by membrane structure are dominated by different processes .The defining feature of membranes which is restricting the transport of certain components, plays a major role in separation processes as acting as selective layer. Due to the gradient in chemical and/or physical properties/potential of between the membrane and components, the membrane will transport one component more willingly. As a result of an acting driving force on the components, the transport takes place. In general, the relation between the driving force and the permeation rate can be explained by the proportionality between the flux (J) and the driving force by [1]

$$J = -A \frac{dX}{dx} \tag{2.1}$$

14

where A is the phenomenological coefficient and dX/dx is the driving force as in Eq. 2.1. The driving force is stated as a gradient of X, which can be concentration, temperature, pressure or any quantity along perpendicular coordinate to the transport barrier (x) [1]. Table 2.1. summarizes the phenomenological equations in this field. Membrane processes can be classified according to nature and magnitude of applied driving forces and the size of components, as shown in Table 2.2. In addition to driving force, material and structure of membrane have effect on the separation processes. The nature of the membrane selective layer plays a major role in the selectivity properties whereas thickness and the pore structure of the cross-section of the membrane will influence the flux performance. As an example, when there is a need to retain particle larger than 200 nm, membrane with an open structure will be a possible choice. Even relatively small driving forces will be enough to obtain high fluxes due to the low hydrodynamic resistance of these microfiltration membranes. Moving from microfiltration to reverse osmosis, higher driving forces will be required due to the high hydrodynamic resistance raised from the dense asymmetric structure of the membrane. As the membrane becomes denser, it will have a higher capability to retain smaller components. However, the flux through the membrane will decrease.

Table 2.1 Phenomenological equations [1]

Mass flux	$J_m = -D \, (dc/dx)$	(Fick's Law)
Volume flux	$J_v = -L_p \, (dP/dx)$	(Darcy's Law)
Heat flux	$J_h = -a \, (dT/dx)$	(Fourier's Law)
Momentum flux	$J_n = -\upsilon \, (dv/dx)$	(Newton's Law)
Electrical flux	$J_i = -1/R \, (dE/dx)$	(Ohm's Law)

Table 2.2 Relation between membrane processes and driving forces [1,4]

Membrane Process	Phase1/Phase 2	Driving Force	Size of materials retained
Microfiltration	L/L	Pressure difference, ΔP (0.1-2 bar)	0.1 - 10 μm microparticles
Ultrafiltration	L/L	Pressure difference, ΔP (1-5 bar)	1 - 100 nm macromolecules
Nanofiltration	L/L	Pressure difference, ΔP (3-30 bar)	0.5 - 5 nm molecules
Reverse Osmosis	L/L	Pressure difference, ΔP (1 - 100 bar)	< 1 nm molecules
Gas separation	G/G	Pressure difference, ΔP (1 - 100 bar)	< 1 nm molecules
Dialysis	L/L	Concentration difference, Δc	< 1 nm molecules
Osmosis	L/L	Concentration difference, ΔC	< 1 nm molecules
Pervaporation	L/G	Vapor pressure difference, Δp	< 1 nm molecules
Electrodialysis	L/L	Electrical potential difference, Δp	< 1 nm molecules
Thermo-osmosis	L/L	Partial pressure difference, ΔT/Δp	< 1 nm molecules
Membrane distillation	L/L	Partial pressure difference, ΔT/Δp	< 1 nm molecules

Table 2.3 Applications and Alternative Separation Processes [1,2,4]

Process	Applications	Alternative Processes
Microfiltration	Separation of bacteria and cells from solutions	Sedimentation, Centrifugation
Ultrafiltration	Separation of proteins and virus, concentration of oil-in-water emulsions	Centrifugation
Nanofiltration	Separation of dye and sugar, water softening	Distillation, Evaporation
Reverse Osmosis	Desalination of sea and brackish water, process water purification	Distillation, Evaporation, Dialysis
Dialysis	Purification of blood (artificial kidney)	Reverse osmosis
Electrodialysis	Separation of electrolytes from nonelectrolytes	Crystallization, Precipitation
Pervaporation	Dehydration of ethanol and organic solvents	Distillation
Gas Permeation	Hydrogen recovery from process gas streams, dehydration and separation of air	Absorption, Adsorption, Condensation
Membrane Distillation	Water purification and desalination	Distillation

2.1.3 Membrane Preperation

2.1.3.1 Synthetic Membrane Preperation

The selection of membrane properties (structure, nature, material, configuration) plays the most important role in manipulation of membrane separation processes. For this reason, it is very critical to prepare the proper membrane for exact membrane process. The basic principle in membrane preparation is to modify the material to obtain a membrane structure with morphology suitable for a specific membrane separation process by the appropriate preparation technique [1]. Since we will just focus on production of the synthetic membranes, important techniques such as sintering coating, stretching, track-etching, phase inversion and their applications are listed in

Table 2.4 [1,2,5]. Table 2.4 shows that asymmetric membranes can be prepared by two main techniques;

1) Utilization of the *phase inversion* process leading to an integral structure with the skin and the support structure made from the same material in a single process [6],

2) Construction of a *composite membrane* where a thin barrier layer is deposited on a microporous substructure that are generally made from different materials in a two step process [7].

In this work, phase inversion technique is preferred to produce asymmetric porous membranes made from a single material by simply tuning their pore sizes.

Table 2.4 Membrane preparation techniques and their applications [1,2,5]

Membrane Preparation Technique	Membrane Material	Types of Membranes	Application
Sintering	Ceramic, metal, polymer, graphite	Symmetric porous membranes (pore size = 0.1-20 μm)	Microfiltration
Stretching	Partially crystalline polymer	Symmetric porous membranes (pore size = 0.1-5 μm)	Microfiltration
Track-etching	Polymer	Symmetric porous membranes (pore size = 0.02-10 μm)	Microfiltration
Template leaching	Glass, polymer, ceramic, metal	Symmetric porous membranes (pore size = 0.5-10 μm)	Microfiltration
Coating	Polymer, glass, ceramic, metal	Composite membranes	Nanofiltration, gas separation, reverse osmosis, pervaporation
Phase inversion	Polymer	Symmetric/asymmetric Porous/nonporous	Microfiltration, ultrafiltration, nanofiltration, gas separation, reverse osmosis, pervaporation

2.1.3.2 Phase Inversion

Phase inversion technique is utilized to manufacture most of the commercial membranes since it is versatile to form almost all possible kind of membrane morphologies. Although phase inversion method can be applied to obtain symmetric membranes, it is mostly popular for preparing asymmetric membranes that are leading the membrane industry. The development of the first integral asymmetric membranes in 60's by phase inversion was a major breakthrough in the development of ultrafiltration and reverse osmosis [2]. Loeb and Sourirajan made these porous asymmetric cellulose acetate membranes that performed with fluxes 10 to 100 times higher than symmetric structures with comparable separation characteristics [8,9].

Phase inversion is a technique where polymer transformation from a liquid to a solid state occurs in a controlled manner. Almost all polymers that are soluble in an appropriate solvent/solvent mixture at a certain temperature can be used to prepare asymmetric phase inversion membranes if they are capable to precipitate as a solid phase. During phase inversion, demixing of liquid phases (transition of one liquid state to two liquid state) initiates the solidification process. The solidification of polymer rich phase will form solid matrix in the membrane. The availability of modifying pore structure of the resulting membrane by controlling the initial step of phase transition is quite important.

The phase inversion processes start with the formation of cast film solution consisting of polymer and solvent/solvent mixture. However, they differ depending on the parameters that induce liquid-liquid demixing. Types of the phase inversion methods can be listed as [1,2];

- Precipitation by solvent evaporation,
- Precipitation from the vapor phase,
- Precipitation by controlled evaporation,
- Thermal precipitation,
- Immersion precipitation.

The most common technique used in industry is the immersion precipitation. In this technique, the polymer-solvent film is cast on a support, which is quenched in a coagulation bath containing a non-solvent. Exchange of the solvent and non-solvent will lead to the precipitation, which will form the membrane later. Predominantly immersion precipitation method is combined with other isothermal phase inversion techniques (i.e. solvent evaporation, precipitation from the vapor phase) to achieve the desired membrane properties. One example of this combination is known as the dry–wet phase inversion technique, also called the Loeb-Sourirajan technique [8,9]. In this method, after casting the polymer/solvent solution on a support, cast polymer solution is exposed to partial evaporation of the solvent and then the cast film is immersed in a non-solvent coagulation bath. In this case, formation of membrane occurs in two steps [10]. In the first step, desolvation forms a thin skin layer on the top of the cast polymer solution. In the second step, when cast film is immersed in coagulation bath diffusion of non-solvent particles through the thin skin will take place while solvent particles will be diffusing out. This exchange will create the pores of polymer membrane.

On the other hand, thermal precipitation, also called temperature induced phase separation (TIPS), is the technique where temperature of polymer solution is systematically lowered in order to induce demixing. TIPS is generally preferred to produce microfiltration membranes.

2.2 Experimental Procedure

2.2.1 Materials

Modified polyether ether ketone (PEEK-WC), shown in Figure 2.3, was supplied from Chanchung Institute of Applied Chemistry, Academia Sinica. N,N-dimethylacetamide (DMA) was purchased from Carlo Erba and used without further purification. Rose Bengal (Sigma-Aldrich, Dye content 95%), Bromothymol blue

(Sigma-Aldrich, Dye content 95%), Methyl orange (Sigma-Aldrich, Dye content 85%), and Methylene blue solution (Sigma-Aldrich, 0.05 wt.% in H_2O) were used without further purification for retention tests to estimate the molecular weight cut-off of the PEEK-WC membranes. Molecular structures, molecular weights (MW) and absorption wavelengths of these dye compounds are listed in Table 2.5. Distilled water was used for coagulation bath whereas ultra pure water was used for the flux and the retention tests.

Table 2.5 Organic Dye Compounds [11]

Molecule	Molecular Weight (g/mol)	Maximum Absorption (λ_{max})	Molecular Structure
Methylene blue	320	663 nm	
Methyl orange	327	505 nm	
Bromothymol blue	624	392 nm, 615 nm	
Rose Bengal	1017	549 nm	
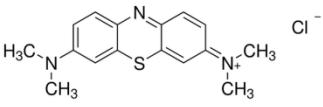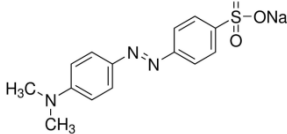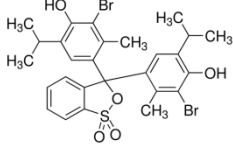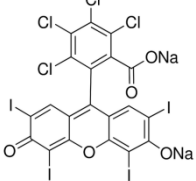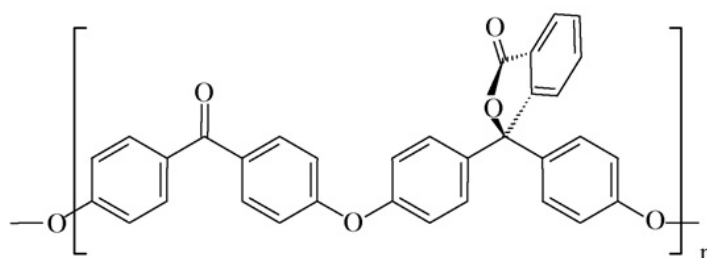
Figure 2.3 Chemical structure of PEEK-WC [12,13]

2.2.2 Membrane Preperation

PEEK-WC was dissolved in DMA to a concentration of 15 wt.% at room temperature (RT). The polymer solution was stirred overnight until PEEK-WC was completely dissolved in DMA. After stirring, the solution was kept under steady state in order to avoid the formation of bubbles in solution that will cause defects in the membrane. The flat membranes were prepared by casting polymeric solution on glass substrate by usage of hand casting knife (BRAIVE instruments) having a gap set arranged to 250 μm (Figure 2.4). Studies on phase inversion techniques indicated that aprotic solvents such as DMA form asymmetric membranes with porous skin that are generally formed upon coagulation in water. However, contact of cast polymer membrane with air before coagulation bath results in formation of sponge-like structure and elimination of the micro-voids [12]. So, the cast polymeric solutions were immediately immersed in coagulation bath after exposure for a fixed time to the air (0 to 120 min.) in order to obtain porous as well as sponge-like dense skin of membrane depending on the contact time with air. The membrane films turned from transparent to opaque in coagulation bath. Membranes were kept at refreshed coagulation bath until all the solvent was removed. Besides evaporation time, the effects of temperature and coagulation bath on the performance of PEEK-WC membranes were investigated. For this reason, the cast membranes were exposed to air for various time at RT and 45°C and then directly immersed to two different of coagulation baths; water and isopropanol (IPA). The operation conditions for PEEK-WC membranes are reported in Table 2.6.
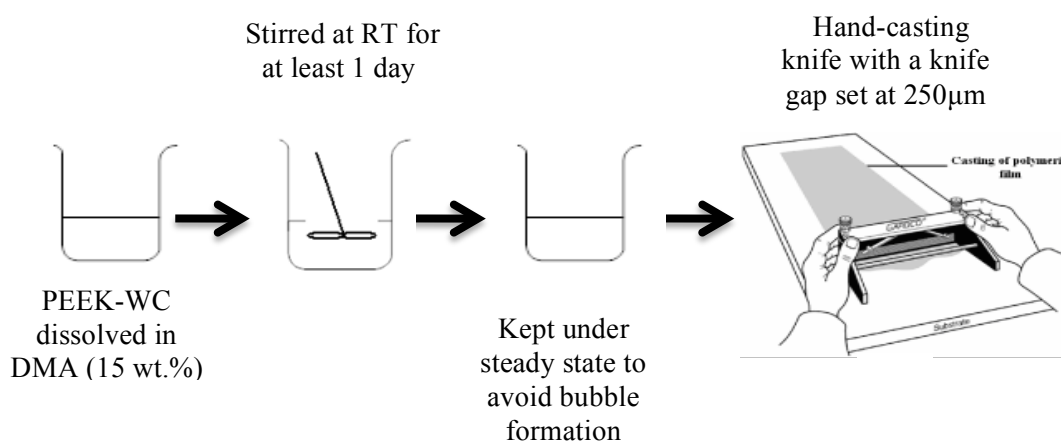
Figure 2.4 Experimental procedure

Table 2.6 Membrane preperation parameters

Membrane	Evaporation Time (min)	Temperature (°C)	Coagulation Bath
DW-0	0	RT	Water
DW-1	1	RT	Water
DW-2	2	RT	Water
DW-5	5	RT	Water
DW-10	10	RT	Water
DW-20	20	RT	Water
DW-40	40	RT	Water
DW-60	60	RT	Water
DW-120	120	RT	Water
DW-5-45	5	45	Water
DW-10-45	10	45	Water
DW-15-45	15	45	Water
DW-20-45	20	45	Water
DW-40-45	40	45	Water
DIPA-0	0	RT	IPA
DIPA-10	10	RT	IPA
DIPA-15	15	RT	IPA
DIPA-20	20	RT	IPA

2.2.3 Membrane Characterization

The morphology of the membranes was examined using scanning electron microscope (SEM, Cambridge Zeiss LEO 400). Cross-sections were prepared by freeze-fracturing each sample in liquid nitrogen in order to have a sharp fracture without modifications of the morphology. In addition to the cross-sections, the "air" and the "glass" sides for each membrane were observed.

The effect of evaporation time was determined by the water flux measurements using both ultrafiltration and nanofiltration cells, shown in Figure 2.5. The permeate flux (J_w) is the ratio of the permeate flow rate to membrane area [1];

$$J = \frac{Permeate\ flow\ rate}{Membrane\ area}$$

(2.2)

The permeance was determined as slope of the linear fitting through the axes origin of the permeating flux as a function of the applied transmembrane pressure (TMP) [1].

The molecular weight cut-off of the membranes was estimated by rejection experiments carried out by filtering of 10 ppm of aqueous solutions of four colorants; methylene blue (310 g/mol), methyl orange (327 g/mol), bromothymol blue (680 g/mol), and rose bengal (1017 g/mol). The retention was calculated by equation [1,2],

$$R(\%) = \left(1 - \frac{C_p}{C_f}\right) \times 100$$

(2.3)

where R is the rejection and C_p and C_f are the concentrations of dye compounds in the permeate and feed solutions, respectively. An UV spectrophotometer (Perkin Elmer Lambda EZ 201), shown in Figure 2.6, was used to analyze the concentration of dye components [12,13].
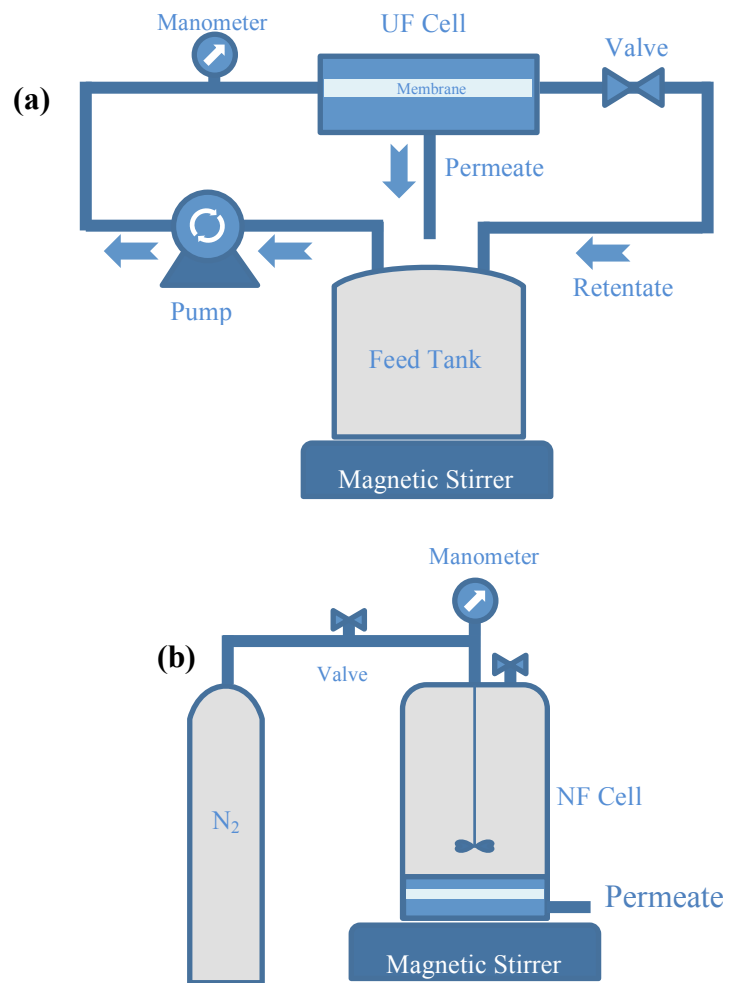
Figure 2.5 Scheme of experimental **a)** ultrafiltration and **b)** nanofiltration set-ups

Figure 2.6 Perkin Elmer lambda EZ 201Spectrometer

2.3 Results and Discussion

2.3.1 Effect of evaporation time

In this part of the work, the influence of evaporation time on the membrane morphology and water permeance was investigated. The evaporation time is known to have an effect on membrane structure [14].

SEM images of PEEK-WC membranes prepared by wet and dry-wet phase inversion technique are shown on the Figure 2.7-2.11. SEM analyses showed that as the membranes exposed to shorter evaporation time, they tend to have a porous asymmetric structure. On the other hand, the membranes prepared with longer evaporation time (5 and 10 min) exhibited denser structure. SEM analyses demonstrated that membranes DW-0, DW-1 and DW-2 have a finger-like macro-void structure across their cross-section. On the other hand, membranes that were exposed to longer evaporation time showed a sponge-like structure with a very fine interconnected pore structure across their cross-section. The cross-section of the membranes, DW-5 and DW-10, also demonstrated the formation of a dense skin layer on the side exposed to the air (Figures 2.10 and 2.11). The cross-section images of all membranes showed a uniform structure along the thickness. SEM analyses showed that as the membranes exposed to shorter evaporation time, they tend to have thicker cross-section.
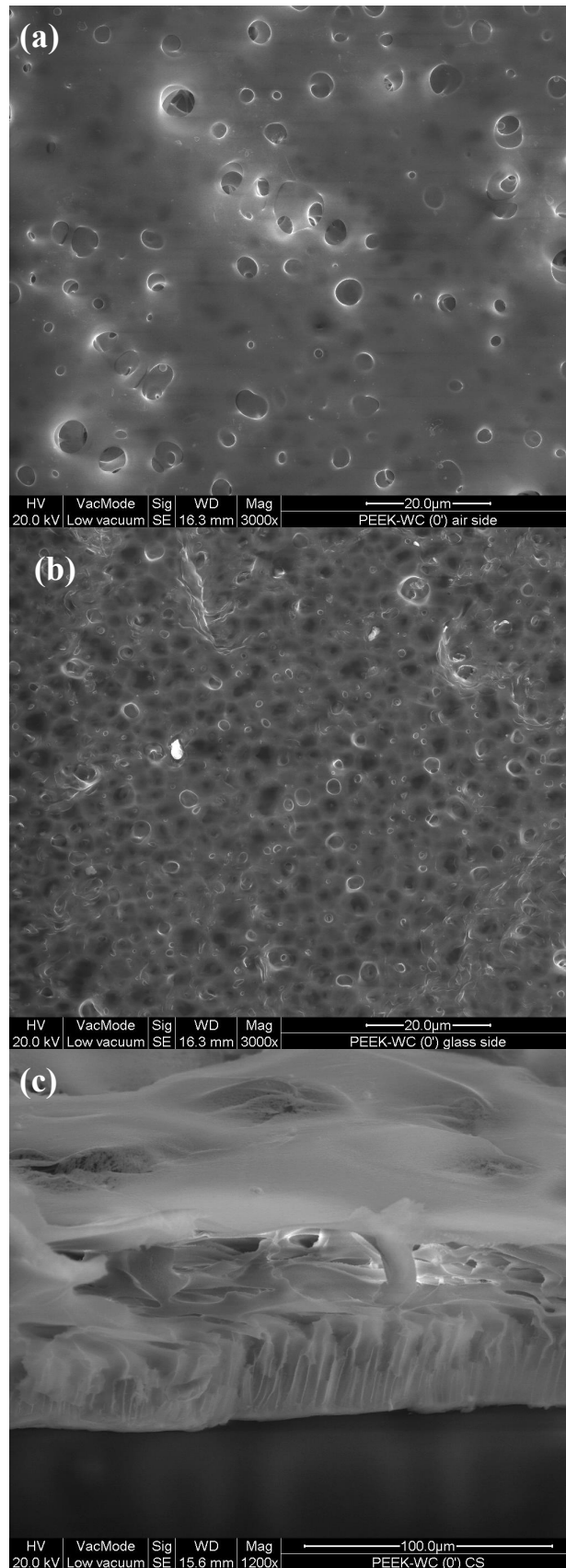
Figure 2.7 SEM micrographs of (a) "air" side, (b) "glass" side, (c) cross-section of membrane prepared by 0 min evaporation time
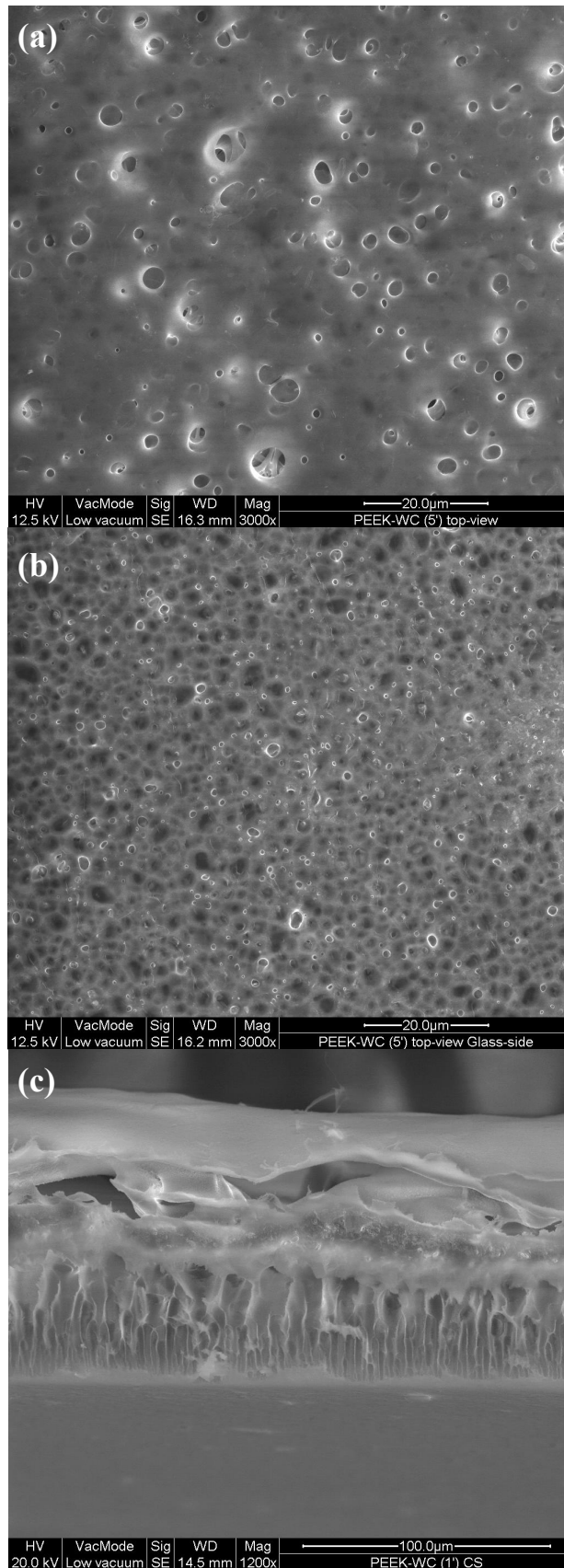
Figure 2.8 SEM micrographs of (a) "air" side, (b) "glass" side, (c) cross-section of membrane prepared by 1 min evaporation time.
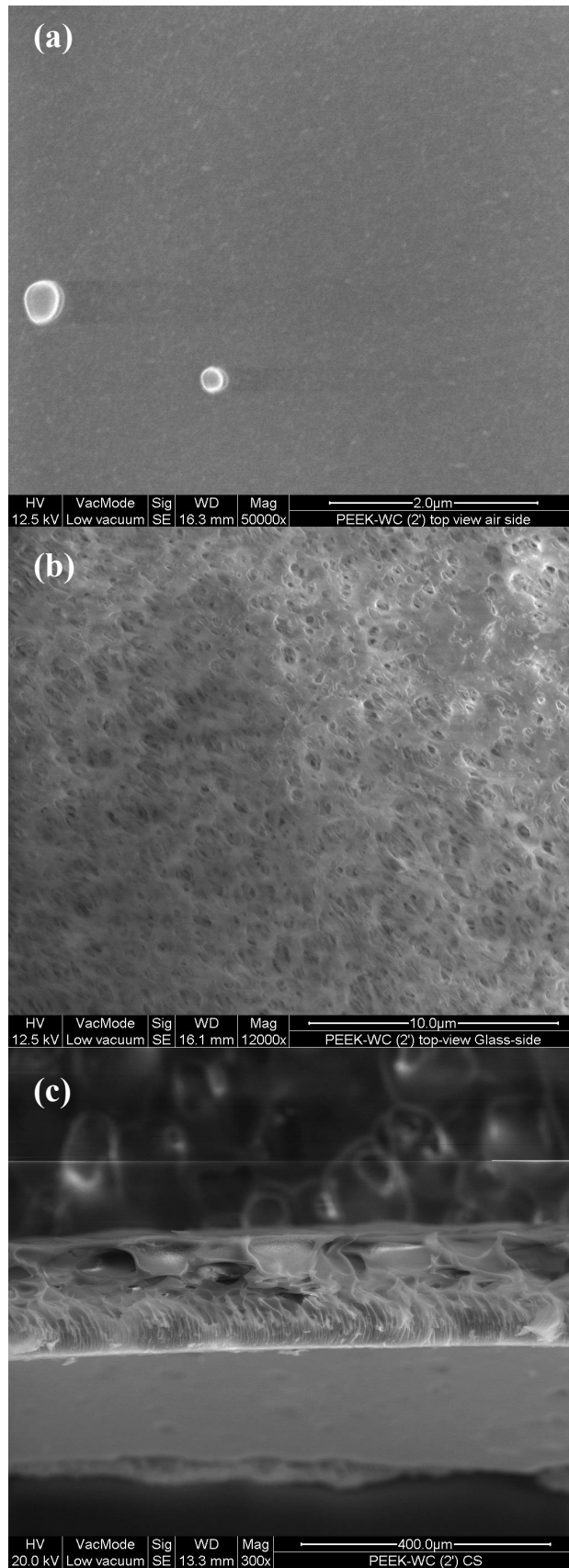
Figure 2.9 SEM micrographs of (a) "air" side, (b) "glass" side, (c)-(d) cross-section of membrane prepared by 2 min evaporation time.

(a)

HV	VacMode	Sig	WD	Mag	
12.5 kV	Low vacuum	SE	16.3 mm	50000x	2.0µm — PEEK-WC (1') top-view air side

(b)

HV	VacMode	Sig	WD	Mag	
12.5 kV	Low vacuum	SE	16.4 mm	12000x	10.0µm — PEEK-WC (1') top view glass side

(c)

HV	VacMode	Sig	WD	Mag	
15.0 kV	Low vacuum	SE	13.2 mm	1500x	50.0µm — PEEK-WC (5') CS
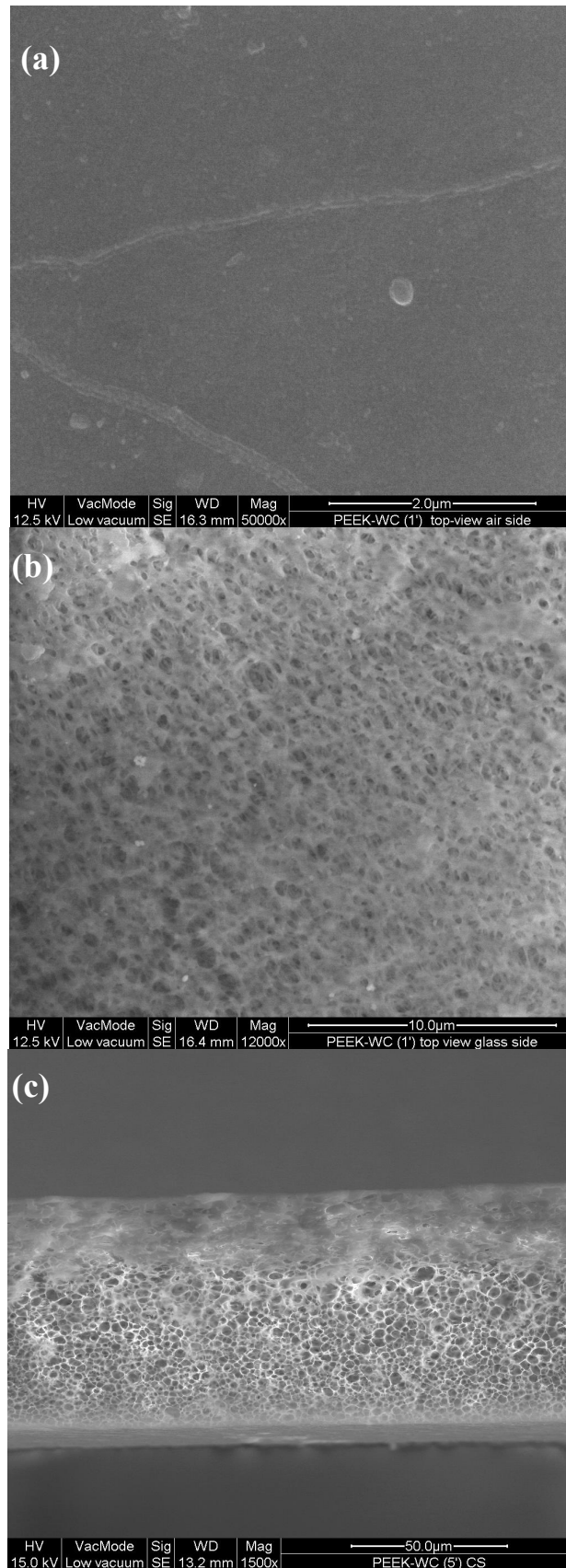
Figure 2.10 SEM micrographs of (a) "air" side, (b) "glass" side, (c) cross-section of membrane prepared by 5 min evaporation time.

30
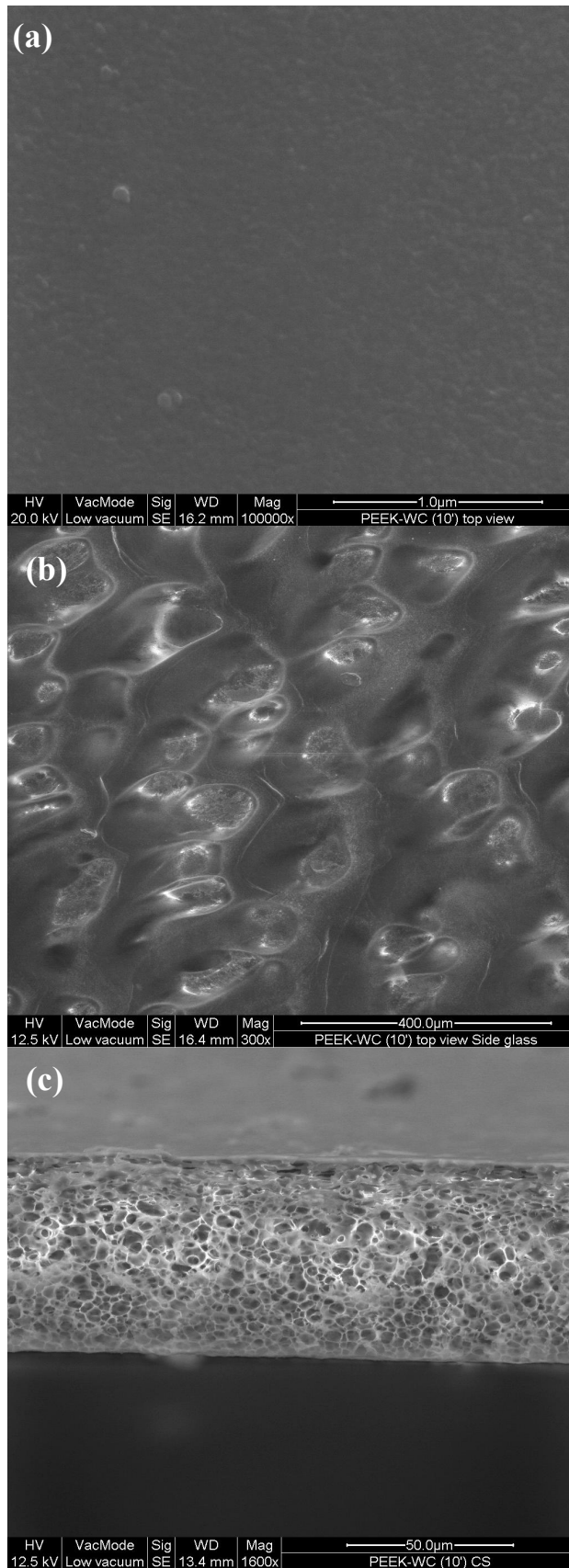
Figure 2.11 SEM micrographs of (a) "air" side, (b) "glass" side, (c) cross-section of membrane prepared by 10 min evaporation time.

The permeability of PEEK-WC membranes was analyzed by water flux measurements. The average water permeances of each membrane are summarized in Table 2.7. The membranes were tested at least three times in order to check the reproducibility and consistency of the membranes prepared under same operation conditions. The error bars denote the standard deviation derived from at least three measurements. It is observed that as the evaporation time of the membrane was increased the flow rate of permeate was decreasing. This expected result indicated that as the evaporation time was increased, PEEK-WC membranes became denser. Figure 2.12 shows the effect of evaporation time on DW membranes that were cast at room temperature and immersed in water as coagulant bath. The evaporation time had remarkable effect on the hydraulic permeance values of DW membranes. As evaporation time increased from 0 to 120 min, hydraulic permeance decreased from 406.4 to 5.8 l/h·m^2·bar. The DW membranes formed after evaporation time of 0-10 minutes were ultrafiltration membranes whereas the membranes formed after 10 minutes of evaporation were in the nanofiltration range.
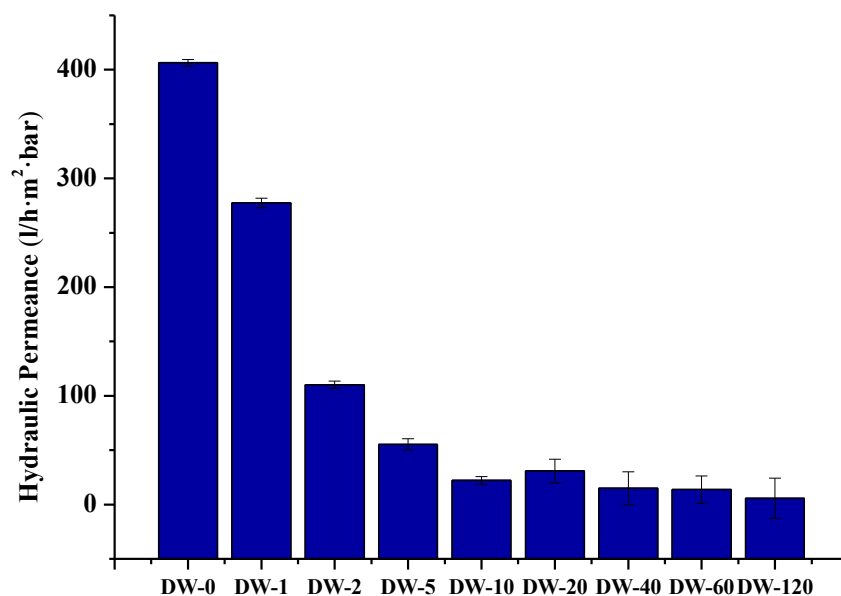
Figure 2.12 Hydraulic permeance of DW membranes with respect to evaporation time

The effect of evaporation time on DW-45 membranes as shown in Figure 2.13 was more distinguished compared to other DW membranes. The only difference in casting DW and DW-45 membranes was applied temperature. At higher temperatures (45°C) membranes tend to be affected more from air exposure, prior to the immersion into the coagulation bath. The DW-45 membranes performed as ultrafiltration membranes having an average permeance of 104 L bar^{-1} h^{-1} m^{-2} when they were exposed to air for 2 min. As the cast membranes were exposed to air for longer time (40 min) at 45°C, they had a more dense structure resulting membranes to operate at nanofiltration processes having an average hydraulic permeance of 5.8 L bar^{-1} h^{-1} m^{-2}.
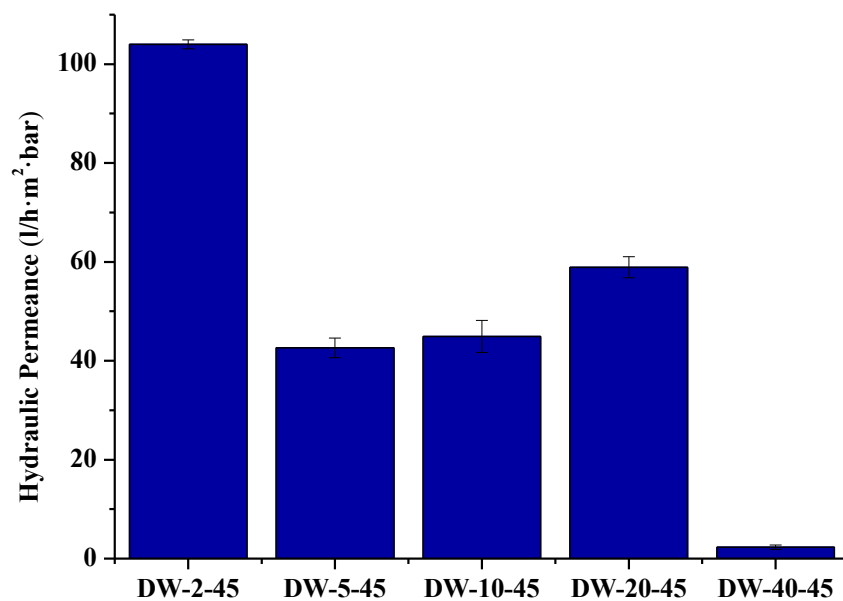
Figure 2.13 Hydraulic permeance of DW-45 membranes with respect to evaporation time

Table 2.7 Permeance and flux of PEEK-WC membranes

Membrane	Evaporation Time (min)	Temperature (°C)	Coagulation Bath	Hydraulic Permeance (L/h·m²·bar)
DW-0	0	RT	Water	406.4
DW-1	1	RT	Water	277.5
DW-2	2	RT	Water	110.2
DW-5	5	RT	Water	55.3
DW-10	10	RT	Water	22.3
DW-20	20	RT	Water	30.8
DW-40	40	RT	Water	14.9
DW-60	60	RT	Water	13.7
DW-120	120	RT	Water	5.8
DW-2-45	2	45	Water	104.0
DW-5-45	5	45	Water	42.6
DW-10-45	10	45	Water	44.9
DW-20-45	20	45	Water	58.9
DW-40-45	40	45	Water	2.3
DIPA-0	0	RT	IPA	1.8
DIPA-10	10	RT	IPA	1.7
DIPA-15	15	RT	IPA	0.9
DIPA-20	20	RT	IPA	1.1
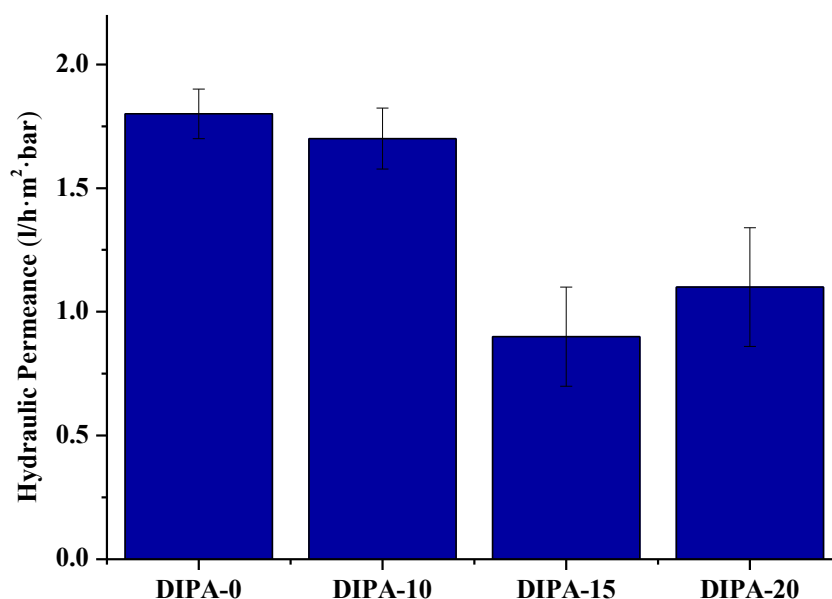
Figure 2.14 Hydraulic permeance of DIPA membranes with respect to evaporation time

When it comes to DIPA membranes, the effect of IPA played the major role in the water flux properties of the membranes, which will be explained in detail in the following section. Since a dense asymmetric structure of the DIPA membranes was formed due to slow demixing in IPA bath, they tend to be affected slightly from the evaporation time (Figure 2.14). The error bars in Figure 2.14 denote the standard deviation derived from at least three measurements. All DIPA membranes were operating at nanofiltration range, which is operating at higher pressures of 3-30 bar [1-4]. As the evaporation time was increased from 0 to 20 min, average hydraulic permeance of membranes decreased from 1.8 to 1.1 L bar^{-1} h^{-1} m^{-2}.

The ultra-pure water flux versus pressure graphs for some of the membranes are illustrated in Figures 2.15-23. Also, the membranes were tested at least three times in order to check the reproducibility and consistency of the membranes prepared under same operation conditions.
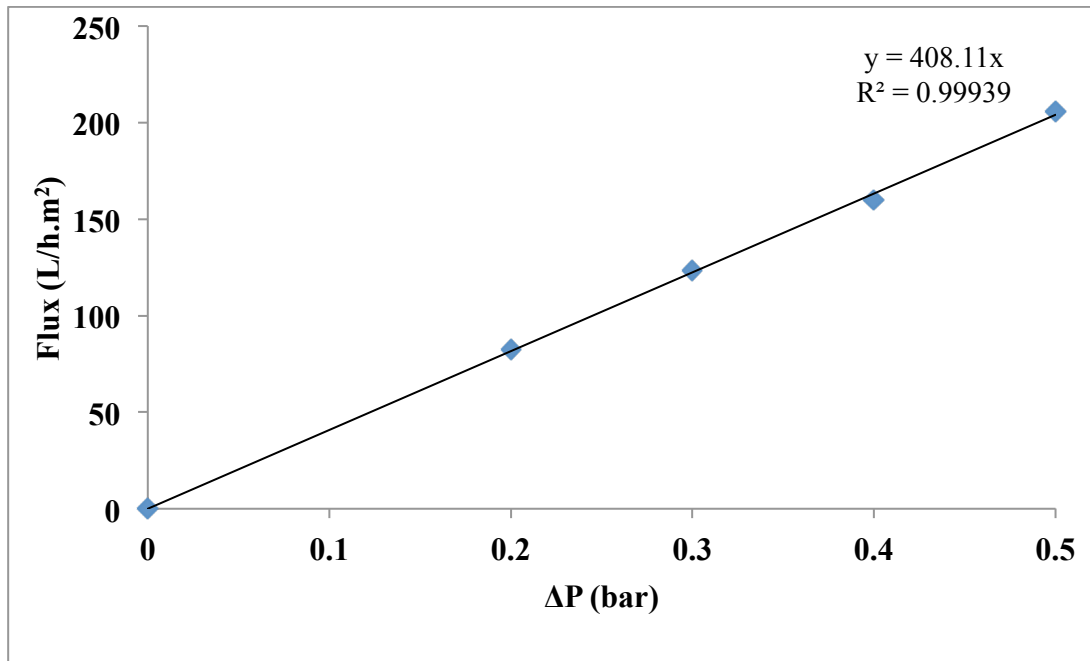
Figure 2.15 Flux vs ΔP curve of DW-0
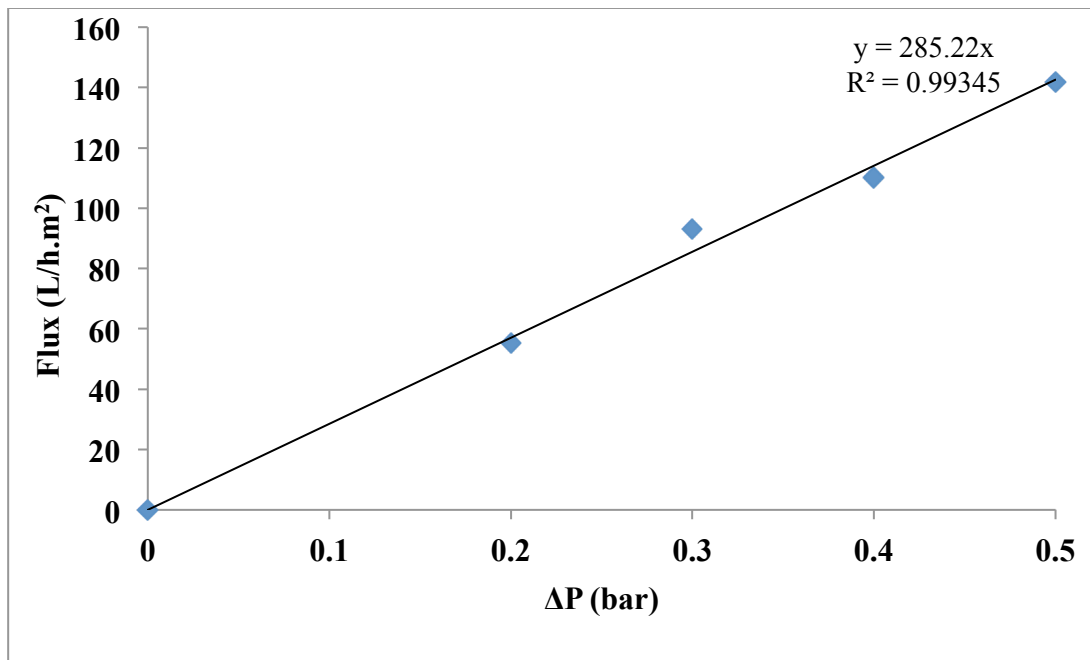
Figure 2.16 Flux vs ΔP curve of DW-1
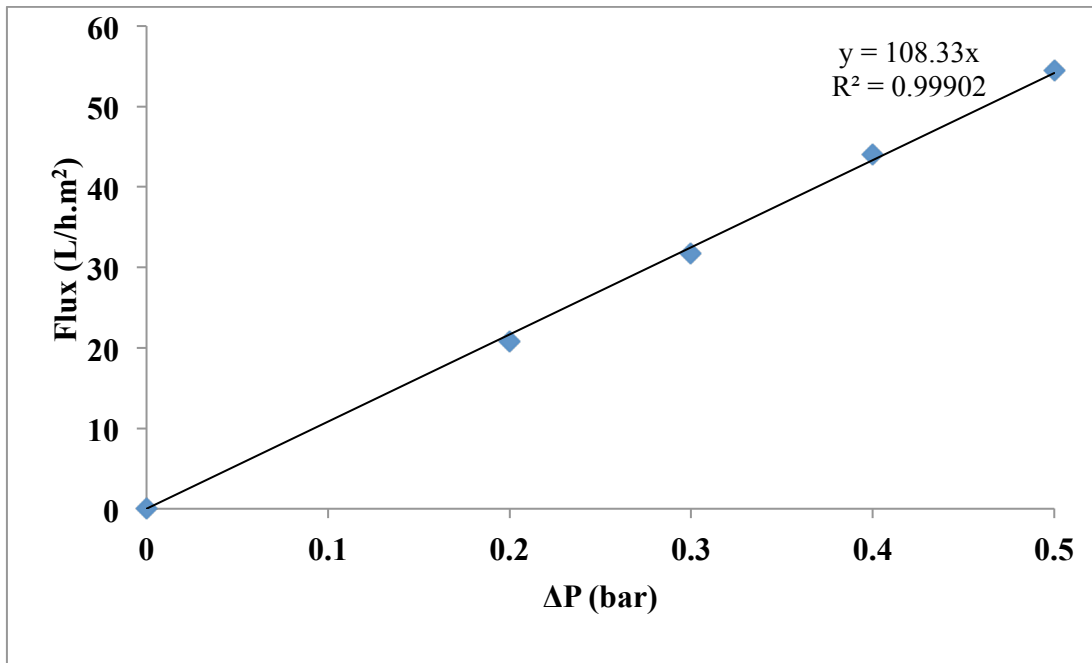
Figure 2.17 Flux vs ΔP curve of DW-2
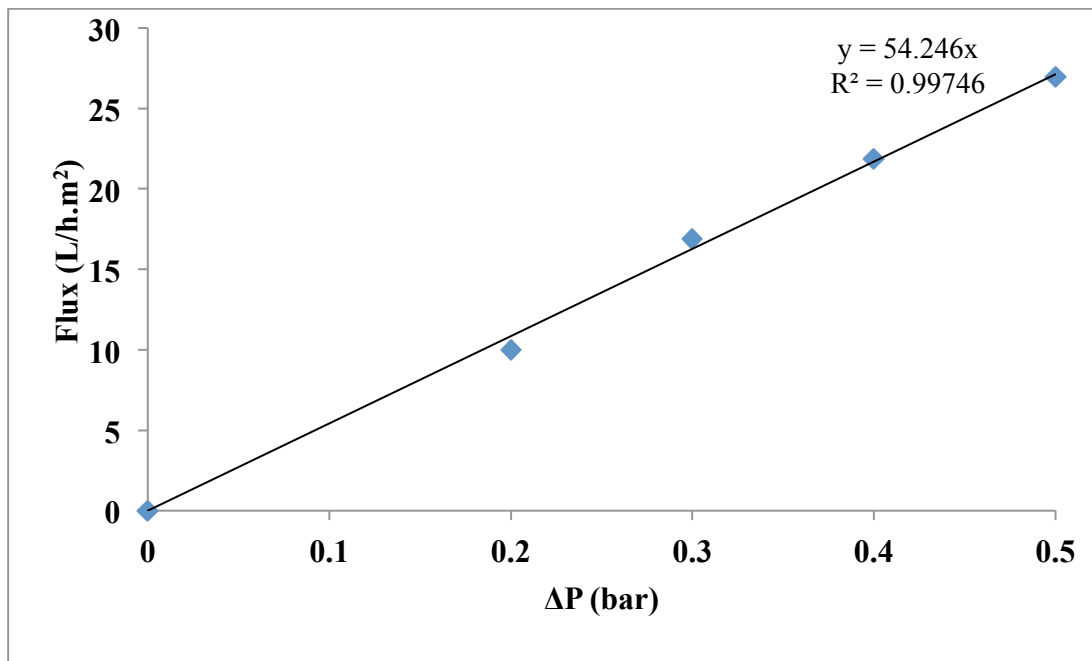
Figure 2.18 Flux vs ΔP curve of DW-5
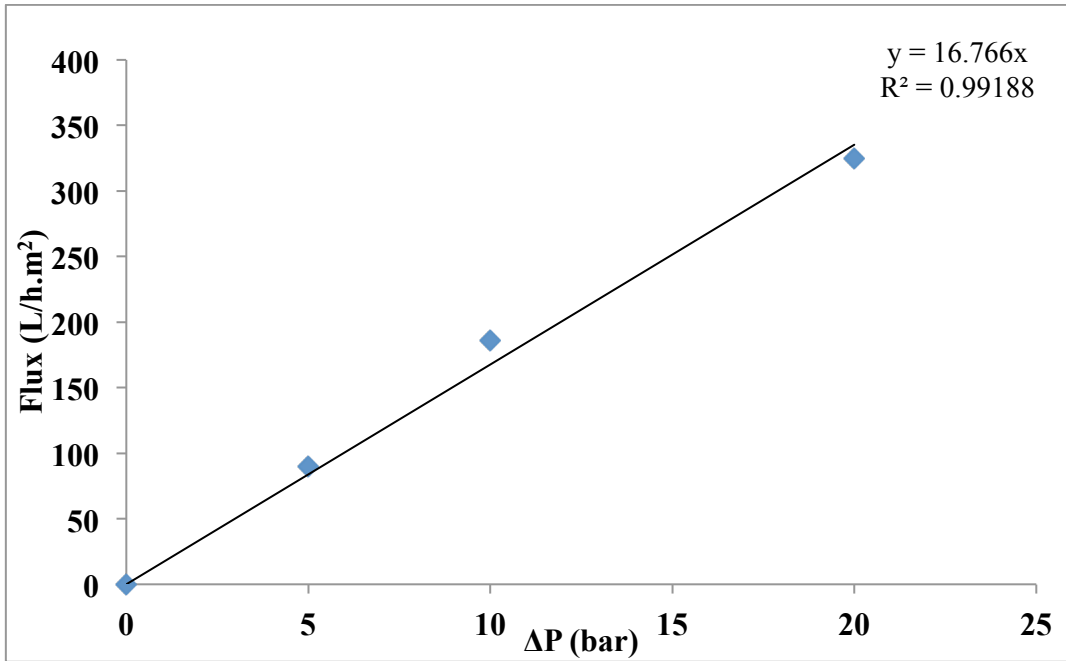
Figure 2.19 Flux vs ΔP curve of DW-60
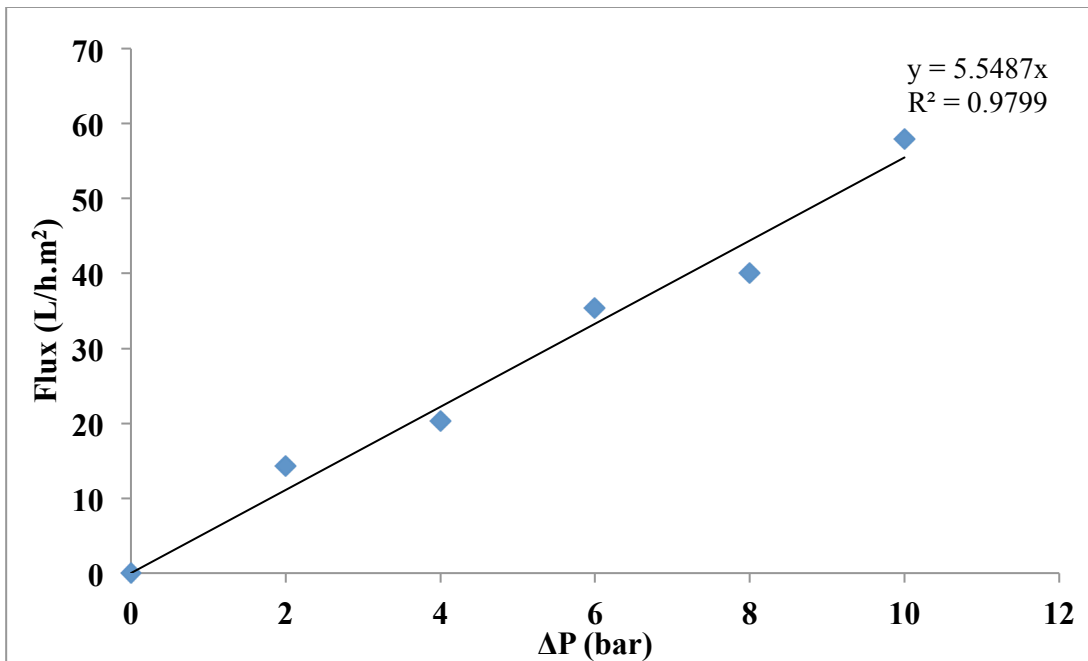
Figure 2.20 Flux vs ΔP curve of DW-120
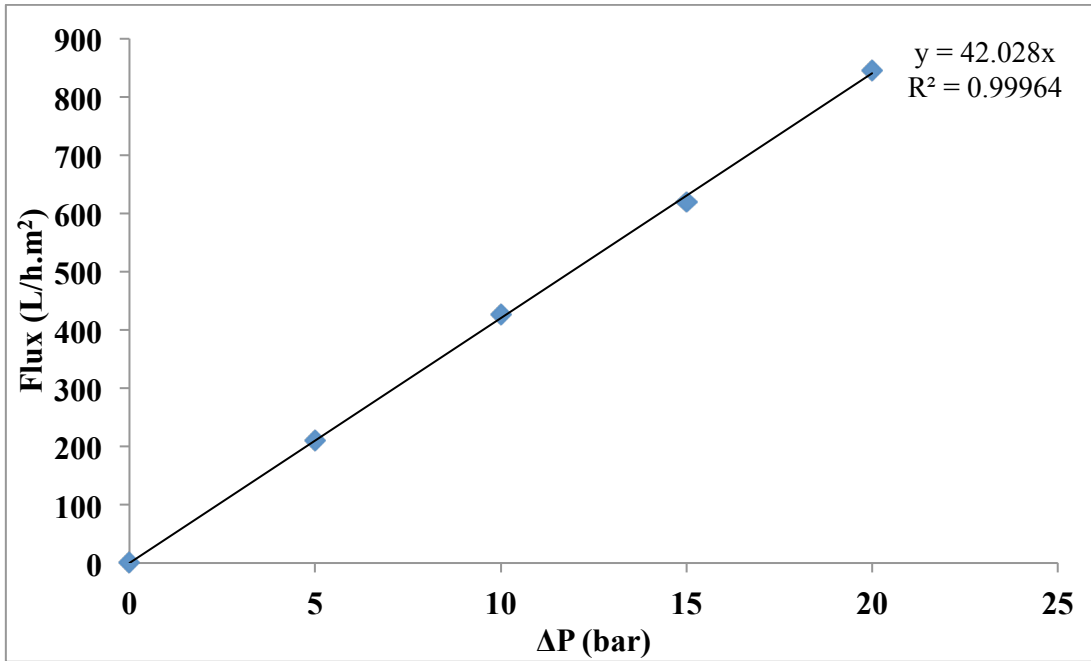
Figure 2.21 Flux vs ΔP curve of DW-10-45
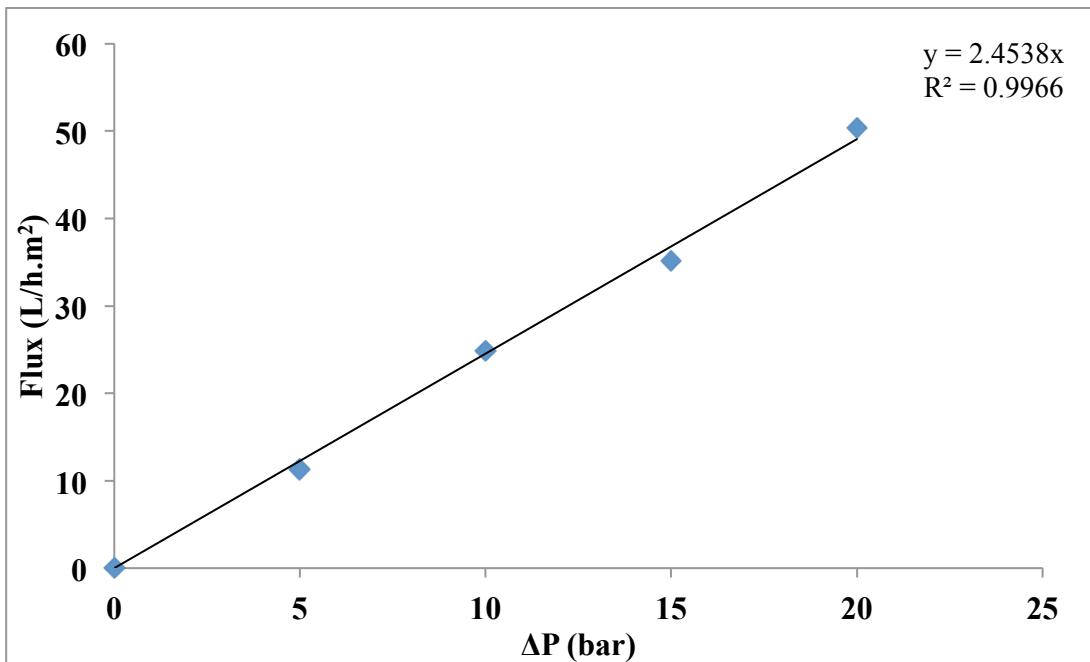
Figure 2.22 Flux vs ΔP curve of DW-40-45
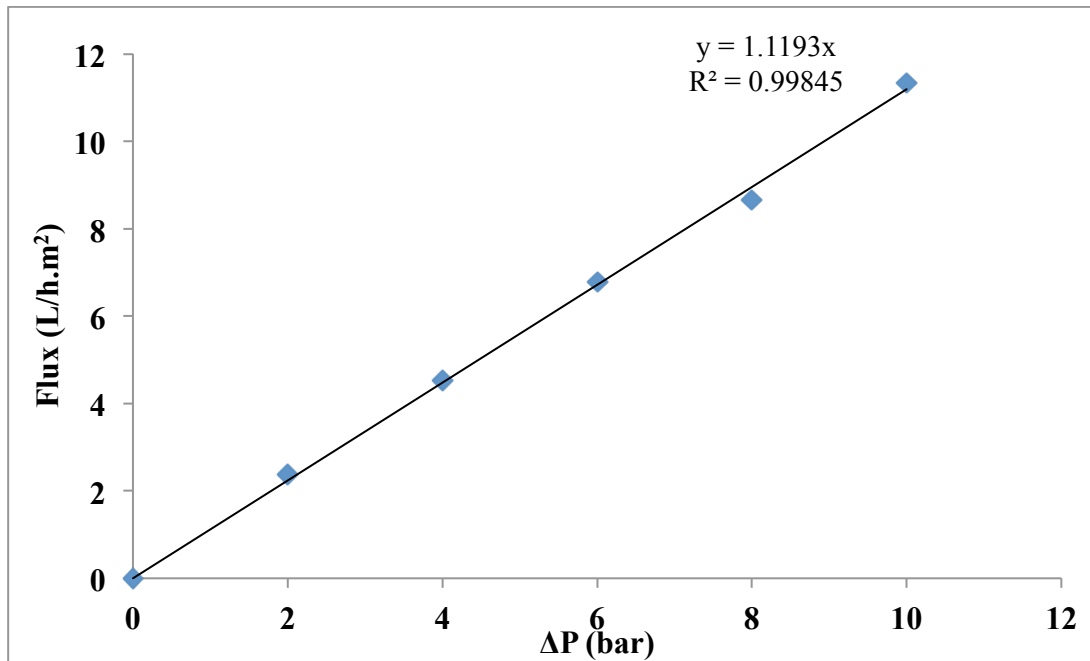
Figure 2.23 Flux vs ΔP curve of DW-10-45

2.3.2 Effect of evaporation temperature

Temperature was the second parameter that was adjusted during membrane casting, in order to investigate its effect on water permeabilities of the membranes. Figure 2.24 represents the effect of temperature on membranes produced with evaporation times of 2, 5 and 40 minutes both at room temperature and at 45°C. As the temperature increased, hydraulic water permeances of DW-45 membranes decreased. This expected fact is due to simple kinetics of increased rate of DMA (solvent) desolvation at 45°C [1,12,13]. When the temperature was increased at evaporation step, higher amount of DMA evaporated and as a result a denser skin layer was formed on the top of the cast polymer solution.
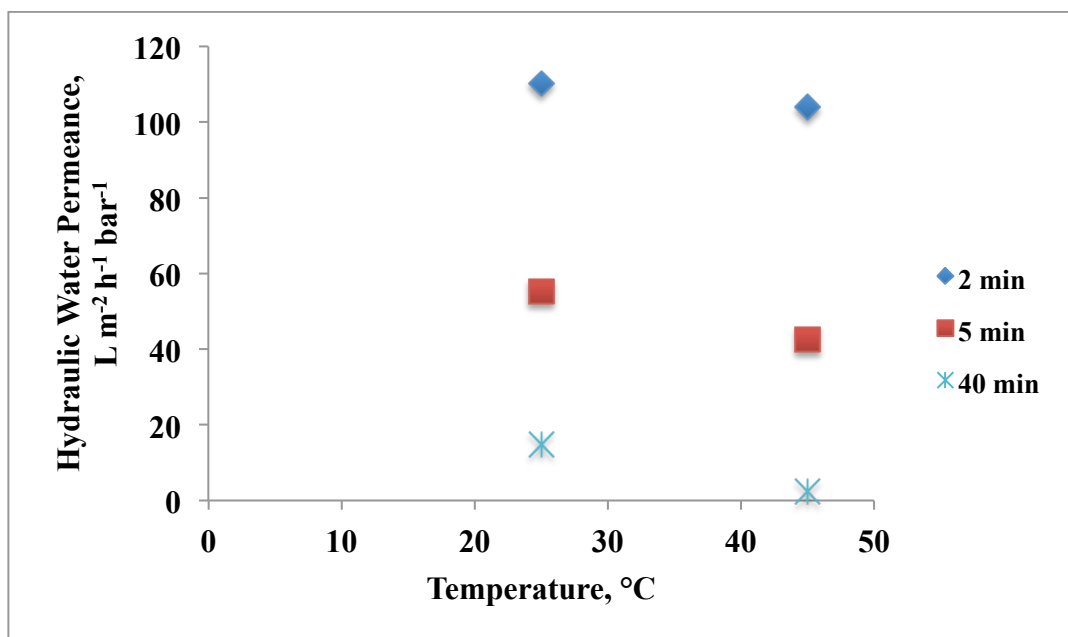
Figure 2.24 Effect of temperature on the permeance values of DW and DW-45 membranes with respect to different evaporation time.

2.3.3 Effect of coagulation bath

The effect of coagulation bath was investigated by using two different non-solvents: water and IPA. When changing the temperature during evaporation time, we were affecting the first step of dry-wet phase inversion that was formation of thin skin layer on top of the cast polymer solution by means of desolvation. However, changing non-solvent affects the second step in which demixing of liquids take place. So, nonsolvent molecules will diffuse through skin layer while solvent particles will diffuse out. As a result, diffusion mechanisms of the non-solvents will affect the pore morphology of formed membranes. Figure 2.25 shows the effect of IPA and water, as non-solvents, on hydraulic permeances of PEEK-WC membranes prepared by wet and dry/wet phase inversion. According to the results, hydraulic permeances of DIPA membranes were drastically lower than DW membranes. This result points out that denser membranes that are founded in nanofiltration range were obtained by the selection of IPA as nonsolvent. Actually, it is a well-known fact that the miscibility of water is much better than IPA [1]. Since, water is more soluble with DMA there was a

41

tendency to form porous DW membranes due to instantaneous de-mixing. On the other hand, low miscibility between IPA and DMA resulted in dense nonporous DIPA membranes due to delayed demixing [1].
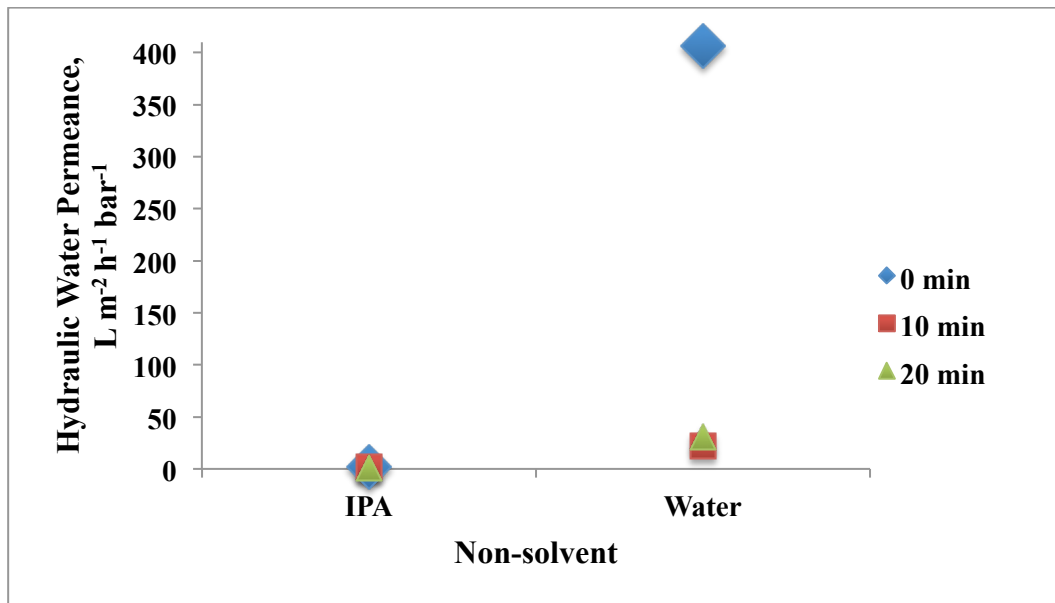
Figure 2.25 Effect of non-solvent type on the permeance values of DW and DIPA membranes with respect to different evaporation time.

In addition, the colorant rejection tests were performed on the densest membranes (DW-120 and DIPA-15) in order to estimate the MW cut-off the membranes in nanofiltration range and to prove the effect of non-solvent choice on the membrane structure. The results of rejection test are reported in Table 2.8. In particular with DW-120 membrane (densest membrane produced at RT in water coagulation bath), Rose Bengal was retained for 57% whereas, for smaller molecules of bromothymol blue and methyl orange observed retentions were 20% and 4%, respectively. These results pointed out the necessity to use colorants with higher molecular weight in order to determine the exact MW cut-off of DW-120. On the other hand, the retention of methylene blue and methyl orange for DIPA-15 membrane were 100% and 83%, respectively. A difference in retention of DIPA-15 membrane was observed while varying component charge. Although the MW of methylene blue and methyl orange were almost same, there was 17% difference in their rejection values. The strong repulsive forces between the positively charged methylene blue and the positively charged membrane can lead this difference. So the local charge effect played

a fundamental role in retention in respect to sieving mechanism. The small negatively charged methyl orange molecules were subjected to attraction forces resulting in less retention. However, still DIPA-15 membranes showed a high retention for both negatively and positively charged component. The high retention of methyl orange occurred on the basis of its larger molecular size than the pore size of membrane. As a result, it can be concluded that DIPA-15 membranes have a MW cut-off of 327 g/mol. This outcome is evidence for the dense sponge-like structured DIPA membranes are in the nanofiltration range.

To sum up, rejection tests were in consistence with water flux measurements. Both results indicated that dense membranes were formed due to delayed demixing in DMA/IPA system whereas instantaneous demixing in DMA/water system formed porous membranes.

Table 2.8 Rejection test results for DW-120 and DIPA-15.

Colorant	MW of the colorant (g/mol)	Rejection in DW-120 (%)	Rejection in DIPA-15 (%)
Methylene blue	320	-	100
Methyl orange	327	4	83
Bromothymol blue	624	20	100
Rose bengal	1017	57	100

2.4 Conclusion

Asymmetric PEEK-WC membranes with a wide range of different morphologies and transport characteristics were prepared by wet and dry-wet phase inversion technique. The influence of the solvent evaporation time, solvent evaporation temperature and non-solvent on phase inversion PEEK-WC membranes were investigated. PEEK-WC membranes were ranging from porous ultrafiltration to dense nanofiltration membranes by changing these three parameters. The SEM analyses and water flux measurements evidenced that solvent evaporation time influenced the final membrane morphology. In particular, as the time increased, membranes exhibited denser structure, especially when water was used as non-solvent in coagulation bath.

As the temperature was increased to 45°C at evaporation step, desolvation of DMA increased and as a result a denser skin layer was formed on the top of the cast polymer solution. Formation of dense skin layer caused the reduction of hydraulic water permeability.

Effect of non-solvent selection was very remarkable on the membrane performance. Both results of retention and water flux tests indicated that dense membranes were formed due to delayed demixing in DMA/IPA system whereas instantaneous demixing in DMA/water system formed porous membranes.

To conclude, the results obtained, in terms of relative flux, SEM and retention, shows producing PEEK-WC membranes ranging from porous ultrafiltration to non-porous nanofiltration is possible by tuning process parameters such as evaporation time, evaporation temperature and non-solvent selection for coagulation bath. Thus, DW membranes having an asymmetric porous structure were good candidates to be used in Polymer Assisted Ultrafiltration applications to remove Cu^{2+} ions from water.

REFERENCES

[1] Mulder M. *Basic Principles of Membrane Technology*. Kluwer Academic Publishers, 1991.

[2] Strathmann H. Giorno L., Drioli E. *Introduction to Membrane Science and Technology*. Consiglio Nazionale delle Ricerche, Rome, 2006.

[3] Lonsdale H. K. What is membrane? Part II. *Journal of Membrane Science*, 1989;43(1):1-3.

[4] Membrane separation processes - An overview, January 1997. [online] http://www.pacificro.com/membrsep.htm.

[5] Li K. Membrane science and membrane separation processes (Online Lecture Notes), Imperial College London.

[6] Kesting R. E. *Synthetic Polymeric Membranes*. McGraw-Hill, New York, 1971

[7] Cadotte J.E. Evolution of Composite Reverse Osmosis Membranes, *187th Meeting of the American Chemical Society* 273, St Louis, MO, USA, (1985)

[8] Loeb S., Sourirajan S. Seawater demineralization by means of a semipermeable membrane. *Advances in Chemistry Series*, 1962;38:117-132.

[9] Loeb S., Sourirajan S. High flow porous membranes for sepration of water from saline solutions. *US- Patent*, 1964;3,133,132.

[10] Khulbe K. C., Feng C. Y., Matsuura T. Synthetic *Polymeric Membranes-Characterization by Atomic Force Microscopy*. Springer, Berlin Heidelberg, 2008.

[11] Sigma-Aldrich, 2013. [online] http://www.sigmaaldrich.com.

[12] Buonomenna M.G., Gordano A., Drioli E. Characteristics and performance of new nanoporous PEEKWC films. *European Polymer Journal*, 2008;44:2051-2059.

[13] WellTech Enterpirses, Perkin-Elmer LAMBDA EZ201 UV-VIS Spectrophotometer, 2010. [online] http://www.welltechinc.com.

[14] Buonomenna M.G., Figoli A., Jansen J.C., Drioli E. Preparation of asymmetric PEEKWC flat membranes with different microstructures by wet phase inversion. *Journal of Applied Polymer. Science*, 2004;92:576-591.

CHAPTER 3

OPTIMIZATION OF METAL-POLYETHYLENIMINE COMPLEXATION CONDITIONS

This chapter is a complementary section that includes the optimization step of the complexation of various heavy metals with water-soluble polyethylenimine (PEI) and provided background information prior to polymer assisted ultrafiltration (PAUF) tests. PAUF testing method, which is described in detail in *Chapter 4*, uses water-soluble polymers that form macromolecular complexes with metallic ions. The ultrafiltration (UF) membranes, having a smaller molecular weight cut-off than the molecular weight of the metal-polymer complex, will block the macromolecular complexes, while still allowing the non-complexed metal ions to pass through the membrane. In this manner, it is very essential to ensure the condition for the maximum binding capacity of polymer-metal complexes. Polyacrylic acid (PAA), polyethylenemine (PEI), poly(dimethylamine–co–epichlorohydrin–co–ethylenediamine) (PDEHED), diethyla-minoethyl cellulose and humic acid are the most commonly used complexing agents providing a selective separation and recovery of heavy metals [1].

3.1 Literature Review

Water-soluble polymer complexes have been attracting interest due to their intrinsic properties and their many potential applications both in scientific and technological fields in recent years. Water-soluble polymer complexes have potential applications such as wastewater treatment, catalysts, biocompatible polymers, liquid crystals,

superconducting materials, and ultra high strength materials [2-12]. Among these applications, wastewater treatment is attracting strong attention since toxic and non-biodegradable heavy metals, i.e. zinc, cadmium, chromium, copper, lead, nickel, cobalt, iron and mercury, in water are growing as a treat to our environment [13]. Generally, these heavy metals and their compounds have been used extensively by various metal finishing, mining, chemical, and electronic industries leading to a sharp increase in the contamination of water [14]. On the other hand, there is also a demand for the recovery of most of the heavy metals due to the decline in the quality and availability of metal ores [3]. As a consequence, it becomes necessary not only to separate metal ions from wastewater but also to recover them, economically. Moreover, the PAUF, which is a hybrid complexation-ultrafiltration process, can meet these requirements [3,14]. The basic principle of PAUF is binding heavy metals and soluble polymers, which have higher molecular weights than molecular weight cut-off (MWCO) of UF membranes, to form macromolecular complexes that will be blocked by the UF membranes [14]. Therefore, it is very critical to ensure a high binding capacity for high retention of metal ions because non-bound metal ions will pass through UF membranes very easily.

These water-soluble polymers can be synthesized or found commercially. In order to be able to use them for industrial applications they must satisfy the following requirements such as [3,15],

- high solubility in water,
- easy route of synthesis,
- adequate molecular weight and distribution,
- good chemical and mechanical stability,
- high metal ion binding capacity,
- high selectivity for the metal of interest
- low toxicity,
- low cost, and
- possibility of regeneration.

High water solubility of polymers results from their high content hydrophilic groups, such as amino, hydroxyl, carboxyl, sulfonic acid and amide groups [2,3]. These groups can be present either as side groups or at the backbone of the polymer. The water-

47

soluble polymers, which are used for the removal of heavy metals, can be categorized as [15],

- nature originated polymers (chitosan, macroalgae),
- lab-scale synthesized/modified polymers (partially exhoxylated PEI), and
- commercial polymers (PAA, PEI, PDEHED)

Although natural polymers are environmentally friendly, their functional group compositions are quite complicated causing problems in separation and polymer regeneration. Individually synthesized polymers are utilized to have high binding capacities and regeneration of polymer. However, their properties like cost, toxicity, and large-scale production ability should be investigated [15]. Since, first two classes are causing difficulties in industrial applications, we will focus on commercially available water-soluble polymers. Among them, polymers having high content of amino group are mainly studied by the PAUF. Especially, PEI, a polymeric amine, is advantageous for PAUF due to its good water solubility, high content of functional groups, adequate molecular weight, and good chemical and mechanical stability [2, 16]. Depending on the polymerization process, PEI can be a linear or a branched polymer with a different ratio of amino groups. Linear polyethylenimine (L-PEI) contains all secondary amines whereas branched PEI (B-PEI) contains primary, secondary and tertiary amino groups [17]. In *this work,* PEI was chosen as water-soluble polymer, due its advantageous properties in the PAUF, to investigate and optimize its binding capacity with various heavy metals (Cu^{2+}, Ni^{2+}, and Co^{2+}).

The binding capacities of metal-polymer complexes can be determined by several characterization methods. The most common method to determine binding capacity is to measure retention of metal-polymer complex during UF process [1-3,16]. The concentration of retained metal-polymer complex solution and unbounded metal ion concentration in permeate can be analyzed by ultraviolet (UV) spectroscopy, inductively coupled plasma mass spectrometry (ICP), infrared (IR) spectroscopy, elemental analysis. Also, binding capacity can be evaluated directly by IR, visible, and UV absorption characteristics of formed metal-polymer complexes [2,16]. In *this work,* we analyzed the binding capacities of metal-PEI complexes by UV-Vis spectroscopy because each metal-PEI complex will absorb a certain wavelength.

Theory

The interaction between water-soluble polymers and metal ions are defined by electrostatic forces and the formation of coordinating bonds [3]. Also other weak interactions, for instance, the trapping of metal ions in the bulk of the polymer phase, may also occur [3]. As a result of these interactions, complexation reactions take place among metal ions and polymeric agents. As an example, the reaction of complex formation between Cu(II) ions and amine groups of PEI can occur, succinctly described as:

$$M + mL \leftrightarrow ML_m \tag{3.1}$$
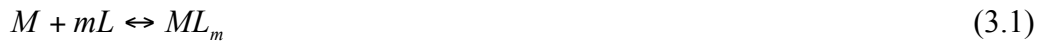
where M represents the metal ions and L represents the monomer units of the polymeric chain. In particular, focusing on the selected polymer, PEI, the complexation reaction takes place in an aqueous solution containing the metal ion. The protonation of PEI, polymer-metal complex formation and soluble metal hydroxyl complexes are the reactions taking place. These reactions can be summarized in the following equations [16-21]:

$$PEI + H \leftrightarrow PEI \cdot H \quad K_p \tag{3.2}$$

$$M + nPEI \leftrightarrow M(PEI)_n \quad K_b \tag{3.3}$$

$$M + mOH \leftrightarrow M(OH)_m \quad K_m \tag{3.4}$$

where n represents the average coordination number of PEI ligands binding to one metal ion, and m represents the number of hydroxide ions present in one soluble metal hydroxy complex. K_p, the protonation constant of PEI, and K_b, binding constant of the metal-PEI complex, are expressed in terms of concentration, which include the contribution of the electrostatic potential field of the polycation [16]. In addition, it is known that chemical binding of PEI-M complex occurs between metal ions and the amino groups of PEI. This complexation form is illustrated in Figure 3.1. Stable complexes are formed from amino groups present in PEI, due to the free electron pair of the nitrogen atom. For this reason, pH has a strong effect on the stability of the complexes. When pH is low, the affinity of metal ions is poor, and the complex has a

low stability, due to the protonation of amino groups. However, at high pH, affinity and stability of the complex molecules increase [3,22].
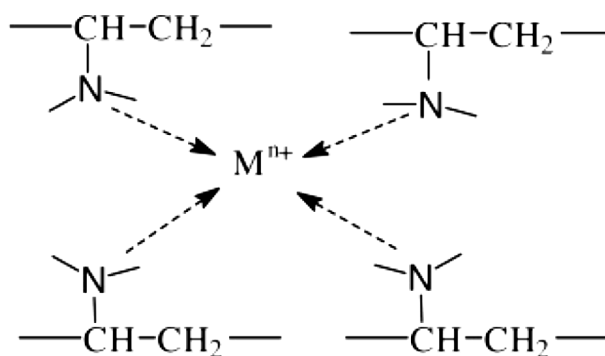
Figure 3.1 Structure of Metal-PEI complex [22]

3.2 Experimental Procedure

3.2.1 Materials

Copper (II) sulphate pentahydrate ($CuSO_4 \cdot 5H_2O$) from Fluka Chemika (MW = 249.09 g/mol, purity <99%), nickel(II) chloride hexahydrate ($NiCl_2 \cdot 6H_2O$) from Horasan (MW = 237.69 g/mol, purity 97-99%), and cobalt(II)chloride hexahydrate ($CoCl_2 \cdot 6H_2O$)from Riedel-de-Haen (MW = 237.93 g/mol, purity <99%) were used as received for preparing various model solutions of wastewater. Ultra-pure (Rephile, Dirctt-Pure UP) water was preferred for model solution preparation in order to prevent the uncontrolled changes in concentration that could be caused by the existent ions in distilled water. Linear polyethylenemine (L-PEI) from Sigma Aldrich (average M_n ~60,000 g/mol by GPC, average M_w ~750,000 g/mol by LS, 50 wt. % in H_2O) and branched polyethylenemine (B-PEI) from Sigma Aldrich (M_w ~25,000 g/mol by LS, average M_n ~10,000 g/mol by GPC, pure), shown in Figure 3.2, were used as complexation agents. Finally, the pH of the metal-PEI complex solutions was adjusted by 0.1 M HCl and 0.1 M NaOH solutions, which were prepared from hydrochloric acid (HCl) from Merck (MW = 36.46 g/mol, 37%) and sodium hydroxide (NaOH) from

LabKim (MW = 39.99 g/mol, purity 99%), respectively. A pH meter (H2211 pH/ORP Meter, Hanna Instruments) with a combined glass electrode was used for pH measurements.
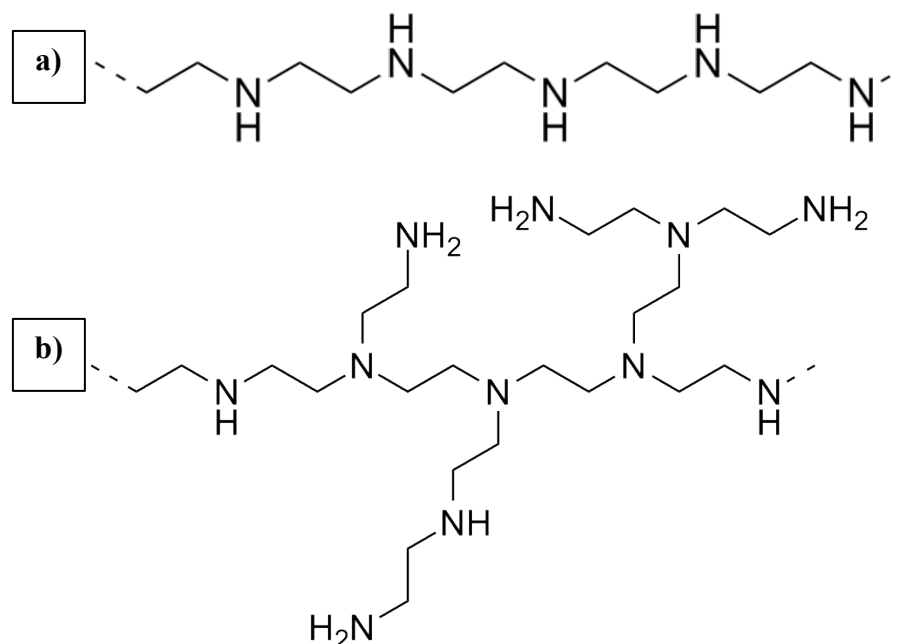
Figure 3.2 Chemical structures of a) L-PEI and b) b-PEI [23].

3.2.2 Preperation and Analysis of Metal-PEI Complex Solutions

Firstly, three different model wastewater solutions having Cu^{2+}, Ni^{2+}, and Co^{2+} content were prepared. Metal salts were dissolved in ultra-pure water with a concentration of 50 mg/L and PEI polymers were added to prepared model wastewater solution with a concentration of 150 mg/L. The solutions containing Cu^{2+}, Ni^{2+}, or Co^{2+} and B-PEI or L-PEI at various pH values were gently agitated in the stirrer. Solutions were stirred until pH values were stabilized. This step, lasting at least for 2 h, was very important to ensure equilibrium binding. Then complexation and maximum bonding capacities of B-PEI-Cu^{2+} and L-PEI-Cu^{2+} were evaluated as a function of pH by UV-Vis spectrophotometric measurements (UV-3150, Schimadzu UV-VIS-NIR Spectrophotometer). Bonding capacities of B-PEI-Cu^{2+} and L-PEI-Cu^{2+} were measured at wavelength of 632 nm whereas bonding capacities of B-PEI-Ni^{2+} and B-PEI-Co^{2+}

were measured at wavelength of 360 nm and 310 nm, respectively. The bonding capacity was evaluated using the equation reported below:

$$Bonding\ Capacity\ \% = \frac{Absorbance}{Absorbance_{max}} \times 100 \qquad (3.5)$$

After optimizing pH values of each polymer-metal complex solution that ensured maximum bonding capability, the concentration of metal ion was varied while fixing both PEI concentration to 150 mg/L and optimum pH value. The maximum metal uptake value of PEI polymers were evaluated by Eq. 3.5, in which absorbance values were measured at the specific wavelength of each B-PEI-Cu^{2+}, L-PEI-Cu^{2+}, B-PEI-Ni^{2+}, and B-PEI-Co^{2+} complex bonding. Also, effect of polymer structure was investigated by comparing the optimum pH and metal concentration values of B-PEI-Cu^{2+} and L-PEI-Cu^{2+} complexations. All solution were prepared and analyzed for at least three times and results were reported as the average values. Finally, optimum chemical conditions for metal complexation, decomplexation and maximum binding capacity were determined.

3.3 Results and Discussion

In order to evaluate the Cu^{2+} bonding capacity of B-PEI, complexation tests were carried out by varying pH and copper concentration. Figure 3.3 shows the effect of pH on B-PEI bonding capacity fixing the polymer and copper concentrations at 150 mg/L and 50 mg/L, respectively. The error bars denote the standard deviation derived from at least three measurements. Results indicate that complexation occurred at pH=6 and higher whereas decomplexation happened due to the poor affinity between polymer and ion at pH values lower than 3. These results were in agreement with those obtained by Molinari *et al*. [24,25]. Specifically, dark blue color of B-PEI-Cu^{2+} complex solutions became a clear solution at pH<3 proving the release of Cu^{2+} ions from polymer. During pH optimization tests, it was observed that it was necessary to provide

enough time to ensure maximum possible binding capacity of copper ions with B-PEI because stabilization of pH of the B-PEI-Cu^{2+} complex solutions was a time consuming process.
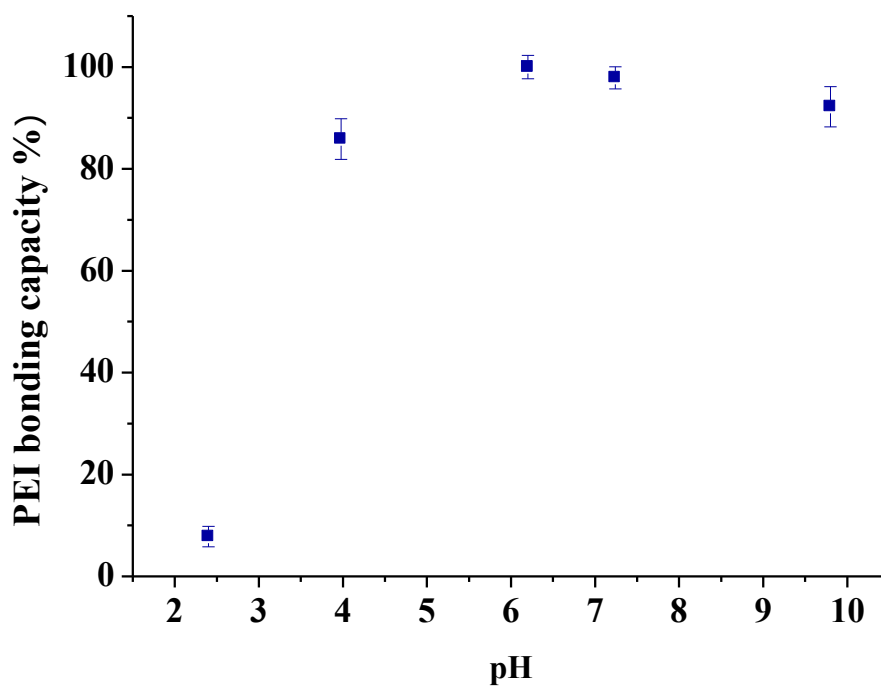
Figure 3.3 . PEI bonding capacity (%) vs pH (B-PEI=150 mg/L; Cu^{2+}= 50mg/L).

After optimizing pH of copper-branched PEI complexation, maximum Cu^{2+} uptake of B-PEI was investigated. On the basis of the results of Figure 3.4, other experiments were performed by fixing the pH at 6 and varying the copper concentration while fixing B-PEI concentration to 150 mg/L. Figure 3.4 shows that the maximum amount of Cu^{2+} complexed by 150 mg/L of B-PEI was equal to 150 mg/L. Moreover, absorbance was almost constant at copper concentrations higher than 150 mg/L. This indicated that there were no more complexation taking place after 150 mg/L. Probably, excess Cu^{2+} remained in solution below its precipitation pH $\approx$ 6 or existed as hydroxide above its precipitation pH [15,24,25]. Many studies in literature reported that maximum bonding capacity of PEI-Cu^{2+} complexation was equal or higher than 3:1 weight ratio of PEI:Cu^{2+} [24,25]. In *this work,* better bonding capacity was obtained at 1:1 weight ratio of B-PEI:Cu^{2+} with respect to reported results for PEI-Cu^{2+}. Higher bonding capacity

(higher copper removal) allows reduction of the PEI amount, thereby reducing processing costs. Additionally, reduction of the polymer concentration will reduce the probability of membrane fouling or concentration polarization during PAUF processes [15].
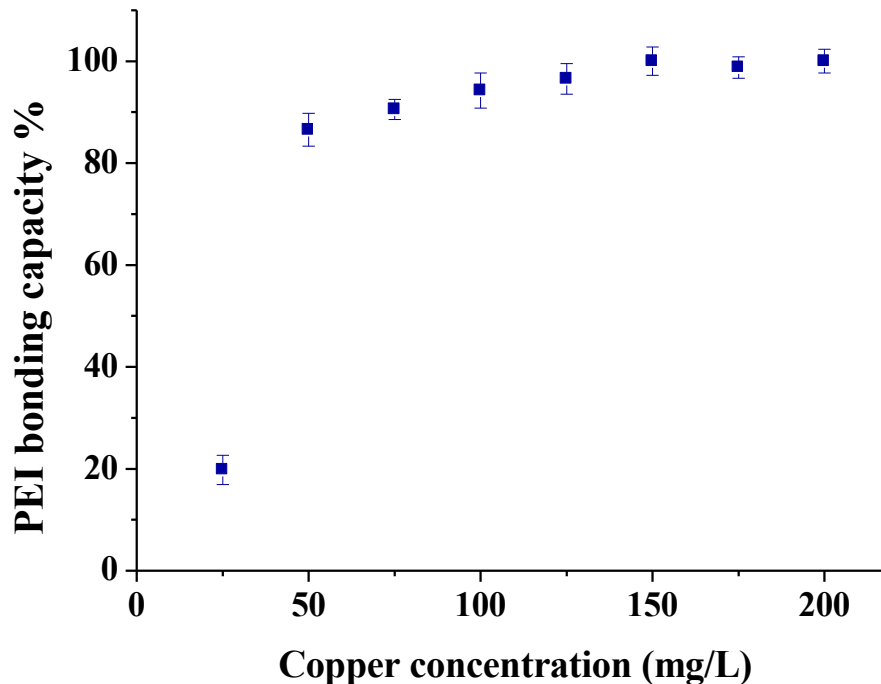
Figure 3.4 PEI bonding capacity (%) percentage vs copper concentration (B-PEI concentration = 150 mg/L, pH=6).

Cu^{2+} bonding capacity of L-PEI, complexation tests were carried out by varying pH and copper concentration in order to compare the effect of different types of amino groups on the bonding capacity. Figure 3.5 shows the effect of pH on L-PEI bonding capacity fixing the polymer and copper concentrations at 150 mg/L and 50 mg/L, respectively. The error bars denote the standard deviation derived from at least three measurements. Similar to B-PEI-Cu^{2+} complexation, results indicate that complexation occurred at pH=6 and higher whereas decomplexation happened due to the poor affinity between polymer and ion at pH values lower than 3. These results were in agreement with those obtained by Molinari et al. [24,25]. Just like the B-PEI-Cu^{2+} solutions, dark blue color of L-PEI-Cu^{2+} complex solutions became a clear solution at pH<3 as a result of releasing Cu^{2+} ions from polymer. During pH optimization tests, it was observed that it was necessary to provide enough time to ensure maximum possible binding capacity

of copper ions with L-PEI because stabilization of pH of the L-PEI-Cu^{2+} complex solutions was a time consuming process.
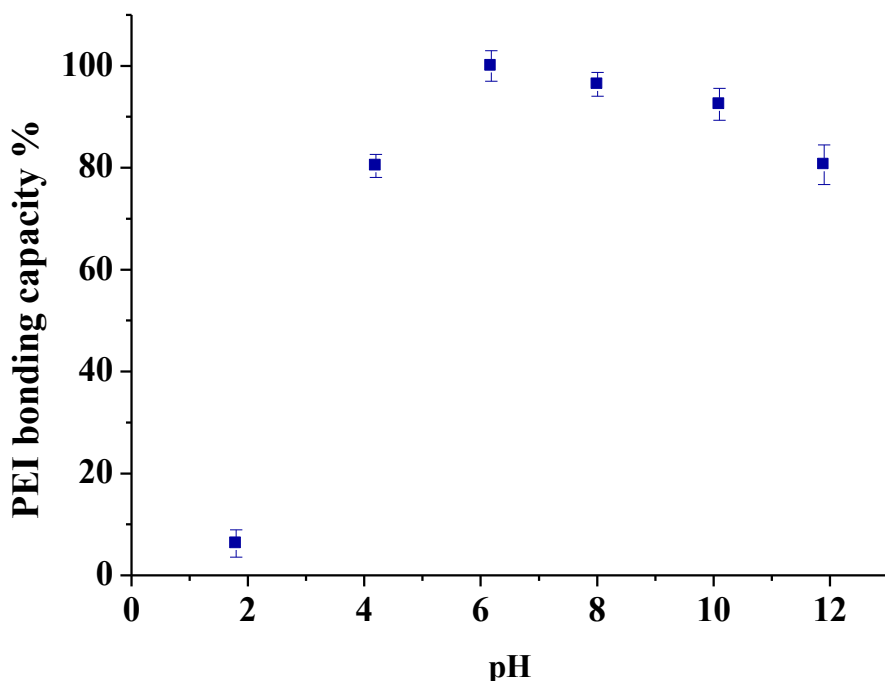
Figure 3.5 PEI bonding capacity (%) vs pH (L-PEI=150 mg/L; Cu^{2+}= 50 mg/L).

After optimizing pH of copper-branched PEI complexation, maximum Cu^{2+} uptake of L-PEI was investigated. Experiments were performed by fixing the pH at 6 and varying the copper concentration while fixing B-PEI concentration to 150 mg/L. Figure 3.6 shows that the maximum amount of Cu^{2+} complexed by 150 mg/L of L-PEI was equal to 75 mg/L. Moreover, there was no more complexation after 50 mg/L of Cu^{2+} since the absorbance was more or less the same at copper concentrations higher than this value. Probably, excess Cu^{2+} remained in solution below its precipitation pH $\approx$ 6 or existed as hydroxide above its precipitation pH [15,24,25]. Many studies in literature reported maximum bonding capacity of PEI-Cu^{2+}, which were close but still lower than our results [24,25]. Maximum metal uptake capacity of L-PEI was obtained at 2:1 weight ratio of L-PEI:Cu^{2+} with respect to reported results for PEI-Cu^{2+}. Although L-PEI:Cu^{2+} ratio was more lower than most of the studies present today, B-PEI-Cu^{2+} bonding capacity was higher. This difference in binding capacities of two PEIs was due their structural differences. Probably branched chains and presence of primary amines

provided a higher number of binding sites to B-PEI. Due to its higher bonding capacity, B-PEI was preferred for studying with other heavy metals, nickel and cobalt.
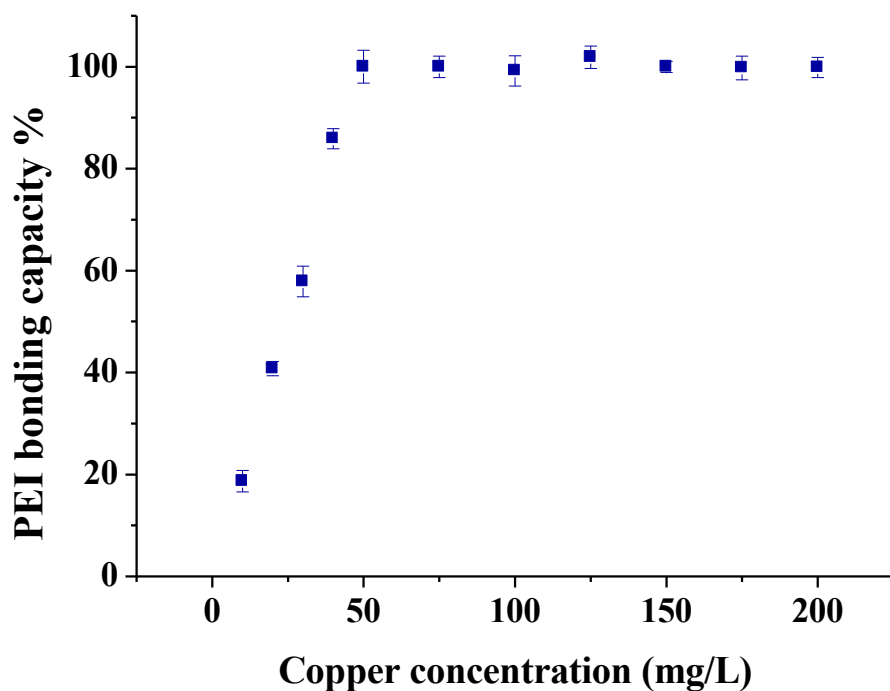
Figure 3.6 PEI bonding capacity (%) percentage vs copper concentration (L-PEI concentration = 150 mg/L, pH=6).

Optimum bonding conditions of B-PEI-Ni^{2+} complex molecule was investigated at various pH and nickel concentrations. At first, the effect of pH on nickel bonding capacity of B-PEI was performed by fixing the polymer and nickel concentrations at 150 mg/L and 50 mg/L, respectively. Unfortunately, the absorbance intensity of B-PEI-Ni^{2+} bonding was so low (at λ=360 nm) that was almost impossible to evaluate the bonding capacity percentages. For this reason, both B-PEI and Ni^{2+} concentrations were doubled to obtain sufficient absorbance intensities to be able to make a proper comparison. Figure 3.7 represents the effect of pH on complexation/decomplexation of B-PEI at fixed concentrations of 300 mg/L and 150 mg/L for B-PEI and Ni^{2+}, respectively. The standard deviation, which was derived from at least three measurements, were denoted by the error bars. According to Figure 3.7, highest complexation was obtained at pH=8, whereas decomplexation was taking place at

lower pH values (pH<3). On the other hand, there was precipitation of hydroxides formed at high pH values (pH>8). These results were in agreement with those obtained by Nagy *et. al.* and Argurio *et.al.* [26,27]. In addition, pale blue-violet color of B-PEI-Ni^{2+} complex solutions observed as a clear solution at pH<3 proving the release of Cu^{2+} ions from polymer and as blurry blue-violet with high amount of precipitates at pH>8 . During pH optimization tests, enough time was provided to ensure maximum possible binding capacity of nickel ions with B-PEI because stabilization of pH of the B-PEI-Ni^{2+} complex solutions was a time consuming process.
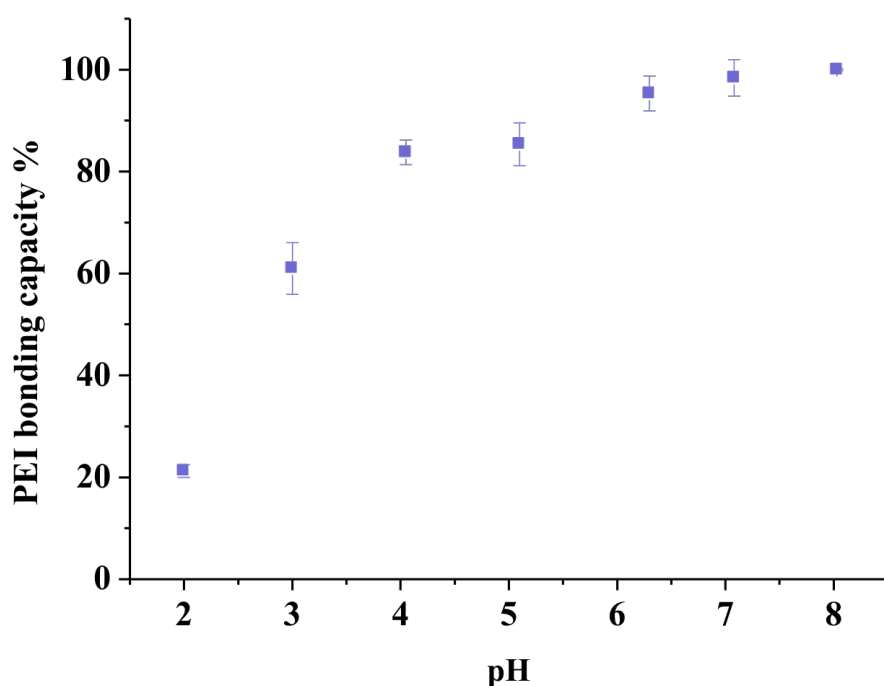

Figure 3.7 PEI bonding capacity (%) vs pH (B-PEI=300 mg/L; Ni^{2+}= 150 mg/L).

The maximum nickel bonding capacity of B-PEI was studied by fixing pH=8 and B-PEI concentration to 300 mg/L. Figure 3.8 shows that the maximum amount of Ni^{2+} complexed by 300 mg/L of B-PEI was 300 mg/L. Specifically, absorbance of B-PEI-Ni^{2+} complex solutions was almost constant at high nickel concentrations ($[Ni^{2+}]$>150 mg/L). So, it was obvious that there were no more complexation taking place after this concentration. It is predicted that excess Cu^{2+} remained in solution below its precipitation pH or existed as hydroxide above its precipitation pH [15,18,19].

Many studies in literature reported maximum bonding capacity of PEI-Ni^{2+} complexation was equal or higher than 5:1 weight ratio of PEI:Ni^{2+} [14,27,28], except Nagy and Borbély reported a bonding capacity of 1:1 [26]. In *this work,* high bonding capacity was obtained at 1:1 weight ratio of B-PEI:Ni^{2+}. Higher bonding capacity (higher nickel removal) allows reduction of the PEI amount, thereby reducing processing costs. Additionally, reduction of the polymer concentration will reduce the probability of membrane fouling or concentration polarization during PAUF processes [15].
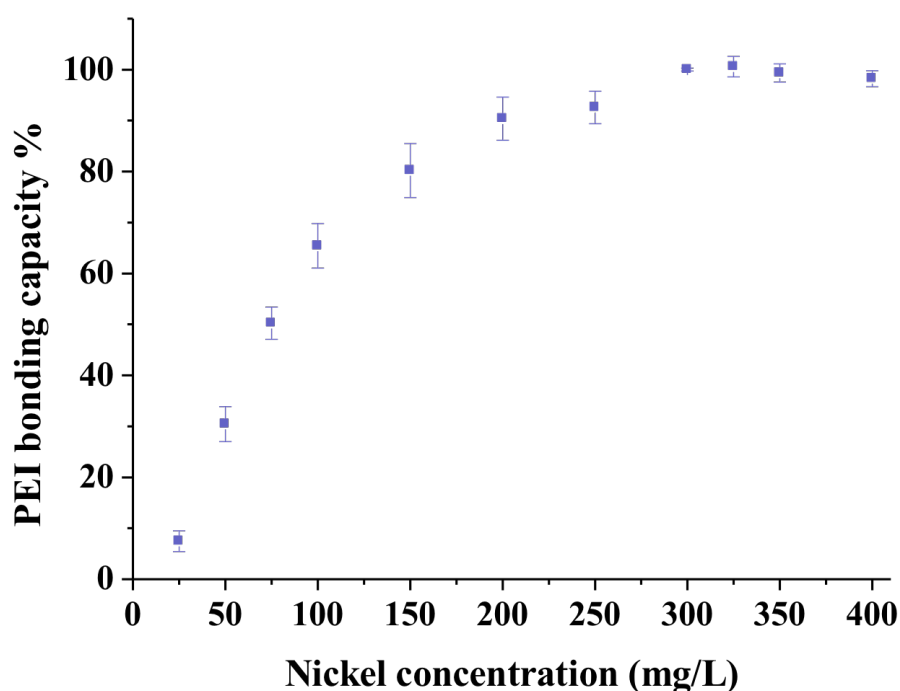

Figure 3.8 PEI bonding capacity (%) percentage vs nickel concentration (B-PEI concentration = 300 mg/L, pH=8).

Finally, optimum bonding conditions of the last heavy metal cobalt was investigated at various pH and cobalt concentrations. The effect of pH on nickel bonding capacity of B-PEI was performed by fixing the polymer and cobalt concentrations at 150 mg/L and 50 mg/L, respectively. Figure 3.7 represents the effect of pH on complexation/decomplexation of B-PEI where the standard deviation was denoted by the error bars. Evaluated bonding capacity percentages show that the best complexation was obtained at pH=8, whereas decomplexation was taking place at

lower pH values (pH<3). On the other hand, there was precipitation of hydroxides formed at high pH values (pH>8). These results were in agreement with those obtained by He *et. al.*[28]. In addition, pale amber color of B-PEI-Co^{2+} complex solutions observed as a clear solution at pH<3 proving the release of Co^{2+} ions from polymer and as blurry amber color with high amount of precipitates at pH>8. During pH optimization tests, enough time was provided to ensure maximum possible binding capacity of nickel ions with B-PEI because stabilization of pH of the B-PEI-Co^{2+} complex solutions was a time consuming process.
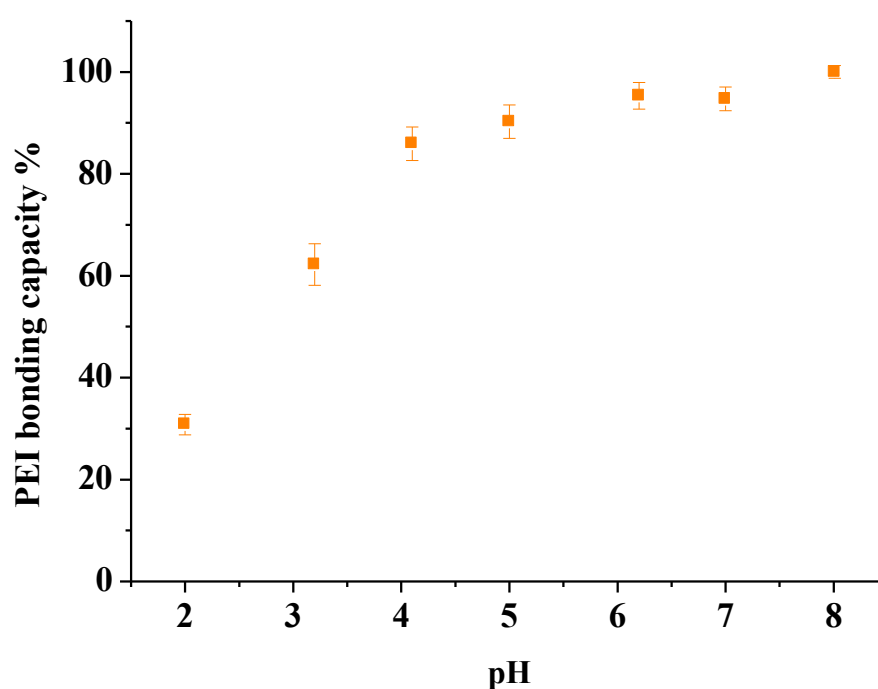

Figure 3.9 PEI bonding capacity (%) vs pH (B-PEI=150 mg/L; Co^{2+}= 50 mg/L).

The maximum cobalt bonding capacity of B-PEI was studied by fixing pH=8 and B-PEI concentration to 150 mg/L. Figure 3.9 represents that the maximum amount of Co^{2+} complexed by 150 mg/L of B-PEI was 150 mg/L. Specifically, absorbance of B-PEI-Co^{2+} complex solutions was almost constant at high cobalt concentrations ([Co^{2+}]>150 mg/L). So, it was obvious that there were no more complexation taking place after this concentration. In *this work,* high bonding capacity was obtained at 1:1 weight ratio of B-PEI:Ni^{2+}. Higher bonding capacity (higher cobalt removal) allows reduction of the PEI amount, thereby reducing processing costs. Additionally, reduction

of the polymer concentration will reduce the probability of membrane fouling or concentration polarization during PAUF processes [15].
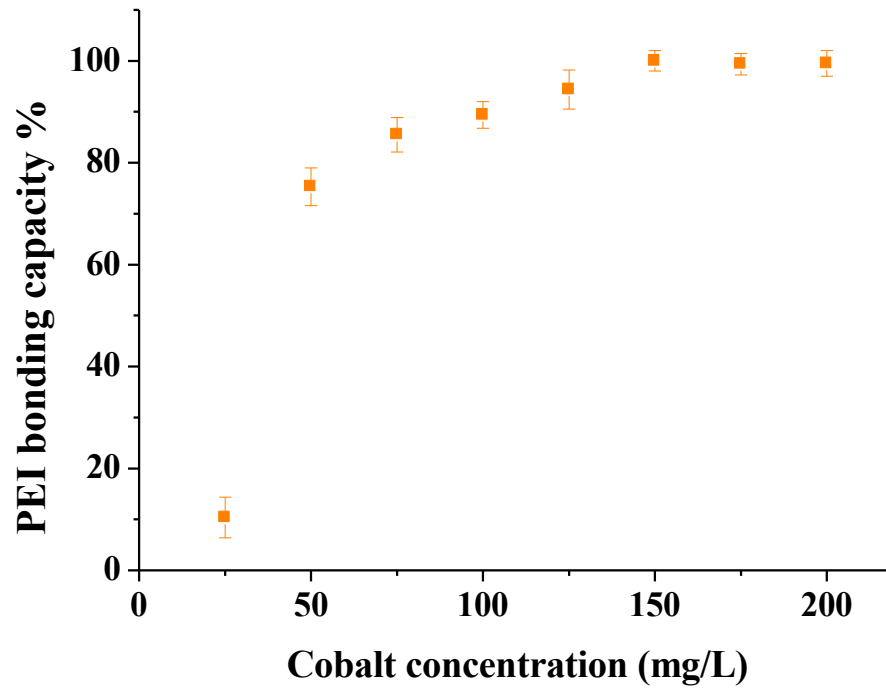
Figure 3.10 PEI bonding capacity (%) percentage vs cobalt concentration (B-PEI concentration = 150 mg/L, pH=8).

3.4 Conclusion

In *this chapter*, the optimum conditions for maximum binding capacities of Cu^{2+}-PEI, Ni^{2+}-B-PEI and Co^{2+}-B-PEI was investigated by varying the pH and metal concentrations of the model wastewater solutions. The comparison of bonding capacities of branched and linear PEIs showed that, B-PEI had the twice as much as the bonding capacity of L-PEI. This was explained by the presence of primary amine groups that were capturing more copper ions. As a result, B-PEI was preferred for further studies since its higher bonding capacity allows reduction of the PEI amount, thereby reducing the cost and the probability of membrane fouling or concentration polarization that can be faced during PAUF processes. Optimum pH conditions of bonding for B-PEI-Cu^{2+} was pH=6 whereas pH was equal to 8 for Ni^{2+}-B-PEI and Co^{2+}-B-PEI complexes. B-PEI provided a high metal uptake of 1:1 (B-PEI:M^{2+} weight ratio) that were better bonding capacities allowing reduction of the PEI amount. The critical step for obtaining a good bonding capacity was resting solutions for at least 2 h until they were completely stabilized. Better bonding capacities obtained for B-PEI will make it a proper choice to be used in industrial applications due to reduction in processing costs, the probability of membrane fouling or concentration polarization during PAUF processes [15].

REFERENCES

[1] Fu F., Wang Q. Removal of heavy metal ions from wastewaters: A review. *Journal of Environmental Management*, 2011;92:407-418.

[2] Geckeler K, Lange G.,Eberhardt H., Bayer E. Preparation and application of water-soluble polymer-metal complexes. *Pure and Applied Chemistry*, 1980;52:1883-1905.

[3] Rivas B.L., Pereira D. Moreno-Villoslada I. Water-soluble polymer-metal ion interations. *Progress in Polymer Science*, 2003;28(2):173-208.

[4] Tsuchida E., Nishide H. Polymer–metal complexes and their catalytic activity. *Advances in Polymer Science*, 1977;24:1–87.

[5] Higashi F., Cho C.S., Hinoki H. A new organic semiconducting polymer from Cu^{2+} chelate poly(vinyl alcohol) and iodine. *Journal of Polymer Science Polymer Chemistry Edition*, 1979;17(2):313–318.

[6] Buchmeiser M.R., Kröll R., Wurst K., Schareina T., Kempe R. Polymer-supported polymerization catalysts via Romp. *Macromolecular Symposia*, 2001;164:187–196.

[7] Michalska Z.M., Strzelec K., Sobczak J.W. Hydrosilylation of phenylacetylene catalyzed by metal complex catalysts supported on polyamides containing a pyridine moiety. *Journal of Molecular Catalysis A: Chemical*, 2000;156(1-2):91–102.

[8] Akelah A., Moet A. *Functionalized Polymers and Their Applications*. Chapman & Hall, London, 1990.

[9] Breslow R., Belvedere S., Gershell L., Leung D. The chelate effect in binding, catalysis, and chemotherapy. *Pure and Applied Chemistry*, 2000;72(2):333–342.

[10] Hojo N., Shirakai H., Hayashi S. Complex formation between poly(vinyl alcohol) and metallic ions in aqueous solution. *Journal of Polymer Science: Polymer Symposia*, 1974;47(1):299–307.

[11] Travers C., Marinsky J.A. The complexing of Ca(II), Co(II), and Zn(II) by polymethacrylic acid and polyacrylic acid. *Journal of Polymer Science: Polymer Symposia*, 1974;47(1):285–297.

[12] Chiang W.Y., Mei W.P. Metal complexation of N-methylthiomethyl-pendant polyimides. *European Polymer Journal*, 1993;29(8):1047–1051.

[13] Dobson R.S., Burgess J.E. Biological treatment of precious metal refinery wastewater: A review. *Minerals Engineering*, 2007;20(6):519–532.

[14] Shao J., Qin S., Davidson J., Li W., He Y., Zhou H.S. Recovery of nickel from aqeous solutions by complexation-ultrafiltration process with sodium polyacrylate and polyethylenimine, *Journal of Hazardous. Materials*, 2013;244-245:472-477.

[15] Qiu Y.R., Mao L.J., Removal of heavy metal ions from aqueous solution by ultrafiltration assisted with copolymer of maleic acid and acrylic acid. *Desalination*, 2013;329:78-85.

[16] Juang R., Chen M. Measurement of binding constants of poly(ethylenimine) with metal ions and metal chelates in aqueous media by ultrafiltration. *Industrial and Engineering Chemistry Research*, 1996;35(6):1935-1943.

[17] Dai Z., Gjetting T., Mattebjerg M. A., Wu C., Andresen T. L. Elucidating the interplay between DNA-condensing and free polycations in gene transfection through a mechanistic study of linear and branched PEI. *Biomaterials*, 2011;32(33):8626-8634.

[18] Kobayashi S., Hiroishi K., Tokunoh M., Saegusa T. Chelating properties of linear and branched poly(ethylenimines). *Macromolecules*, 1987;20(7):1496-1500.

[19] Nguyen Q. T., Jyline Y., Neel J. Concentration of cupric and nickel ions by complexation-ultrafiltration-Synergic effect of succinic acid. *Desalination*, 1981;36(3);277-283.

[20] Rumeau M., Persin F., Sciers V., Persin M., Sarrazin J. Separation by coupling ultrafiltration and complexation of metallic species with industrial water soluble polymers-Application for removal or concentration of metallic cations. *Journal of Membrane Science*, 1992;73(2-3):313-322.

[21] Volchek K., Krentsel E., Zhilin Y., Shtereva G., Dytnersky Y. Polymer binding/ultrafiltration as a method for concentration and separation of metals. *Journal of Membrane Science*, 1993;79(2-3):253-272.

[22] Rivas B. L., Geckeler K. E. Polymer Synthesis Oxidation Processes. *Advances in Polymer Science*, 1992;102:171–88.

[23]Polyethylenimine, 2013. [online] http://en.wikipedia.org/wiki/Polyethylenimine.

[24] Molinari R., Argurio P., Poerio T. Ultrafiltration of polymer-metal complexes for metal ion removal from wastewaters. *Macromolar Symposia*, 2006;235(1):206–214.

[25] Molinari R., Argurio P., Poerio T. Comparison of polyethylenimine, polyacrylic acid and poly(dimethylamine-co-epichlorohydrin-co-ethylenediamme) in Cu^{2+} removal from wastewaters by polymer-assisted ultrafiltration. *Desalination*, 2004;162:217–228..

[26] Borbély G., Nagy E. Removal of zinc and nickel ions by complexation-membrane filtration process from industrial wastewater. *Desalination*, 2009;240:218-226.

[27] Molinari R., Poerio T., Argurio P. Selective separation of copper(II) and nickel(II) from aqueous media using the complexation–ultrafiltration process. *Chemosphere*, 2008;70:341-348.

[28] Shao J., Qin S., Li W., He Y. Simultaneous recovery of nickel and cobalt from aqeous solutions using complexation-ultrafiltration process. *Separation Science and Technology,* 2013;48(18):2735-2740.

CHAPTER 4

REMOVAL OF COPPER IONS FROM WASTEWATER BY POLYMER ASSISTED ULTRAFILTRATION

4.1 Literature Review

Water pollution is today a serious problem, due to fresh water being a vital and limited resource. Due to rapid and intensive industrialization, large volumes of aqueous wastes containing dangerous materials, such as heavy metals, are introduced into the environment [1]. These metal ions are non-biodegradable and can be toxic and carcinogenic even at very low concentrations, creating a serious threat to the environmental and public health [2,3]. Generally, cadmium, lead, zinc, nickel, copper and/or their compounds have been used extensively by various metal finishing, mining, chemical and electronic industries, leading to a sharp increase in the toxic contamination of water [4, 5]. In particular, copper is essential to human life and health, but its excess in the human body leads to stomach and intestinal distress, such as nausea, diarrhea and stomach cramps [6]. In addition, the toxicity of copper has been implicated in various neurodegenerative disorders, such as Wilson's disease and Alzheimer's disease. In fact, free copper in the brain has been associated with neuronal and cellular damage, promoting free radical production [7].

Although in some cases groundwater contains high levels of copper, the average copper concentration in lakes, rivers and groundwater is about 4 μg/L [1]. In order to prevent the harmful effects of copper, the U.S. Environmental Protection Agency

(EPA) stated that the limit of the concentration of copper allowed in drinking water is 1.3 mg/L [1].

As a consequence, there is strong demand to develop efficient and low-cost treatment methods for wastewater. The general processes developed to clean up these heavy metals from wastewater include chemical precipitation [8,9], ion exchange, coagulation, complexation, solvent extraction, and membrane separation [1-12]. However, these techniques come with significant disadvantages, such as their high maintenance costs due to high energy consumption the incomplete removal of metals, and the production of toxic sludge [8,12]. To overcome these limitations and to reduce the heavy metals concentration to the required level, considerable efforts have been devoted to removing heavy metal cations by membrane separation, which offers a promising approach to the treatment of wastewater [13-20].

The development of membrane technology offers significant advancement in achieving metal removal and/or recovery from wastewater. Their importance on the industrial scale is exemplified especially in gas and liquid separation, due to their simple operation, ease of scale-up and efficient energy usage. Emphasis placed on fabricating structures with controlled and novel pore architectures has led to more efficient and cost effective purification [21,22]. The membrane processes used for heavy metal removal are reverse osmosis, nanofiltration, electrodialysis and ultrafiltration. During the reverse osmosis and nanofiltration operations, it is necessary to apply high transmembrane pressures, which increases operating cost while yielding relatively low permeate flow rate. However, ultrafiltration process takes place at low transmembrane pressures. Even though this would reduce the operation cost of the filtration processes, low molecular weight complexes and metal ions may still pass easily through ultrafiltration membranes as a result of their large pore sizes. In order to overcome these problems an solution for the removal of heavy metals from water, called polymer-assisted ultrafiltration (PAUF), has been proposed [8,18,19]. The PAUF method uses water-soluble polymers that form macromolecular complexes with metallic ions. The UF membranes, having a smaller molecular weight cut-off than the molecular weight of the metal-polymer complex, will block the macromolecular complexes, while still allowing the non-complexed metal ions to pass through the membrane. Polyacrylic acid (PAA), polyethylenemine (PEI), poly(dimethylamine–co–

65

epichlorohydrin–co– ethylenediamine) (PDEHED), diethylaminoethyl cellulose and humic acid are the most commonly used complexing agents providing a selective separation and recovery of heavy metals [8].

Polymeric membranes are widely produced due to their simple processability, intrinsic transport properties and low cost, albeit at the expense of selectivity and permeability. Such membranes are also vulnerable to fouling and weakened in chemical resistance [21].

Instead, a viable alternative is polyether ether ketone (PEEK), which is a glassy polymer with high degree of crystallinity, high thermal and chemical stability as well as good mechanical properties [23]. Unfortunately, PEEK is not soluble in water or in most organic solvents. Thus, it is not possible to apply the commonly used phase-inversion technique for membrane production [24]. However, this problem is solved by the synthesis of PEEK-WC with a phthalidecardo group by polycondensation of dichlorobenzophenone and phenolphthalein [25]. The more amorphous structure of PEEK-WC due to the presence of bulky phenolphthalein allows it to become more soluble in some organic solutions, such as DMA, DMF, THF, NMP [24,25]. Since solubility of the polymer with this modification is improved, the PEEK-WC membranes can be prepared by simple, conventional solution-casting or phase-inversion methods. The phase-inversion method is well-suited toward producing thin and asymmetric membranes [26]. Moreover, PEEK-WC still offers the outstanding mechanical, chemical, and thermal properties of the parent polymer. To complement the advantageous material characteristics of PEEK-WC, it also enables the production of both asymmetrically dense and porous membranes, depending on the proper choice of solvent/non-solvent system [27]. Finally, the low-cost and simple, single-step preparation of PEEK-WC membranes is a compelling advantage over commercial composite hydrophilic membranes [28].

In this work, the removal of the PEI-Cu complex from aqueous solutions was carried out by using flat PEEK-WC membranes prepared at lab-scale. The aim of the study was to develop an alternative typology of membranes with respect to those normally employed for the Cu^{2+} extraction, able to reduce the fouling of membrane, while ensuring good rejection of Cu^{2+} transport from the feed to the extractant.

66

Asymmetric flat PEEK-WC membranes were casted from a polymer solution containing PEEK-WC as the polymer and DMA as the solvent, by the dry/wet phase-inversion process. The effect of evaporation time on membrane morphology and properties was investigated.

4.2 Experimental Procedure

4.2.1 Materials

PEEK-WC, shown in Figure 2.3, used as membrane forming material, was supplied from Chanchung Institute of Applied Chemistry, Academia Sinica. N,N-dimethylacetamide (DMA), used as polymer solvent, was purchased from Carlo Erba and used without further purification. Branched polyethylenimine (B-PEI), shown in Figure 3.2-b, polymer complexing agent, was purchased from Sigma-Aldrich. The polymer, having average M_w 25,000 g/mol and M_n 10,000 g/mol, was used without any purification. Copper sulphate penta-hydrate ($CuSO_4 \cdot 5H_2O$) from Fluka Chemika (purity <99%) was used for preparing Cu^{2+} solutions. Distilled water was used for coagulation bath whereas ultra-pure water (Millipore Qwater systems) was used for membrane permemability measurements and complexation tests. These tests were carried out in the laboratories of ITM-CNR, Rende, Italy. These tests, identical to studies in *Chapter 3,* were performed for a second time, prior to PAUF tests in order to validate the optimization conditions were consistent.

4.2.2 Membrane Preparation

Preparation of PEEK-WC membranes were explained in detail in *Section 2.2.1.* According to the same procedure, the membranes were prepared by wet and dry-wet phase-inversion techniques [34]. With respect to the results in *Chapter 2,* only

ultrafiltration membranes were chosen to be studied in this part of the work. Among the membranes listed in Table 2.7, DW-0, DW-1, and DW-2 membranes were preferred for PAUF applications due to their high water permeances. As explained in *Chapter 2,* PEEK-WC was dissolved in DMA at a concentration of 15 wt.% at room temperature. The polymer solution was magnetically stirred for at least 24 hours to ensure complete dissolution of the polymer. Afterwards, the solution was sonicated for 15 minutes to remove the air bubbles in the solution that could potentially cause defects to form in the membrane. The solution was cast uniformly onto a glass support by means of a hand-casting knife with a knife gap set at 250 μm and followed by immersion in a coagulation bath after exposure for a fixed time to the air (0, 1, and 2 minutes). After complete coagulation, the membranes were transferred into a pure water bath, which was refreshed frequently for at least 24 hours to remove the traces of solvent. The membranes were stored in a water bath until tested for water permeability. In Table 4.1, the membranes and the experimental conditions used for their preparation are listed.

Table 4.1 Experimental conditions used for the preparation of PEEKWC membranes

Membrane Code	Method	Evaporation Time (s)
DW-0	Wet inversion	0
DW-1	Dry-wet inversion	1
DW-2	Dry-wet inversion	2

4.2.3 Membrane Characterization

Different characterization techniques were used to evaluate the effect of evaporation time on the structure of the prepared membranes. The morphology of the membranes was examined by scanning electron microscopy (SEM, Cambridge Zeiss

LEO 400). Cross-sections were prepared by freeze-fracturing each sample in liquid nitrogen, in order to obtain a sharp fracture without modification to the morphology. In addition to the cross-sections, the "air" and the "glass" sides for each membrane were analyzed.

The membrane thickness was measured by using a digital micrometer (Carl Mahr D 7300 Esslingen a.N.), averaging five measurements, and by SEM analysis of the freeze-fractured cross-sections of the membranes.

Pore size distribution was determined by a Capillary Flow Porometer (CFP 1500 AEXL). The porometry tests were performed in dry-up/wet-up mode. The dry samples were immersed in the wetting fluid Porewick, from PMI—(surface tension = 16×10-5 J $\times$ cm^{-1} (16 dyne $\times$ cm^{-1})—for at least 15 min and then placed in the sample chamber with an effective area of 3.14 cm^2.
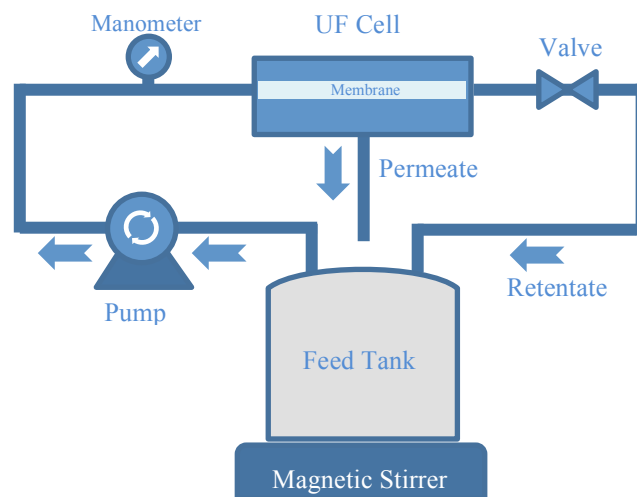
Figure 4.1 Scheme of experimental ultrafiltration set-up

The membrane flux was determined (before and after membrane use) using the system shown in the schematic in Figure 4.1. The core of the system is a permeation cell operating in cross-flow mode (Figure 4.2) with a membrane area of 12.6 cm^2. The hydraulic permeance was calculated as a slope of the linear fitting through the axes origin of the permeating flux as a function of the applied trans-membrane pressure (0.2-0.8 bar).
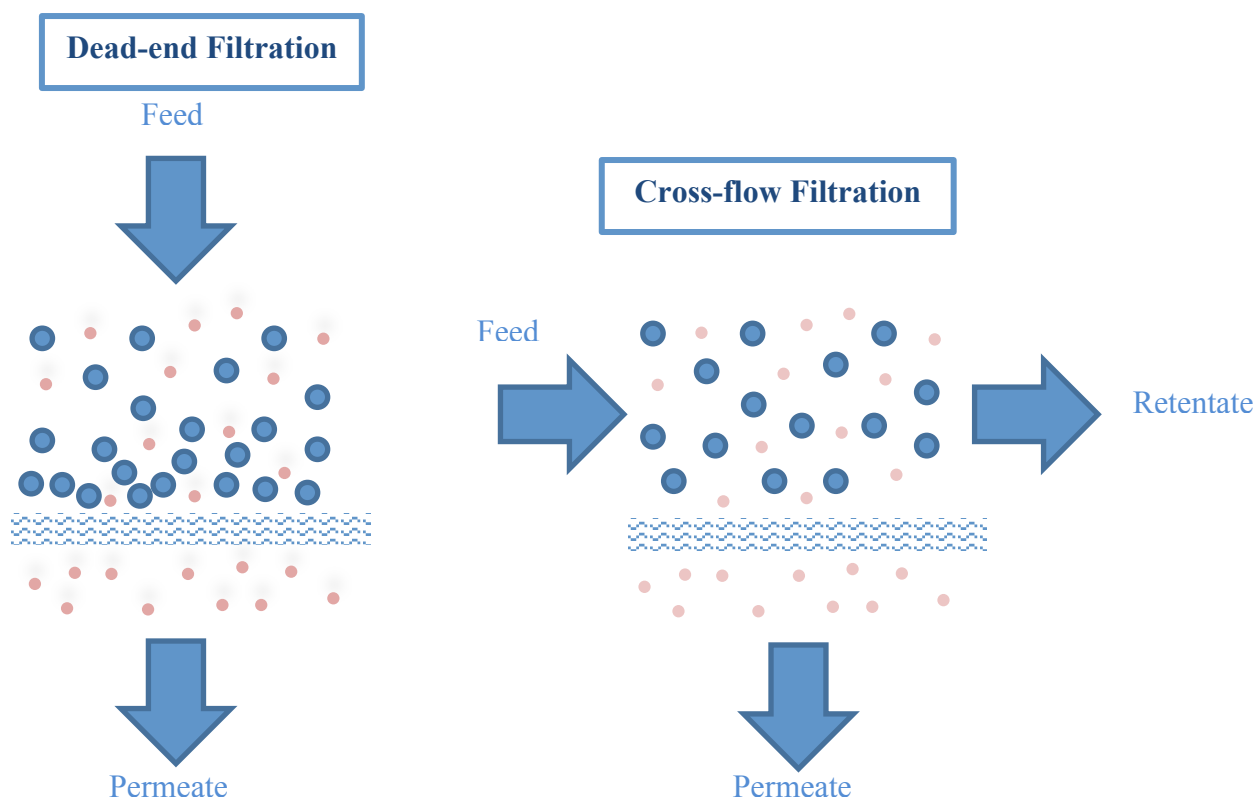
Figure 4.2 Dead-end and cross-flow filtration

4.2.4 Complexation Tests

Copper complexation and maximum bonding capacity between PEI-Cu^{2+} were evaluated as a function of pH and copper concentration by spectrophotometric measurement at wavelength of 632.5 nm (Perkin Elmer lambda EZ 201). The bonding capacity was evaluated using Eq. 3.5.

4.2.5 PAUF Tests

The PAUF tests were carried out setting the operative pressure at 0.5 bar. The system operated in batch mode recycling the permeate into the feed tank. The measurements were performed every 30 minutes collecting 1 mL of the permeate that

was analyzed for the determination of the copper concentration. Each test was stopped after reaching the steady-state. The rejection percentage R (%) was determined using the following equation:

$$R(\%) = \left(1 - \frac{C_p}{C_f}\right) \times 100$$

(4.1)

where C_f and C_p indicate the PEI-Cu complex concentration in the initial feed and in the permeate, respectively. In addition, other experiments were carried out in concentration mode using the same operating conditions. The experiments were replicated three times.

4.3 Results and Discussion

4.3.1 Membrane Characterization

SEM images of PEEK-WC membranes are shown in Figures 4.3-4.5. SEM analyses demonstrated that membranes have a finger-like macro-void structure. The cross-section images of all membranes showed a regular structure along the thickness. Moreover, the membranes exposed to shorter evaporation time are thinner. Membrane thickness was affected by the exposure time to air as demonstrated by SEM images and thickness measurements. The average thicknesses were 103.5, 100.1 and 98.8 μm for membranes having 0, 1 and 2 minutes of evaporation time, respectively.
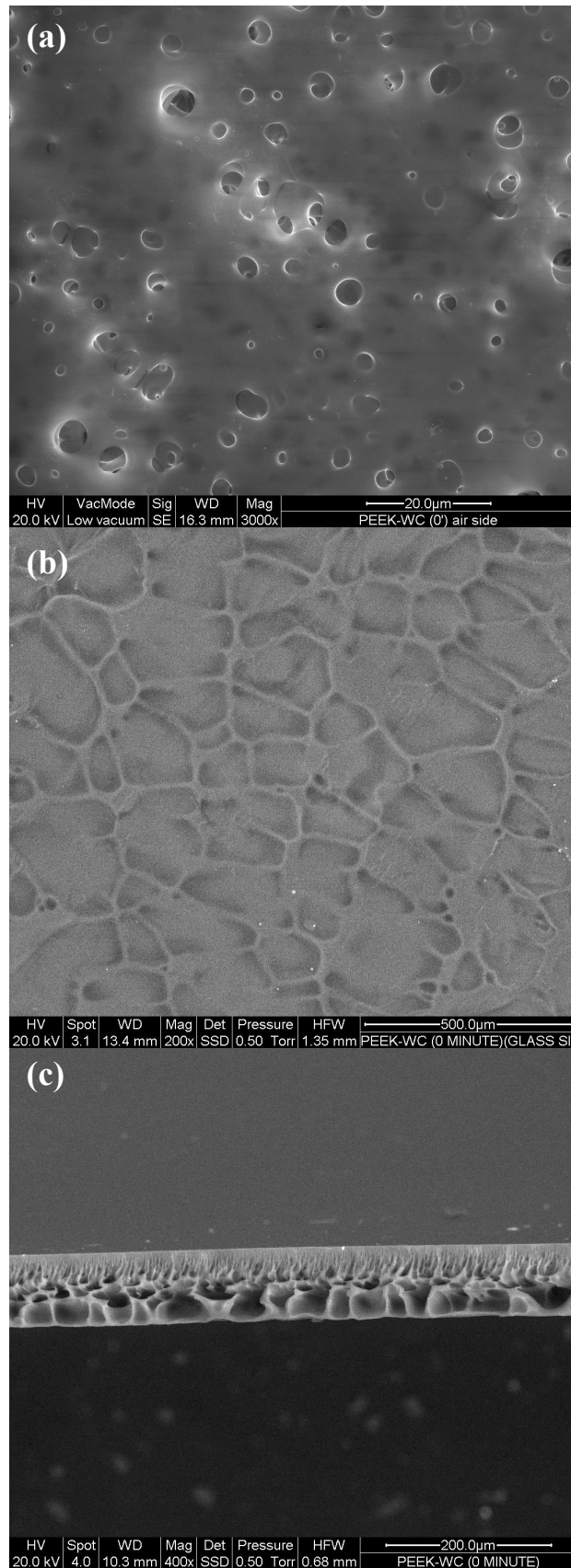
Figure 4.3 SEM micrographs of (a) "air" side, (b) "glass" side, (c) cross-section of membrane prepared by 0 min of evaporation time (wet method).
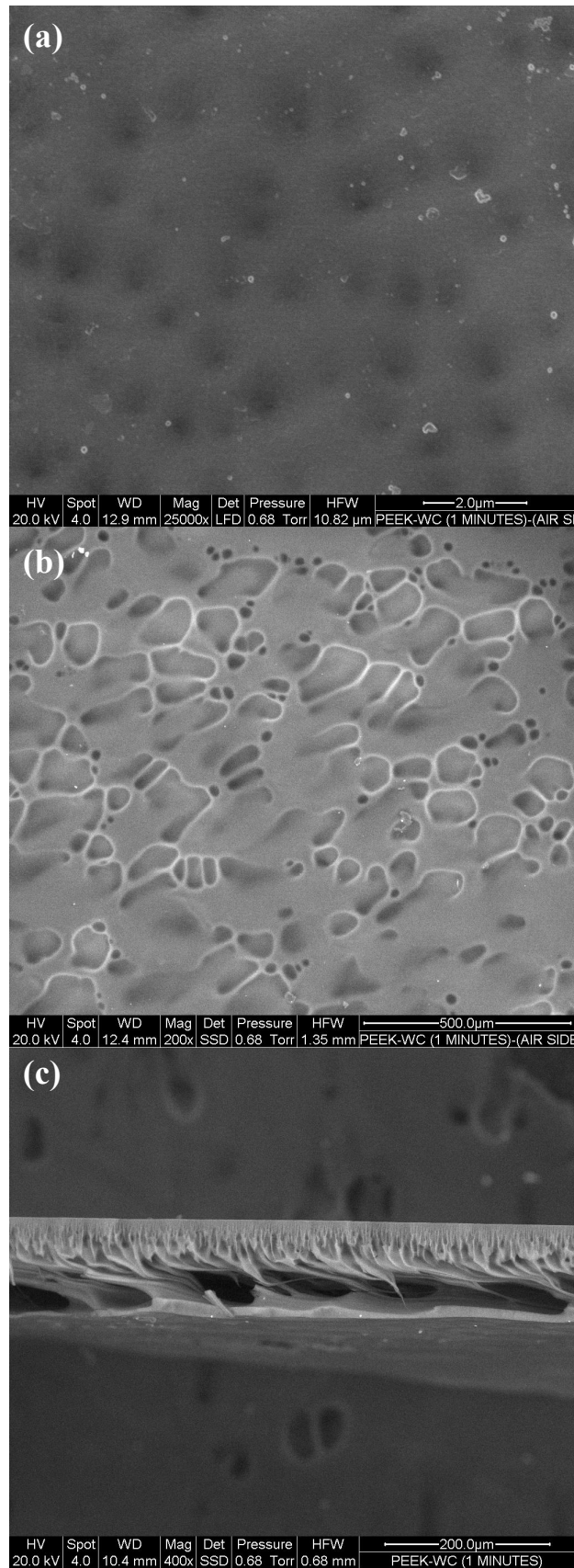
Figure 4.4 SEM micrographs of (a) "air" side, (b) "glass" side, (c) cross-section of membrane prepared by 1min evaporation time (dry-wet method).
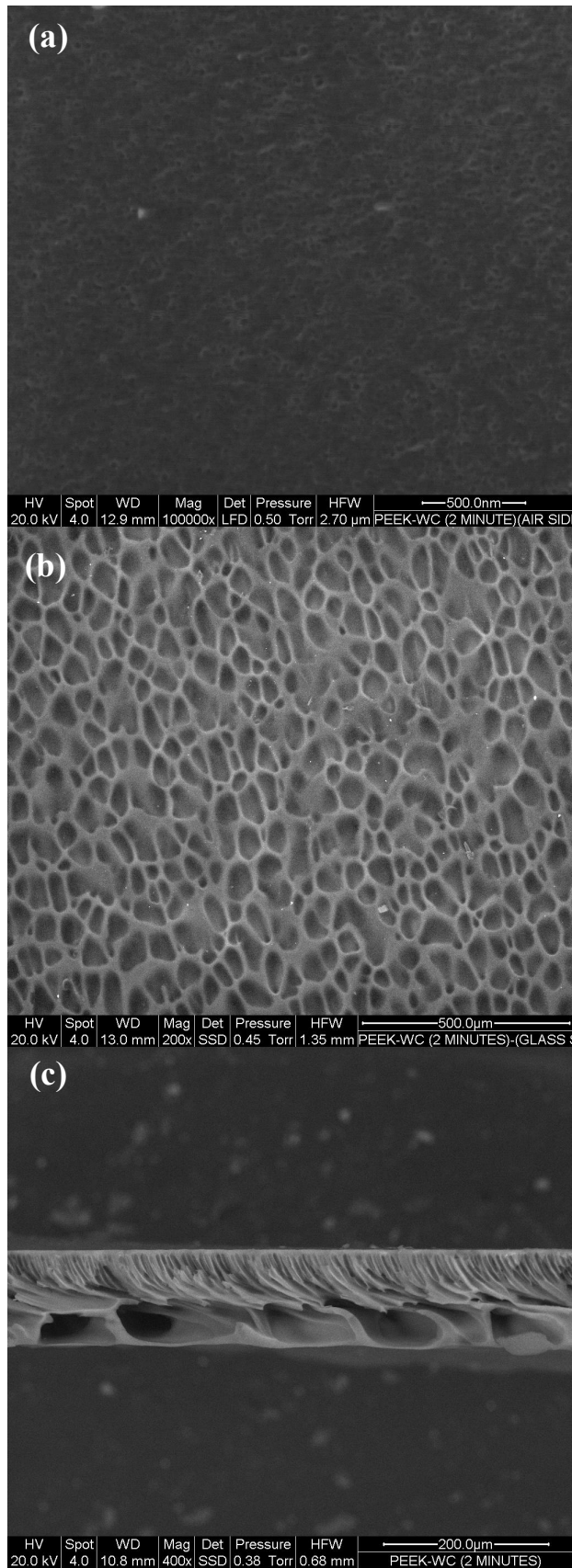
Figure 4.5 SEM micrographs of (a) "air" side, (b) "glass" side, (c)-(d) cross-section of membrane prepared by 2 min evaporation time (dry-wet method)
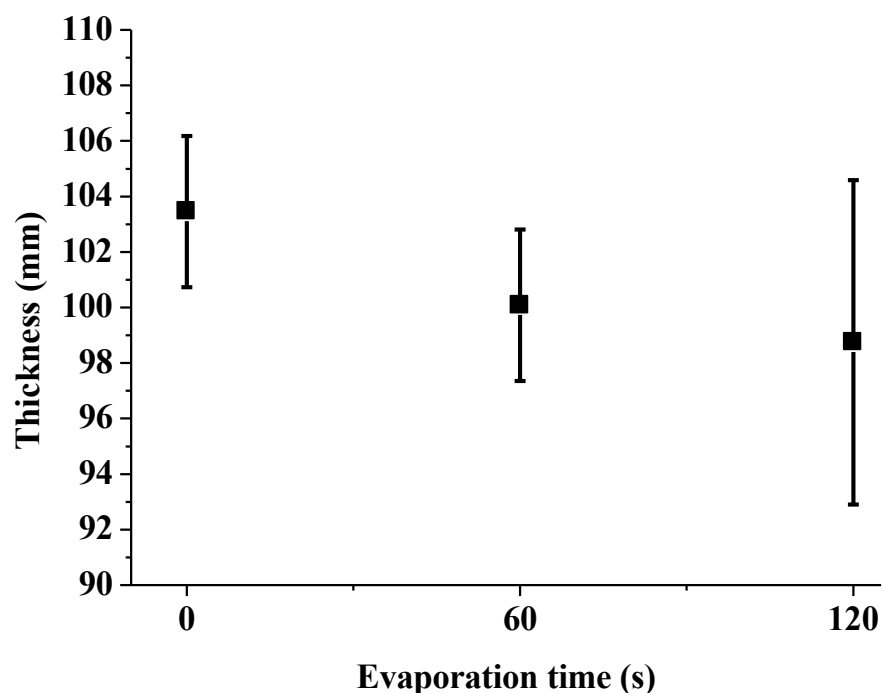
Figure 4.6 Average thickness of membranes with respect to evaporation time

Table 4.2 reports the diameter at maximum pore size distribution of membranes prepared at different evaporation time. These results indicated as the solvent evaporation time influences the pore size and pore size distribution as shown in Figure 4.7. In fact, the cast solution exposed to the air for 1 min and 2 min exhibited similar pore diameter (0.05 μm), while, a larger pore diameter (0.08 μm) was observed to have emerged from immediately quenching the cast solution into a coagulation bath. In addition, a narrow pore size distribution was obtained by avoiding air exposure of the cast solution (Figure 4.7-DW-0). A possible explanation of this behavior is a very rapid demixing between the two liquids that occurs in the wet method.

Table 4.2 Pore diameter of the PEEK-WC membranes

Membrane	Diameter at maximum pore size distribution (μm)
DW-0	0.08
DW-60	0.05
DW-120	0.05
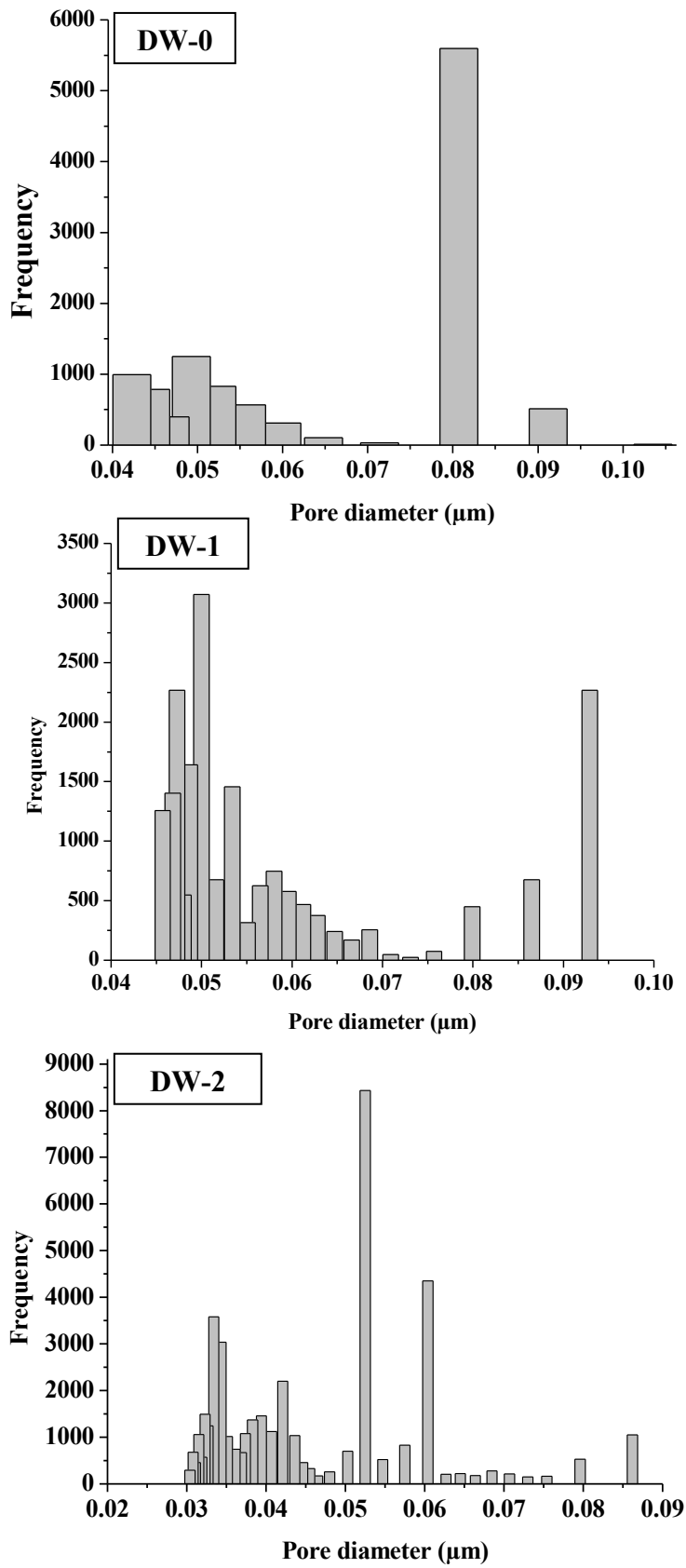
Figure 4.7 Pore size distributions of the PEEK-WC membranes prepared using different evaporation times.

Table 4.3 summarizes the water flux at 0.5 bar and the hydraulic permeance characteristics of the prepared membranes. The hydraulic permeance of the membranes decreased as the solvent evaporation time increased.

Table 4.3 Water flux and hydraulic permeance of PEEK-WC membranes.

Membrane	Evaporation Time (min)	Water Flux at 0.5 bar (L/h·m^2)	Hydraulic Permeance (L/h·m^2·bar)
DW-0	0	181 ±7	361 ±14
DW-1	1	136±3	272±6
DW-2	2	55±5	110±8

In order to evaluate the bonding capacity of PEI, complexation tests were carried out by varying pH and copper concentration. Figure 4.8 shows the effect of pH on PEI bonding capacity fixing the polymer and copper concentrations at 150 mg/L and 50 mg/L, respectively. Results indicate that the maximum bonding percentage was observed at pH 6. At low pH (pH < 3), due to the poor affinity between polymer and ion, the bonding capacity is very low. These results are in agreement with those obtained by Molinari *et al.* [18,19].

On the basis of the results of Figure 4.9, other experiments were performed by fixing the pH at 6 and varying the copper concentration. Better bonding capacity was obtained at 1:1 weight ratio of PEI:Cu^{2+}. Higher bonding capacity (higher copper removal) allows reduction of the PEI amount , thereby reducing processing costs.
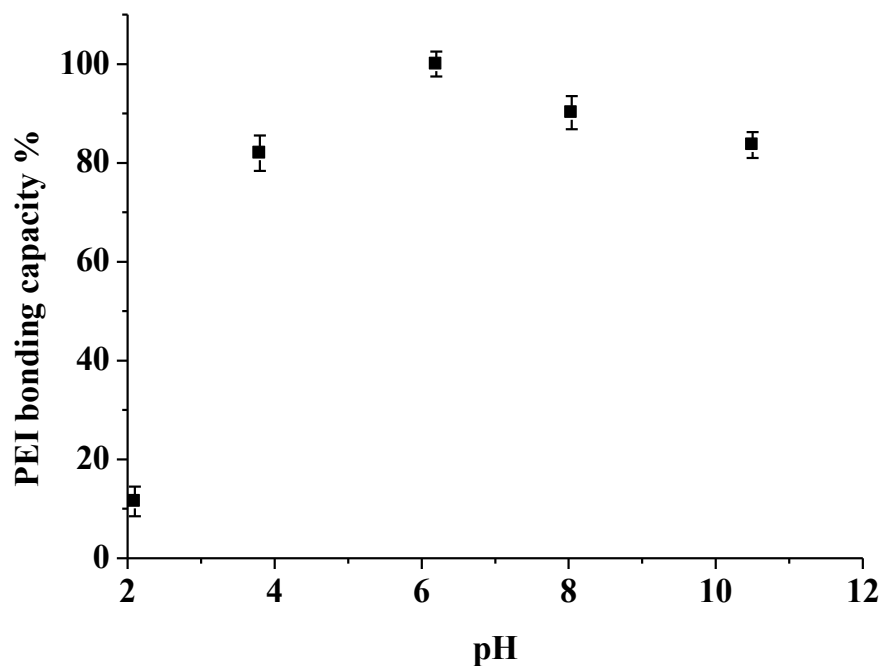
Figure 4.8 PEI bonding capacity (%) vs pH (B-PEI = 150 mg/L; Cu^{2+}= 50mg/L).
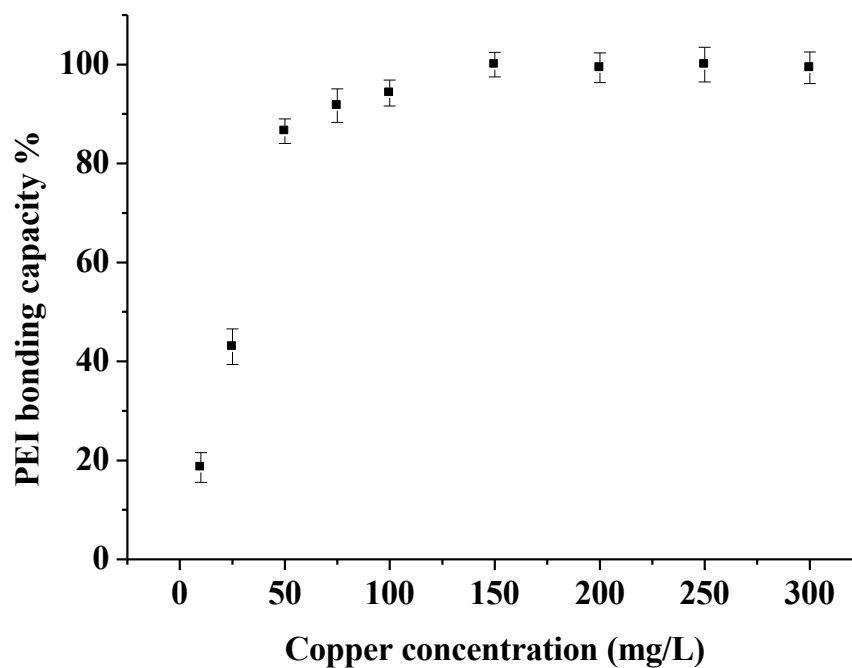
Figure 4.9 PEI bonding capacity (%) percentage vs copper concentration (B-PEI concentration = 150 mg/L, pH=6).
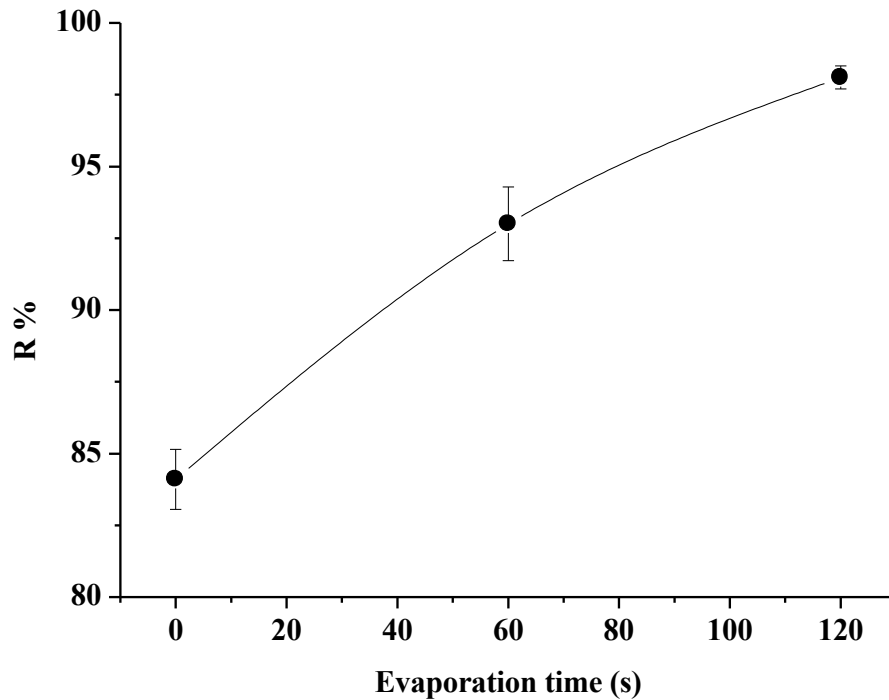
Figure 4.10 Effect of evaporation time on the rejection of PEI-Cu complexes

PAUF tests were carried out using the optimized operating conditions: 150 mg/L of PEI, 150 mg/L of copper concentrations and pH 6. Figure 4.10 shows the rejection, R (%), for the different prepared membranes. Higher rejection (98 %) was obtained for the DW-2 membrane. This result is due the membrane preparation method, which favored both the formation of a thicker skin layer and pores with diameter in the range of 0.03-0.04 μm, which are not present in the membranes DW-0 and DW-1. Table 4.4 compares and summarizes the permeance and rejection characteristics of different membranes reported in the literature. Although, PAN membranes showed a better rejection with higher permeance values, it should be noted that the average MW of PEI (average MW=60 kDa) used by Poerio et al. in these study was higher than B-PEI used in this work (average MW = 10 kDa). Taking this into consideration, the values reported below showed that PEEK-WC membranes can be candidates for PAUF applications, due to their metal ion rejection capacity.

Table 4.4 Heavy metal removal by PAUF

Membrane	Membrane Material	Polymer-Metal Complex x	Polymer-Metal Complex Concentration (per L)	Average MW of Polymer (kDa)	Hydraulic Water Permeance (l/h·m²·bar)	Hydraulic Permeance of PAUF test (l/h·m²·bar)	R, %	Reference
DW-0	PEEK-WC	PEI-Cu	150 mg/150 mg	10	406.4	92.6	84.1	This work
DW-1	PEEK-WC	PEI-Cu	150 mg/150 mg	10	277.5	74.4	93.0	This work
DW-2	PEEK-WC	PEI-Cu	150 mg/150 mg	10	110.2	33.9	98.1	This work
Ceramic 15	Carbon/zirconia composite	PEI-Cu	1000 mg/500 mg	25	42.5	24.0	94.0	[38]
Iris 10	PES	PEI-Cu	150 mg/50 mg	60	99.1	60.3	99.0	[18,19]
PANGKSS HV3/T	PAN	PEI-Cu	150 mg/50 mg	60	211.6	120.6	99.1	[18,19]
PANGKSS HV2/T	PAN	PEI-Cu	150 mg/50 mg	60	217.9	126.9	99.1	[18,19]
UTC 60 ROPUR	Cross-linked polyamide	PEI-Cu	150 mg/50 mg	60	59.3	14.8	99.9	[18,19]
PES	PES	CMC-Cu	1000 mg/10 mg	-	-	39.0	97.6	[14]
PES	PES	CMC-Cu	1000 mg/100 mg	-	-	39.0	98.5	[14]
M1	PVA/cellulose	PVA-Cu	0.2 mg/6.4 mg	72	217.4	713.3	44	[37]
SIKA-R 0.1 AS	Metallic (tubular)	PAA-Cu	300 mg/108 mg	250	-	592.9	91.5	[16]
Regenerated Cellulose	Regenerated cellulose	PEI-Co	382 mg/65mg	750	14.3	9.9	91.5	[15]

The flux degradation over time is a very critical problem in pressure driven membrane processes. Concentration polarisation and membrane fouling are the main reasons that cause decline of the flux over time during actual separation processes [39]. In order to determine the effect of fouling and concentration polarisation in UF membranes, concentration mode operation tests were carried out after the PAUF tests. PEI-Cu complex solutions were filtered through PEEK-WC membranes in concentration mode (without any recycling of the permeate). The results (Table 4.5) show that there was a decrease in hydraulic permeance, since it was 406.4 for an ultra-pure water flux test, 92.6 for PAUF, and 65.9 for a concentration mode test for DW-0. In contrast, an increase was observed in the rejection values, *i.e.* from 84.1% to 94.8% for DW-0. The membranes DW-1 and DW-2 also showed similar behavior. This was an expected result due to the PEI-Cu complex concentration increase in the retentate. Additionally, as the membrane structure became denser, the difference in the results of PAUF and concentration mode test decreased. On the other hand, the low reduction in permeate flux values during concentration mode tests showed that there is a very slight effect of concentration polarization on PEEK-WC membranes. Also, this effect can be seen from plots of hydraulic permeance versus time, recorded *in-situ* during the analysis (Figure 4.11). At the end of the experiments, the formation of a light blue thin layer of polymer-copper complexes on the filtering surface of the membrane was observed.

Table 4.5 Results of concentration mode operation tests

Membrane	Hydraulic Pure Water Permeance $(l/h \cdot m^2 \cdot bar)$	Hydraulic Permeance of PAUF Test $(l/h \cdot m^2 \cdot bar)$	Hydraulic Permeance of Concentration Mode Test $(l/h \cdot m^2 \cdot bar)$	R,% after PAUF Test	R*, % after Concentration Mode Test
DW-0	406.4	92.6	65.9	84.1	94.8
DW-1	277.5	74.4	62.3	93.0	93.9
DW-2	110.2	33.9	34.7	98.1	98.0
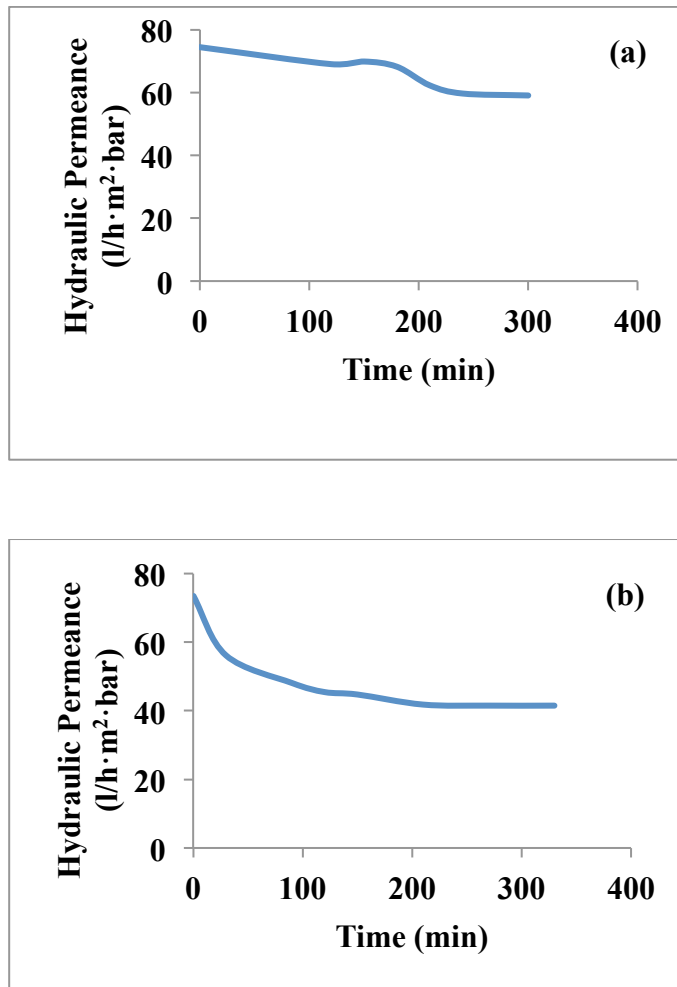
Figure 4.11 Flux behavior of DW-1 during a) first and b) second concentration mode operation

4.3.2 Membrane Washing and Reuse

The possibility of reusing membranes in PAUF process and consequent loss in performance was evaluated by carrying out three UF tests. After initial water flux analysis of the PEEK-WC membranes, the following steps were performed:

(i)   UF test was carried out until steady state condition was reached

(ii)   Concentration mode operation test was performed

(iii)   The membrane was washed with 15 *l* of distilled water without recycling

(iv)   Membrane characterization, UF_1

(v)   Repeat steps (i)-(iv), UF_2

(vi)   Membrane was washed with 1 *l* of diluted HCl (pH = 3) without recycling

(vii)   Membrane characterization, UF_3

In order to avoid cake compaction, membrane washing processes were performed at minimum transmembrane conditions. The results are summarized in Figure 4.12. According to these results, the reduction of membrane performance was 29.4, 32.7, and 27.3% for UF_1, UF_2, and UF_3. Although washing the membrane with acid having pH = 3 provided a 5.4% increase in the performance of membrane, due to the decomplexation of PEI-Cu complexes, the membrane performance was almost constant after UF_1. These results were important for long-standing use of same membrane.
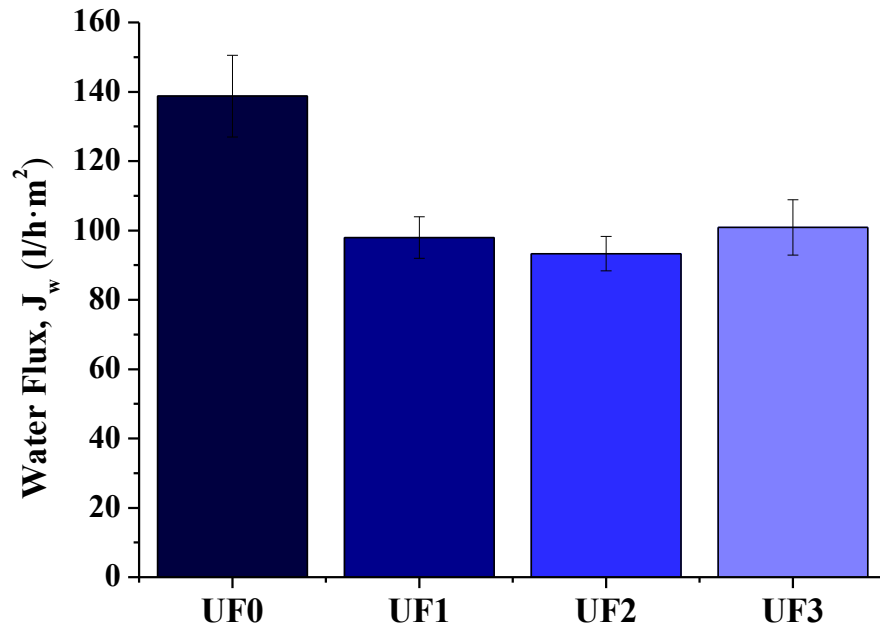
Figure 4.12 Water flux at 0.5 bar for DW-0 after PAUF tests

In addition, DW-2 membrane was washed with only 5 liters of distilled water without recycling. Specifically, the following procedure was followed;

(i)   UF test was carried out until steady state condition was reached

(ii)   Concentration mode operation test was performed

(iii)   The membrane was washed with 5 *l* of distilled water without recycling

(iv)   Membrane characterization, UF_1

(v)   Repeat steps (i)-(iv), UF_n

Subsequent testing with ultra-pure water exhibited almost a full recovery of the membrane, around 94.5 %, as shown in Figure 4.13. This high degree of recovery can be explained by the more compact nature of the membrane, which prevented the PEI-Cu complexes from blocking its pores. So, a simple washing of the membrane can lead to remove the formed thin layer of PEI-Cu complexes.
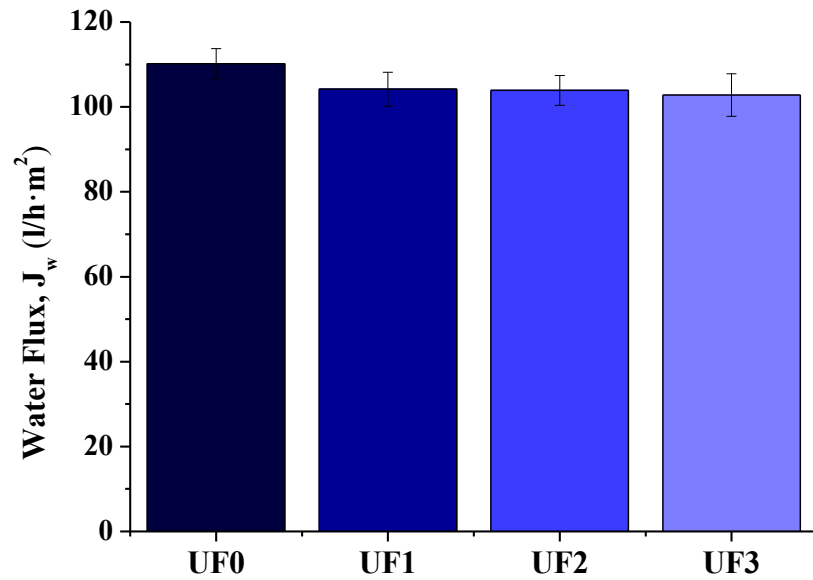
Figure 4.13 Water flux at 0.5 bar for DW-2 after PAUF tests

4.4 Conclusions

PEEK-WC membranes, exposed to various evaporation times, were produced by wet and dry-wet phase inversion method. The membranes were in the range of ultrafiltration membranes for separation of PEI-Cu from water. Polymer-copper complexation tests revealed that the optimum condition for binding occurred at pH ~6.2 with concentrations of 150 mg/L copper and 150 mg/L B-PEI. These results were consistent with the optimization conditions, which are mentioned in *Chapter 3*. DW-0 membranes, prepared without exposing to air, demonstrated a sufficient rejection of Cu^{2+} (93%) during PAUF tests. Also, washing processes revealed that performance of these membranes can be recovered up to 72.7%. A denser structure of PEEK-WC membranes, DW-120, corresponded to a higher rejection of Cu^{2+} (98%), although there was a sharp reduction in permeance. All membranes showed a constant permeance profile with respect to time. This strongly indicated that there was no effect of concentration polarization on the membranes. Also, both long-term and short-term stability (in means of flux and selectivity) of these membranes validated the reduction of fouling effect due to the chemical stabilility of PEEK-WC. In spite of the decrease in permeances, reusability and almost complete recovery (94.5%) of the used membranes make these membranes an attractive alternative for industrial applications. Specifically, almost full recovery of performance of PEEK-WC membranes, just by washing with water, makes them significant among commercially used membranes.

REFERENCES

[1] Khan M.N., Wahab M.F. Characterization of chemically modified corncobs and its application in the removal of metal ions from aqueous solution. *Journal of Hazardous Materials*, 2007;141: 237–244.

[2] Liu C., Bai R., Ly Q.S. Selective removal of copper and lead ions by diethylenetriamine- functionalized adsorbent behaviours and mechanisms. *Water Research*, 2008;42:1511–1522.

[3] Vilar V.J.P., Botelho C.M.S., Boaventura R.A.R. Copper desorption from Gelidium algal biomass. *Water Research*, 2007;41:1569–1579.

[4] Dobson R.S., Burgess J.E. Biological treatment of precious metal refinery wastewater: A review. *Minerals Engineering*, 2007;20:519–532.

[5] Aziz H.A., Adlan M.N., Ariffin K.S. Heavy metals (Cd, Pb, Zn, Ni;Cu and Cr(III)) removal from water in Malysia: Post treatment by high quality limestone. *Bioresource Technology*, 2008;99:1578–1583.

[5] Bertinato J., L'Abbé M.R. Maintaining copper homeostasis: Regulation of copper-trafficking proteins in response to copper deficiency or overload. *Journal of Nutritional Biochemistry*, 2004;15:316–322.

[7] Parmar P., Daya S. The effect of copper on (3H)-tryptophan metabolism in organ cultures of rat pineal glands. *Metabolic Brain Disease*, 2001;16(3-4):199–205.

[8] Fu F., Wang Q. Removal of heavy metal ions from wastewaters: A review. *Journal of Environmental Management*, 2011;92:407-418.

[9] Ku Y., Jung I.L. Photocatalytic reduction of Cr(VI) in aqueous solutions by UV irradiation with the presence of titanium dioxide. *Water Research*, 2001;35(1):135-142.

[10] Kurniawan T.A., Chan G.Y.S., Lo W.H., Babel S. Physico–chemical treatment techniques for wastewater laden with heavy metals. *Chemical Engineering Journal*, 2006;118(1-2):83–98.

[11] Meunier N., Drogui P., Montan'e C., Hausler R., Mercier G., Blais J.F. Comparison between electrocoagulation and chemical precipitation for metals removal from acidic soil leachate. *Journal of Hazardous Materials*, 2006;137(1):581–590.

[12] Sanchez A.G., Ayuso E.A. Sorption of Zn, Cd and Cr on calcite-Application to purification of industrial wastewaters. *Minerals Engineering*, 2002;15(7):539–547.

[13] Danisa, U., Aydiner, C. Investigation of process performance and fouling mechanisms in micellar-enhanced ultrafiltration of nickel-contaminated waters. *Journal of Hazardous Materials*, 2009;162(2-3):577-587.

[14] Barakat, M.A., Schmidt, E. Polymer-enhanced ultrafiltration process for heavy metals removal from industrial wastewater. *Desalination*, 2010;256(1-3):90-93.

[15] Cojocaru C., Zakrzewska-Trznadel G., Jaworska A. Removal of cobalt ions from aqueous solutions by polymer assisted ultrafiltration using experimental design approach. part 1: Optimization of complexation conditions. *Journal of Hazardous Materials*, 2009;169(1-3):599–609.

[16] Cojocaru C., Zakrzewska-Trznadel G. Response surface modeling and optimization of copper removal from aqua solutions using polymer assisted ultrafiltration. *Journal of Membrane Science*, 2007;298(1-2):56–70.

[17] Camarillo R., Pérez Á., Cañizares P., de Lucas A. Removal of heavy metal ions by polymer enhanced ultrafiltration: Batch process modeling and thermodynamics of complexation reactions. *Desalination*, 2012;286:193–199.

[18] Molinari R., Argurio P., Poerio T. Ultrafiltration of polymer-metal complexes for metal ion removal from wastewaters. Macromolar Symposia, 2006;235(1):206–214.

[19] Molinari R., Argurio P., Poerio T. Comparison of polyethylenimine, polyacrylic acid and poly(dimethylamine-co-epichlorohydrin-co-ethylenediamme) in Cu^{2+} removal from wastewaters by polymer-assisted ultrafiltration. *Desalination*, 2004;162:217–228.

[20] Molinari R., Poerio T., Argurio P. Selective separation of copper(II) and nickel(II) from aqueous media using the complexation–ultrafiltration process. *Chemosphere*, 2008;70:341-348.

[21] Ismail A.F., Goh P.S., Sanip S.M., Aziz M. Transport and separation properties of carbon nanotube-mixed matrix membrane. *Separation and Purification Technology*, 2009;70(1):12-26.

[22] Clarizia G., Algieri C., Regina A., Drioli E. Zeolite-based composite PEEK-WC membranes: Gas transport and surface properties. *Microporous and Mesoporous Materials*, 2008;115(1-2):67–74.

[23] Brunetti A., Simone S., Scura F., Barbieri G., Figoli A., Drioli E. Hydrogen mixture separation with PEEK-WC asymmetric membranes. *Separation and Purification Technology*, 2009;69(2):195-204.

[24] Gordano A., Clarizia G., Torchia A., Trotta F., Drioli E. New membranes from PEEK-WC and its derivatives. *Desalination*, 2002;145(1-3):47-52.

[25] Jansen J.C., Drioli E. Poly(ether ether ketone) derivative membranes—A review of their preparation, properties and potential. *Polymer Science Series A*, 2009;51(11):1355-1366.

[26] Jack U. *Fabrication of wet phase inversion capillary membrane, dimension and diffusion effects*. (2006). MTech thesis, Cape Peninsula University of Technology, 2006.

[27] Yampolskii Y., Pinnau I., Freeman B.D. *Materials Science of Membranes for Gas and Vapor Separation*. Wiley, Chichester, 2006.

[28] Buonomenna M.G., Golemme G., Jansen J.C., Choi S.-H. Asymmetric PEEKWC membranes for treatment of organic solvent solutions. *Journal of Membrane Science*, 2011;368(1-2):144-149.

[29] Rivas B.L., Pereira D. Moreno-Villoslada I. Water-soluble polymer-metal ion interations. *Progress in Polymer Science*, 2003;28:173-208.

[30] Juang R., Chen M. Measurement of binding constants of Poly(ethylenimine) with metal ions and metal chelates in aqueous media by ultrafiltration. *Industrial and Engineering Chemistry Research*, 1996;35(6):1935-1943.

[31] Kobayashi S., Hiroishi K., Tokunoh M., Saegusa T. Chelating properties of linear and branched poly(ethylenimines). *Macromolecules*, 1987;20(7):1496-1500.

[32] Nguyen Q. T., Jyline Y., Neel J. Concentration of cupric and nickel ions by complexation-ultrafiltration-Synergic effect of succinic acid. *Desalination*, 1981;36(3):277-283.

[33] Rumeau M., Persin F., Sciers V., Persin M., Sarrazin J. Separation by coupling ultrafiltration and complexation of metallic species with industrial water soluble polymers-Application for removal or concentration of metallic cations. *Journal of Membrane Science*, 1992;73(2-3):313-322.

[34] Volchek K., Krentsel E., Zhilin Y., Shtereva G., Dytnersky Y. Polymer binding/ultrafiltration as a method for concentration and separation of metals. *Journal of Membrane Science*, 1993;79(2-3):253-272.

[35] Rivas B.L., Pereira D. Moreno-Villoslada I. Water-soluble polymer-metal ion interations. *Progress in Polymer Science*, 2003;28:173-208.

[36] Rivas B. L., Geckeler K. E. Polymer Synthesis Oxidation Processes. *Advances in Polymer Science*, 1992;102:171–88.

[37] Ciftci C., Kaya A. Preparation of poly(vinyl alcohol)/cellulose composite membranes for metal removal from aqueous solutions. *Desalination*, 2010;253(1-3):175-179.

[38] Canizares P., Perez A., Camarillo R. Recovery of heavy metals by means of ultrafiltration with water-soluble polymers: calculation of design parameters. *Desalination*, 2002;144(1-3):279-285.

[39] Mulder M. *Basic Principles of Membrane Technology*. Kluwer Academic Publishers, 1991.

CHAPTER 5

ZEOLITE MEMBRANES FOR METAL ION
REMOVAL FROM WATER

5.1 Literature Review

Interest in alternative ways to achieve separation in industry has led to increasing attention for zeolite membranes due to their attractive properties. The zeolites are alumino-silicate microporous materials with pore diameters -close to molecular size of different species. Furthermore, zeolite membranes give the possibility to separate gaseous or liquid mixtures in a continuous way on the basis of different molecular size and shape and also on the basis of different adsorption properties. Beside these, chemical and thermal resistivities of zeolite membranes are some of their advantages over the organic membranes, as reported in Table 5.1.

Table 5.1 Advantages and disadvantages of zeolite membrane [1]

Advantages of zeolite membranes	Disadvantages of zeolite membranes
Long-term stability at high temperatures	Brittleness
Resistance to high pressure drops	High capital cost
Resistance to harsh environments	Difficult to achieve high selectiveness in large scale microporous membranes
Inertness to microbiological degradation	Low permeability of the highly selective membranes at medium temperatures
Easy to clean after fouling	Difficult to module sealing at high temperatures
Catalytic activity	Low membrane surface area per module volume

The potential applications of zeolite membranes can be summarized as separation membrane, chemical sensor and catalytic membrane reactors [1,2]. Zeolite membranes may offer an alternative choice for produced water treatment as well. Zeolites are crystalline aluminosilicate materials with uniform sub-nanometer- or nanometer-scale pores. The zeolite membranes can be prepared from different topologies such as; LTA, FAU, MOR, FER, MEL, CHA, SAPO-34, DDR, AFI and mixed tetrahedral-octahedral oxides [2]. Among these, FAU membranes came into prominence for the separation of benzene/cyclohexane, CO_2/N_2, ethylene/methane, propylene/propane mixtures with separation factors of 160, 20-100, 8.4, and 6.2, respectively [3]. FAU type zeolite can be classified as X-type (Si/Al=1.0-1.5) and Y-type (Si/Al>1.5) depending on the Si/Al ratio [3].

Besides, MFI-type zeolite has a three-dimensional pore system with straight channels in the b-direction (5.4Å×5.6 Å) and sinusoidal channels in the a-direction (5.1Å×5.5 Å). Due to the inert property of aluminosilicate crystal, zeolite membranes

have superior thermal and chemical stabilities, hence holding great potential for application in difficult separations such as produced water purification and radioactive wastewater treatment [6].

On the other hand, cost and the reproducibility problems in the preparation step limits the applications of zeolite membranes in the industrial level. Recently, only LTA zeolite membranes for pervaporation and vapor permeation are produced and developed in industrial companies such as BNRI (Bussan Nanotech Research Instute Inc.) which is a 100% subsidiary of Mitsui & Co. Ltd. Japan [2]. However, stability of LTA zeolite membranes is limited in a pH range of 6.5-7.5 due to the high Al content. Hence, FAU membranes attracted attention, especially in pervaporation processes, owing to their higher chemical stability.

In addition, difficult formation of self-standing zeolite layers, with dimensions larger than a few square centimeters due to their fragility, is another problem in production of these membranes. Hence, alumina, stainless steel and mullite are the main mechanically resistant supports used for zeolite membrane preparation. Compared to alumina, stainless steel supports have rougher surfaces, larger pore sizes (>100 nm) and higher thermal expansion coefficient causing less resistivity to thermally induced cracks and adhesion problems [3]. On the other hand, alumina supports are capable of high quality micro-, nano- and ultra-filtration membranes with smooth top surfaces. Since smooth top surface is important for thin continuous zeolite layer preparation, alumina supports are generally preferred. Also, it is very critical to synthesize a supported defect-free zeolite membranes. Secondary growth is the most promising method offering a way to control the growth of zeolite layer on surface of support means of using seeds. Secondary growth method has two main steps; seeding and hydrothermal treatment. The support is covered with seed crystals in seeding procedure followed by hydrothermal treatment of seeded support in order to favor the crystal growth of seeds. Therefore, secondary growth method avoids the nucleation step and by this means parameters of each step can be optimized independently [3].

The seeding procedure is the critical step of the secondary growth method because its influence has a direct effect on the improvement of the membrane quality. There are four main ways described in literature to attach the seeds on the support surface [3-5];

- Dip-coating,

- Spin-coating,

- Rubbing and

- Cationic polymer use.

Beyond these, filtration of water suspension of zeolite crystals is a more convenient method to seed porous supports due to its dynamic coverage modality. In this procedure, zeolite crystals facilitate the formation of complete seed coverage on support surface with appliance of pressure differences. In this dynamic process, although filtration takes place primarily through the larger pores, smaller pores enlarge and involve in the mechanism with time. There are two possible modes for applying the filtration process; dead-end and cross-flow. As illustrated in Figure 1-a, fluid flow is perpendicular to the filter surface and the filter rapidly becomes clogged with particles in the dead-end filtration. Particles larger than the filter's pore size may be retained by sieving whereas particles smaller than the pore size may be retained by sticking to the elements of the filter (hydrosol filtration). On the other hand, fluid flow is parallel to the filter surface and particles become more concentrated as filtrate leaves through the filter's pores in the cross-flow filtration (Figure 5.1-b) [4]. Compared to dead-end mode, cross-flow filtration offers a more uniform and compact zeolite layer due to tangentially flow of suspension along to the surface of the support. The shear stresses on the deposited layer should be prevented by low linear velocity to achieve a uniform coverage on the support [3].
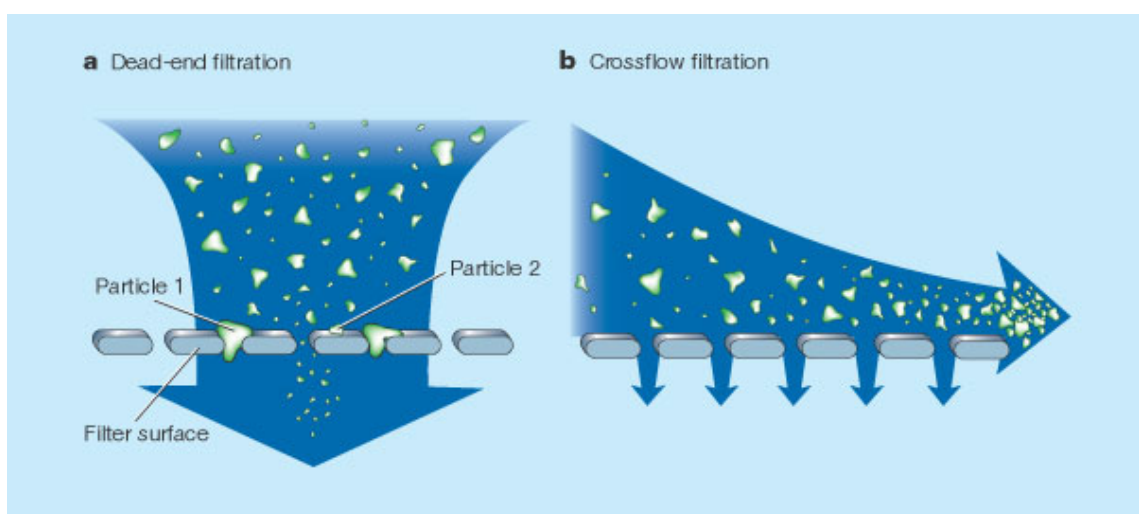
Figure 5.1 Dead-end (a) and cross-flow (b) filtration [4]

In addition, uniformity of the zeolite coverage on the support surface is dependent on the geometry of the support. Uniformity of the deposited layer can be destroyed because of the gravitational force when tubular supports are used. For example, a vertically placed support will cause a thicker seed layer on the lower part whereas a horizontally placed one will cause deposition of the seed on the bottom surface. In order to prevent this effect of gravitational force, rotation of the support during the seeding process becomes necessary [3].

The present work used the method, designed by C. Algieri *et. al.* [3], which is a combination of the following:

i.   cross-flow filtration of zeolite-water suspension through porous alumina support;

ii.   tilting of the support with respect to the horizontal plane;

iii.   rotation of the support along its longitudinal axis.

5.2 Experimental Procedure

5.2.1 Membrane Synthesis

A series of FAU and ZSM-5 zeolite membranes, with different permeation properties, were synthesized by secondary growth method. The zeolite layer was synthesized on the inner surface of α-Al_2O_3 tubes, which were used as the membrane supports (I.D.=7 mm, O.D.=10 mm, L=100 mm, d_{pore}=100-200 nm, INOCERMIC). NaX crystals purchased by Sigma Aldrich (particle size of about 5 μm) and synthesized ZSM-5 and silicalite were used during the seeding step.

The tilt angle, the concentration, zeolite topology, and the pH of the zeolite suspension, and the hydrothermal treatment were the changing parameters for investigation of their effects on the performance of the membrane. In the first series of membranes, the concentration and pH of the zeolite suspension were set constant to 0.2 wt% and 9, respectively.

The first step was to prepare a homogeneous 0.2 wt% zeolite suspension. The first sample was seeded with a tilt angle of 10°. After seeding for 20 minutes the α-Al_2O_3 support tube was rotated slowly for 180° and the seeding continued for another 20 minutes. The second zeolite membrane was seeded with a suspension having pH around 9 and with a tilt angle of 5°. The seeding time and the rotation was same with the previous sample. The last sample of this series was seeded by changing only the tilt angle to 0°.

The second series of zeolite membranes were prepared by seeding the inner surface of α-Al_2O_3 tubes with a more dilute zeolite suspension (1.60×10^{-2} wt%) having a pH around 11. The samples were seeded with a tilt angle of 0° with a total synthesis time of 20 minutes. One of the samples was seeded under continuous rotation for 20 minutes while the other was seeded for 10 minutes then rotated 180° and seeded for another 10 minutes. The remaining membranes were seeded with 1.60×10^{-2} wt% zeolite suspension having a pH 7. Membranes FAU-1-7 were seeded by using zeolite suspension immediately after reaching the expected pH value by adding some drops of HNO_3. Membranes FAU-8 and FAU-9 seeded after stabilizing the pH of the zeolite suspension.

The third series of zeolite membrane were prepared by seeding the inner surface of α-Al_2O_3 tubes (d_{pore}=100 nm) with silicalite suspension (1.60×10^{-2} wt%). The samples were seeded with a tilt angle of 7° under continuous rotation for 20 minutes. One of the samples were seed at pH 7 while the other was seeded at pH=9.

Finally, the last series of zeolite membranes were seeded with ZSM-5 suspension having a stabilized pH of 9 (1.60×10^{-2} wt%) with a tilt angle of 7° under continuous rotation for 20 minutes. In this case, the pore diameter of support materials was the changing parameter. ZSM-3 and ZSM-4 were seeded on the inner surface of α-Al_2O_3 tubes having d_{pore} equal to 100 nm and 200 nm, respectively. The operative conditions for the seeding are summarized in Table 5.2.

Table 5.2 Operative conditions used for the seeding procedure

Sample	Concentration of zeolite in suspension (wt %)	Seeding crystal	pH of the zeolite suspension	Total seeding time (min)	Rotation	Tilt angle (°)	Pore diameter of α-Al$_2$O$_3$ supports (nm)
FAU-1						0	
FAU-2	0.2	NaX	9	40	180° after 20 min	5	100
FAU-3						10	
FAU-4	1.6x10^{-2}	NaX	11	20	180° after 10 min continuous	0	100
FAU-5							
FAU-6	1.6x10^{-2}	NaX	7	20	180° after 10 min continuous	0	100
FAU-7							
FAU-8	1.6x10^{-2}	NaX	7	20	continuous	0	100
FAU-9							
ZSM-1	1.6x10^{-2}	Silicalite	7	20	continuous	7	100
ZSM-2			9				
ZSM-3	1.6x10^{-2}	ZSM-5	9	20	continuous	7	100
ZSM-4							200

All of the seeded samples were dried under room conditions for 24 hours and then they were weighted before the growth step. Next step was to prepare a growth solution in order to favor the crystal growth of the zeolite membrane inside the α-Al$_2$O$_3$ tubes. After the preparation of growth solution, the outside α-Al$_2$O$_3$ tubes were covered with Teflon tape in order to prevent the membrane formation on the outer part of the tubes. The tubes were inserted in the Teflon-lined autoclaves, filled with the synthesis solution for the growth of the zeolite layer, were placed vertically in pre-heated furnace for hydrothermal treatment. Membranes FAU-1-7 were subjected to the hydrothermal

treatment in which crystallization is carried out at 90°C for 24 hours. On the other hand, membranes FAU-8 and FAU-9 were crystallized through second hydrothermal treatment in which 6 hours hydrothermal treatments at 100°C were repeated in order to minimize the intercrystal pores and defects [7]. ZSM-1 and ZSM-2 membranes were subjected to a 2 step hydrothermal treatment each last for 4 days at 175°C whereas ZSM-3 and ZSM-4 were exposed to a first hydrothermal treatment for 6 days and second hydrothermal treatment for 2 days at 175°C. The operative conditions of hydrothermal treatment are reported in Table 5.3. After the heat treatment process, the membranes were washed with distilled water up to the pH was neutral. Finally, the washed membranes were placed in oven at 110° to evaporate the water.

Table 5.3 Operative conditions used for the hydrothermal treatment

Chemical Reagents	Sodium silicate solution (Aldrich, NaOH 14 wt.% and SiO_2 27 wt.%) Sodium aluminate (Carlo Erba Reagenti, 53-55% Al_2O_3) Sodium hydroxide (NaOH pellets, 97%, Carlo Erba Reagenti), Tetrapropylammonium hydroxide (Aldrich, TPAOH 1 M soln.), Tetraethyl orthosilicate (Aldrich, TEOS), Aluminum isoproxide (Aldrich, 99.99% AIP), Deionized water
FAU Synthesis solution 1 composition	14 SiO_2:32 NaOH:2 Al:1030 H_2O [3]
FAU Synthesis solution 2 composition	10.7 SiO_2:37.4 NaOH:2 Al:850 H_2O [5]
ZSM-5 Synthesis solution composition	1 Al_2O_3:46 SiO_2:2.7 TPA:5 Na_2O:2500 H_2O
Solution aging	24 h
Temperature	90°C, 100°C, 175°C
Time (h)^a	1/(24), 2/(6,6), 3/(96,96), 4/(144,48)

[a] The number of the slash indicates the number of repetitions; numbers in the brackets are the durations (hour) for each hydrothermal treatment. For example, "2/(6,6)" means that the membrane was obtained by two repetitions of hydrothermal treatment: 6 h for the first time and 6 h for the second time.

As a final step, ZSM-1 and ZSM-2 were calcinated at 480°C for 5 hours with a heating rate of 0.2 °C/min, in order to remove all decomposition products from the zeolite crystal.

5.2.2 Membrane Characterization

The performance of the zeolitic membranes was initially analyzed by single gas permeation tests with N_2 and CO_2 at room temperature. The permeation tests were carried out according to the pressure drop method (PDM). In PDM, one end of the membrane tube was closed and the trans-membrane pressure difference (ΔP^{TM}) was set by controlling the feed pressure with atmospheric pressure on the permeate side. The permeating flux was measured in steady state via bubble soap flow-meters, and used for calculating the gas permeance as;

$$Permeance = \frac{Flux}{\Delta P^{TM}}$$

(5.1)

The ideal selectivity is the ratio of the permeances of the two gases measured under the same conditions;

$$Ideal\ Selectivity\ (i\,/\,j) = \frac{Permeance_i}{Permeance_j}$$

(5.2)

5.3 Results and Discussion

The deposited amount of zeolite on the inside surface of α-Al$_2$O$_3$ tubes after seeding and growth steps of each membrane are reported in the Table 5.4. The membranes seeded with NaX at pH value 9 were not good quality due to reduction in the zeolite layer during hydrothermal treatment As reported in Table 5.4, reduction in the mass of the zeolite layer after hydrothermal treatment proved that zeolite layer after seeding step was not stable for FAU-1, FAU-2, and FAU-3. On the other hand, zeolite membranes seed with ZSM-5 at pH 7 and 9 did not show reduction in their masses after hydrothermal treatment. However, seeding and crystal growth of ZSM-1 and ZSM-2 membranes were exactly the same, except pH of their seed suspensions. The difference only in their pH showed that ZMS-5 crystals could be seeded and grown better when the pH of the seed suspension was 9. For this reason, at latter experiments of ZSM-5, pH was fixed to 9. In addition, the effect of pore size difference of the α-Al$_2$O$_3$ on membrane performance was investigated by ZSM-3 and ZSM-4. Results showed that, when α-Al$_2$O$_3$ support having larger pore diameter (~200 nm) was used, deposited seed layer was increased on the inside layer of the support tube. This can be explained by the blockage of larger pores during the cross-flow seeding process. Larger pores caused higher possibility of blockage of pores by small ZSM-5 zeolite particles. In addition, ZSM-5 seeded membrane ZSM-3 had higher amount of seed deposited on the inner layer of the support than that of ZSM-2, which was seeded with silicalite suspension.

Table 5.4 Mass deposited on inner surface of α-Al$_2$O$_3$ support tubes after seeding and growth step

Membrane	pH (seed suspension)	m$_{after\ seeding}$ (g)	m$_{after\ growth\ step}$(g)
FAU-1		0.7055	0.0871
FAU-2	9	0.6960	0.1307
FAU-3		0.0202	0.0557
FAU-4		0.0139	0.0685
FAU-5	11	0.0249	0.1039
FAU-6		0.0099	0.0459
FAU-7	7	0.0070	0.0396
FAU-8		0.0143	0.1031
FAU-9	7 (stable)	0.0280	0.0997
ZSM-1	7 (stable)	0.0042	0.3764
ZSM-2	9 (stable)	0.0072	0.5747
ZSM-3	9 (stable)	0.0181	0.4465
ZSM-4	9 (stable)	0.0249	0.5175

The results of the single gas permeation tests for the prepared FAU membranes were listed in Table 5.5. Ideal selectivities of the membranes (1.2-1.3) are very close to the bare support's ideal selectivity (1.2) corresponding to Knudsen transport [5]. The lower permeances of the membranes with respect to the bare support indicated that the large pores are covered with zeolitic layer. For the seeding step, decreasing the zeolite concentration of the seeding suspension from 0.2 wt.% to 1.6×10^{-2} wt.% decreased the permeances of both N_2 and CO_2 gases. These results indicated that pores of the support were covered with less defects into the zeolite layer by use of lower concentration value. The high decrease in N_2 and CO_2 permeance of FAU-8 and FAU-9 with respect to the other membranes indicated the strong effect of the stability of the pH during the seeding step on the membranes' quality. In fact, FAU-7 and FAU-9 synthesized under

exactly same conditions with difference on the stabilization time of the suspension, their N_2 permeances were 9.8 and 1.1 µmol m^{-2} s^{-1} Pa^{-1}, respectively. This indicated the formation of a very uniform and compact zeolite layer. Table 5.5 shows that the membrane quality was improved by increasing the selectivity to 1.5 by repeating short-duration (6 hours) hydrothermal treatment. As Gu *et.al.* [7] explained, above 90°C crystallinity of zeolite reaches a maximum within 4 hours so that short-duration repetitions of hydrothermal treatment reduces the defect formation. Also, Walk *et. al.* stated that existing defects (partial coverage of the substrate and micro-cracks) can be repaired by a second hydrothermal synthesis step by using a shorter reaction time [8]. As reported in Table 5.5, Keh and coworkers [5] obtained N_2/CO_2 selectivity as 1.3 whereas Li and coworkers [9] obtained as 1.1 using membranes with same topology. Weh and coworkers [5] found, using the same membrane, higher N_2/CO_2 selectivity value considering a binary system CO_2-N_2 (50:50). The single gas permeation test put in evidence that the N_2 was the more permeable gas. CO_2 presented a lower permeance due to the electrostatic interactions between these quadrupolar molecules and Na^+ ions within the supercages of NaX zeolite [5]. Also, Carbon dioxide permeation data shows the lower values due to its higher size than nitrogen [10].

The results of the single gas permeation tests for the prepared ZSM-5 membranes were listed in Table 5.6. Ideal selectivities of the membranes (~1.1-1.3) were very close to the ideal selectivity (1.2) of the bare support corresponding to Knudsen transport [5]. In addition, lower permeances of ZSM-1, ZSM-2, ZSM-3, and ZSM-5 obtained without the calcination steps showed that there was a reduction in existing defects. ZSM-5 crystals showed a better formation of zeolite membrane having fewer defects than FAU membranes. This indicated the formation of a more uniform and compact zeolite layer. In addition, the reduction in permeance after second heat treatment proved that existing defects was repaired during the second hydrothermal synthesis step. The high increase in N_2 and CO_2 permeance of membranes ZSM-1 and ZSM-2 after calcination step indicated the strong effect calcination process on the quality of the membranes. N_2 permeance of ZSM-1 increased from 0.9x10^{-2} to 1.17 µmol m^{-2} s^{-1} Pa^{-1} whereas N_2 permeance of ZSM-2 increased from 0.5x10^{-2} to 1.5 µmol m^{-2} s^{-1} Pa^{-1}. This high increase in permeance indicated the deformation and/or crack formation of zeolite layers during calcination. During calcination step, membranes were cooled without a fixed cooling rate. Since cooling rate is very critical for crystal growth process, cooling

membranes with out a controlled heating rate cause defects and/or micro cracks on zeolite membrane layer. As a result, N_2/CO_2 selectivity of ZSM-1 and ZSM-2 were around 1, which shows membranes lost their selectivity after calcination step. In addition, ZSM-3 and ZSM-4 membranes, after second hydrothermal treatment, showed N_2/CO_2 selectivities of 1.27 and 1.29, respectively. Although this behaviour is in agreement with the size of N_2 and CO_2 molecules, the selectivities were still low. However, it would be a proper way to analyse these membranes a binary system of CO_2-N_2 (50:50) for determination of the actual selectivities of these membranes.

Table 5.5 Permeances and the ideal selectivities of FAU membranes for N_2 and CO_2

Membrane	Hydrothermal Treatment[b] (pH)	N_2 Permeance ($\mu mol\ m^{-2}\ s^{-1}\ Pa^{-1}$)	CO_2 Permeance ($\mu mol\ m^{-2}\ s^{-1}\ Pa^{-1}$)	Ideal Selectivity$_{(N2/CO2)}$
Support		24.3	19.5	1.2
FAU-1		20.8	16.3	1.3
FAU-2	H1 (9)	15.8	14.2	1.1
FAU-3		6.8	5.0	1.4
FAU-4		4.2	3.6	1.2
FAU-5	H1 (11)	5.4	4.6	1.2
FAU-6		6.9	5.5	1.3
FAU-7	H1 (7)	9.8	7.4	1.3
FAU-8	H2 (7)$_{(stable)}$	2.8	1.9	1.5
FAU-9	H1 (7)$_{(stable)}$	1.1	0.9	1.3
Weh *et.al.*[5]		0.053	0.041	1.3 8.4*
Li *et.al.* [8]		10×10^{13}	9.2×10^{13}	1.1

[b] **H1: Hydrothermal treatment at 90°C for 24 h, using FAU growth solution 1**
H2: Hydrothermal treatment at 100°C for two times of 6 h, using FAU growth solution 2
* N_2/CO_2 selectivity measured by a binary CO_2-N_2 (50:50) system

Table 5.6 Permeances and the ideal selectivities of ZSM-5 membranes for N_2 and CO_2

Membrane	Hydrothermal Treatment[b] (pH)	N_2 Permeance (μmol m^{-2} s^{-1} Pa^{-1})	CO_2 Permeance (μmol m^{-2} s^{-1} Pa^{-1})	Ideal Selectivity$_{(N2/CO2)}$
Support	-	24.3	19.5	1.2
ZSM-1[1]	H3 (7)$_{(stable)}$	1.0×10^{-2}	-	-
ZSM-2[1]	H3(9)$_{(stable)}$	0.3×10^{-2}	-	-
ZSM-1[2]	H3 (7)$_{(stable)}$	0.9×10^{-2}	-	-
ZSM-2[2]	H3(9)$_{(stable)}$	0.5×10^{-2}	-	-
ZSM-1	H3 (7)$_{(stable)}$	1.17**	1.15**	1.02**
ZSM-2	H3(9)$_{(stable)}$	1.50**	1.43**	1.05**
ZSM-3[1]	H4(9)$_{(stable)}$	1.50×10^{-2}	1.32×10^{-2}	1.14
ZSM-4[1]		0.52×10^{-2}	0.41×10^{-2}	1.27
ZSM-3[2]	H4(9)$_{(stable)}$	0.14×10^{-2}	0.11×10^{-2}	1.27
ZSM-4[2]		0.27×10^{-2}	0.21×10^{-2}	1.29
Weh *et.al.*[5]		0.053	0.041	1.3 / 8.4*
Li *et.al.* [8]		10×10^{13}	9.2×10^{13}	1.1

[b] **H3: Hydrothermal treatment at 175°C for two times of 96 h, using ZSM-5 growth solution**
H4: Hydrothermal treatment at 175°C for two times of 144 and 48 h, using ZSM-5 growth solution
[1] **First hydrothermal treatment**
[2] **Second hydrothermal treatment**
* **N_2/CO_2 selectivity measured by a binary CO_2-N_2 (50:50) system**
**These values were observed after calcinations step

5.4 Conclusions

Tubular FAU and ZSM-5 type supported membranes were prepared by a secondary growth method. The novel seeding procedure designed by Algieri et.al [3] was applied in this study to form a uniform and selective zeolite membrane on the inner surface of α-Al$_2$O$_3$ supports. The results of single gas permeation tests proved that the pH of the seeding suspension and its stabilization was important to form better seal of the inter-crystalline spaces improving the performance of the membrane. FAU membranes with lower permeance values were synthesized using a stable zeolite suspension having a fixed pH value of 7 during the seeding step. Also, applying a two-step hydrothermal treatment with shorter times improved the selectivity of the membrane. These results were due to a better uniform and compact zeolite layer formation on the inner surface of the α-Al$_2$O$_3$ support.

On the other hand, lower permeances of ZSM-5 seeded membranes showed more uniform and compact zeolite layer formation on the inner surface of the α-Al$_2$O$_3$ support. The reduction in the N$_2$ permeances of ZSM-5 membranes after second heat treatment proved that existing defects was repaired during this step. However, increase in permeances of ZSM-1 and ZSM-2 membranes after the calcination step proved deformation of uniform and compact zeolite layer due to possible defect and/or micro crack formation.

These preliminary results shows that FAU and ZSM-5 membranes can be used for water purification treatments by reverse osmosis. However, it should be noted that calcination step of zeolite membranes should be improved by a controlled cooling rate. In order to reach a conclusion, water flux measurements, selectivity of zeolite layer for the metal ions, fouling, and recovery of these membranes must be tested. All these requirements to finish this work are the future work of this study.

REFERENCES

[1] Caro J., Noack M., Kölsch P., Schäfer R. Zeolite membranes – state of their development and perspective. *Microporous and Mesoporous Materials*, 2000;38(1):3-24.

[2] Caro J., Noack M. Zeolite membranes – Recent developments and progress. *Microporous and Mesoporous Materials*, 2008;115(3):215-233.

[3] Algieri C., Bernardo P., Barbieri G., Drioli E. A novel seeding procedure for preparing tubular NaY zeolite membranes. *Microporous and Mesoporous Materials*, 2009;119(1-3):129-136.

[4] Brainerd E. L. Caught in the crossflow. *Nature*, 2001;412:387-388.

[5] Weh K., Noack M., Sieber I., Caro J. Permeation of single gases and gas mixtures through faujasite-type molecular sieve membranes. *Microporous and Mesoporous Materials*, 2002;54(1-2): 27-36.

[6] Liu N., Li L., McPhersona B., Lee R. Removal of organics from produced water by reverse osmosis using MFI-type zeolite membranes. *Journal of Membrane Science*, 2008;325(1);357–361.

[7] Gu X., Dong J., Nenoff T.M. Synthesis of defect-free FAU-type zeolite membranes and separation for dry and moist CO_2/N_2 mixtures. *Industrial and Engineering Chemistry Research*, 2005;44(4):937-944.

[8] Welk M. E., Bonhomme F., Nenoff T. M. Silicalite – 1 Zeolite Membranes For CO_2 Separation. *Preprint Paper-American Chemical Society, Division of Fuel Chemistry*, 2004;49:245.

[9] Li S., Tuan V.A., Falconer J.L., Noble R.D. X-type zeolite membranes: preparation, characterization, and pervaporation performance. *Microporous and Mesoporous Materials*, 2002;53(1-3):59-70.

[10] López A. B., García-Abuín A., Gómez-Díaza D., Navaza J. M. Gases separation by ZSM-5 based membranes. *Procedia Engineering*, 2012;42:795-801.

CHAPTER 6

CONCLUSION AND FUTURE WORK

Membrane separation processes have attracted remarkable attention as promising candidates for water treatments. In particular, membrane processes offer high stability, low energy consumption, simple operation, low operation and capital cost, and high efficiency when compared to conventional separation methods. Main membrane processes for removal of heavy metals from water are reverse osmosis, nanofiltration and ultrafiltration. In *this thesis*, polymer assisted ultrafiltration (PAUF) is preffered due to its capability to remove metal ions by binding them to large water soluble polymers under low transmembrane pressures. In order to have a feasible application of PAUF, the following requirements should be satisfied:

- high water flux (low capital cost),
- high metal retention (high water quality and high metal recovery),
- long-term stability of water flux and rejection (membrane fouling),
- recovery and reusability of membranes (low capital cost),
- mechanical, chemical and thermal stability of membranes,
- minimum pre-treatment (back-flushing and chemical treatment),
- simple and large-scale processability,
- cost effective materials.

Considering these requirements, the aim of *this dissertation* was to produce polymer membranes ensuring high flux, high selectivity, high recovery and reduced fouling properties by simple and inexpensive synthesis method. In this manner, PEEK-

WC was preffered as membrane material due to its outstanding mechanical, chemical, and thermal properties. Additionally, the low-cost and simple, single-step preparation of PEEK-WC membranes is a compelling advantage over commercial composite hydrophilic membranes. Producing flat PEEK-WC membranes for water purification applications for the first time, in literature is one of the novelties of *this work*.

In the first part of *this thesis,* which is covered in *Chapter 2,* asymmetric PEEK-WC membranes with a wide range of different morphologies and transport characteristics were prepared by wet and dry-wet phase inversion technique. The influence of the solvent evaporation time, solvent evaporation temperature and non-solvent on phase inversion PEEK-WC membranes were investigated. It was found that, tuning these three parameters enabled production of PEEK-WC membranes, which were ranging from porous ultrafiltration to dense nanofiltration membranes. The SEM analyses and water flux measurements proved that solvent evaporation time influenced the final membrane morphology. In particular, as the time increased, membranes exhibited denser structure, especially when water was used as non-solvent in coagulation bath. As the temperature was increased to 45°C at evaporation step, desolvation of DMA increased and as a result a denser skin layer was formed on the top of the cast polymer solution. Formation of dense skin layer caused the reduction of hydraulic water permeability. Effect of non-solvent selection was very remarkable on the membrane performance. Both results of retention and water flux tests indicated that dense membranes were formed due to delayed demixing in DMA/IPA system whereas instantaneous demixing in DMA/water system formed porous membranes. Water flux, SEM and retention, shows producing PEEK-WC membranes ranging from porous ultrafiltration to non-porous nanofiltration is possible by tuning process parameters such as evaporation time, evaporation temperature and non-solvent selection for coagulation bath. Thus, DW-0, DW-1, and DW-2 membranes, having an asymmetric porous structure with high water permeances (406, 277, and 110 L/h·m^2·bar, respectively), are good candidates to be used in polymer assisted ultrafiltration applications to remove Cu^{2+} ions from water.

In *Chapter 3*, the optimum conditions for maximum binding capacities of Cu^{2+}-PEI, Ni^{2+}-B-PEI and Co^{2+}-B-PEI was investigated by varying the pH and metal concentrations of the model wastewater solutions. The comparison of bonding capacities of branched and linear polyethlenimine (PEI) showed that, B-PEI has twice

107

as much the bonding capacity as L-PEI. This was explained by the presence of primary amine groups that were capturing more copper(II) ions. As a result, B-PEI was preferred for further studies since its higher bonding capacity allows reduction of the PEI amount, thereby reducing the cost and the probability of membrane fouling or concentration polarization that can be faced during PAUF processes. Optimum pH conditions of bonding for B-PEI-Cu^{2+} was pH=6 whereas pH was equal to 8 for Ni^{2+}-B-PEI and Co^{2+}-B-PEI complexes. B-PEI provided a high metal uptake of 1:1 (B-PEI:M^{2+} weight ratio) that had a better bonding capacity allowing reduction of the PEI amount. The critical step for obtaining a good bonding capacity was resting solutions for at least 2 h after they were completely stabilized. Better bonding capacities obtained for B-PEI will make it a proper choice to be used in industrial applications due to reduction in processing costs, the probability of membrane fouling or concentration polarization during PAUF processes.

Our purpose in *Chapter* 4 was to validate the significant properties of PEEK-WC membranes providing high selectivity, long-term stability, reduced fouling, and high recovery. DW-0, DW-1, and DW-2 membranes, mentioned in *Chapter 2,* were in the range of ultrafiltration membranes for separation of PEI-Cu from water. Polymer-copper complexation tests revealed that the optimum condition for binding occurred at pH ~6.2 with concentrations of 150 mg/L copper and 150 mg/L PEI. DW-0 membranes, prepared without exposing to air, demonstrated a sufficient rejection of Cu^{2+} (93%) during PAUF tests. Also, washing processes revealed that performance of the membranes can be recovered up to 72.7%. A denser structure of PEEK-WC membranes corresponded to a higher rejection of Cu^{2+} (98%), although there was a sharp reduction in permeance. All membranes showed a constant permeance profile with respect to time. This strongly indicated that there was no effect of concentration polarization on the membranes. Also, both long-term and short-term stability (in means of flux and selectivity) of these membranes validated the reduction of fouling effect due to the chemical stabilility of PEEK-WC. In spite of the decrease in permeances, reusability and almost complete recovery (94.5%) of the used membranes make these membranes an attractive alternative for industrial applications. Specifically, almost full recovery of performance of PEEK-WC membranes, just by washing with water, makes them significant among commercially used membranes.

In *Chapter 5,* tubular FAU and ZSM-5 type supported membranes were prepared by a secondary growth method. The novel seeding procedure was applied in this study to form a uniform and selective zeolite membrane on the inner surface of α-Al_2O_3 supports. The results of single gas permeation tests proved that the pH of the seeding suspension and its stabilization was important to form better seal of the inter-crystalline spaces improving the performance of the membrane. FAU membranes with lower permeance values were synthesized using a stable zeolite suspension having a fixed pH value of 7 during the seeding step. Also, applying a two-step hydrothermal treatment with shorter times improved the selectivity of the membrane. These results were due to a better uniform and compact zeolite layer formation on the inner surface of the α-Al_2O_3 support. On the other hand, lower permeances of ZSM-5 seeded membranes showed more uniform and compact zeolite layer formation on the inner surface of the α-Al_2O_3 support. The reduction in the N_2 permeances of ZSM-5 membranes after second heat treatment proved that existing defects was repaired during this step. However, increase in permeances of ZSM-1 and ZSM-2 membranes after the calcination step proved deformation of uniform and compact zeolite layer due to possible defect and/or micro crack formation.

The forthcoming studies on PEEK-WC membranes can be listed as,

- *Improvement of Permeate Flux:* The permeance of PEEK-WC membranes decrease very sharply in the beginning of the PAUF test. This was due to high rejection of Cu^{2+}-B-PEI complexes, which form a thin cake layer on the membrane. The permeance of membranes can be improved by tuning the feed flux. The feed flux rate can be optimized so that solid particles can be flushed more effectively during cross-flow filtration.

- *Recovery of Metal Ions:* In order to have a more feasible separation process, retained metal ions should be recovered. In *Chapter 3,* we already proved that decomplexation occurs in M^{2+}-PEI complexes at pH<3, so that PEI can be regenerated for futher analysis. Also, the efficiency of metal recovery during decomplexation step should be determined.

- *Possible Candidates for PEEK-WC:* Since PEEK is not a very cheap polymer and it is not possible to find commercial PEEK-WC, alternative hydrophilic, chemically and mechanically stable polymers, other than available polymers on the membrane industry, can be investigated.

The forthcoming studies on zeolite membranes can be listed as,

- *Improvement of Calcination Step:* A proper cooling rate will probably prevent the formation of cracking and/or defect formation during calcination step.

- *Membrane Characterization:* Water flux measurements should be carried out. Also, morphology of zeolite membranes will be analysed by SEM. However, in order to analyze their morphology membranes should be broken, which means they cannot be used for further analysis. As a consequence, SEM analysis will be the final analysis.

- *Metal Ion Removal by Reverse Osmosis:* Selectivity of FAU and ZSM-5 membranes for the metal ions, fouling, and recovery of these membranes must be tested by reverse osmosis tests.